NBS MONOGRAPH 116

Hydrogen Stark Broadening Calculations With the Unified Classical Path Theory

U.S. DEPARTMENT OF COMMERCE
National Bureau of Standards

NATIONAL BUREAU OF STANDARDS

The National Bureau of Standards [1] was established by an act of Congress March 3, 1901. Today, in addition to serving as the Nation's central measurement laboratory, the Bureau is a principal focal point in the Federal Government for assuring maximum application of the physical and engineering sciences to the advancement of technology in industry and commerce. To this end the Bureau conducts research and provides central national services in four broad program areas. These are: (1) basic measurements and standards, (2) materials measurements and standards, (3) technological measurements and standards, and (4) transfer of technology.

The Bureau comprises the Institute for Basic Standards, the Institute for Materials Research, the Institute for Applied Technology, the Center for Radiation Research, the Center for Computer Sciences and Technology, and the Office for Information Programs.

THE INSTITUTE FOR BASIC STANDARDS provides the central basis within the United States of a complete and consistent system of physical measurement; coordinates that system with measurement systems of other nations; and furnishes essential services leading to accurate and uniform physical measurements throughout the Nation's scientific community, industry, and commerce. The Institute consists of an Office of Measurement Services and the following technical divisions:

Applied Mathematics—Electricity—Metrology—Mechanics—Heat—Atomic and Molecular Physics—Radio Physics [2]—Radio Engineering [2]—Time and Frequency [2]—Astrophysics [2]—Cryogenics.[2]

THE INSTITUTE FOR MATERIALS RESEARCH conducts materials research leading to improved methods of measurement standards, and data on the properties of well-characterized materials needed by industry, commerce, educational institutions, and Government; develops, produces, and distributes standard reference materials; relates the physical and chemical properties of materials to their behavior and their interaction with their environments; and provides advisory and research services to other Government agencies. The Institute consists of an Office of Standard Reference Materials and the following divisions:

Analytical Chemistry—Polymers—Metallurgy—Inorganic Materials—Physical Chemistry.

THE INSTITUTE FOR APPLIED TECHNOLOGY provides technical services to promote the use of available technology and to facilitate technological innovation in industry and Government; cooperates with public and private organizations in the development of technological standards, and test methodologies; and provides advisory and research services for Federal, state, and local government agencies. The Institute consists of the following technical divisions and offices:

Engineering Standards—Weights and Measures — Invention and Innovation — Vehicle Systems Research—Product Evaluation—Building Research—Instrument Shops—Measurement Engineering—Electronic Technology—Technical Analysis.

THE CENTER FOR RADIATION RESEARCH engages in research, measurement, and application of radiation to the solution of Bureau mission problems and the problems of other agencies and institutions. The Center consists of the following divisions:

Reactor Radiation—Linac Radiation—Nuclear Radiation—Applied Radiation.

THE CENTER FOR COMPUTER SCIENCES AND TECHNOLOGY conducts research and provides technical services designed to aid Government agencies in the selection, acquisition, and effective use of automatic data processing equipment; and serves as the principal focus for the development of Federal standards for automatic data processing equipment, techniques, and computer languages. The Center consists of the following offices and divisions:

Information Processing Standards—Computer Information — Computer Services — Systems Development—Information Processing Technology.

THE OFFICE FOR INFORMATION PROGRAMS promotes optimum dissemination and accessibility of scientific information generated within NBS and other agencies of the Federal Government; promotes the development of the National Standard Reference Data System and a system of information analysis centers dealing with the broader aspects of the National Measurement System, and provides appropriate services to ensure that the NBS staff has optimum accessibility to the scientific information of the world. The Office consists of the following organizational units:

Office of Standard Reference Data—Clearinghouse for Federal Scientific and Technical Information [3]—Office of Technical Information and Publications—Library—Office of Public Information—Office of International Relations.

---

[1] Headquarters and Laboratories at Gaithersburg, Maryland, unless otherwise noted; mailing address Washington, D.C. 20234.
[2] Located at Boulder, Colorado 80302.
[3] Located at 5285 Port Royal Road, Springfield, Virginia 22151.

UNITED STATES DEPARTMENT OF COMMERCE
Maurice H. Stans, *Secretary*
National Bureau of Standards Lewis M. Branscomb

Hydrogen Stark Broadening Calculations With the Unified Classical Path Theory

C. R. Vidal, J. Cooper, and E. W. Smith

Institute for Basic Standards
National Bureau of Standards
Boulder, Colorado 80302

National Bureau of Standards Monograph 116

Nat. Bur. Stand. (U.S.) Monogr. 116, 143 pages (May 1970)
CODEN: NBSMA

Issued May 1970

Library of Congress Catalog Card Number: 75-606028

TABLE OF CONTENTS

HYDROGEN STARK BROADENING CALCULATIONS WITH THE UNIFIED CLASSICAL PATH THEORY*

C. R. Vidal, J. Cooper, and E. W. Smith

The unified theory has been generalized for the case of upper and lower state interaction by introducing a more compact tetradic notation. The general result is then applied to the Stark broadening of hydrogen. The thermal average of the time development operator for upper and lower state interaction is presented. Except for the time ordering it contains the effect of finite interaction time between the radiator and perturbers to all orders, thus avoiding a Lewis type cutoff. A simple technique for evaluating the Fourier transform of the thermal average has been developed. The final calculations based on the unified theory and on the one-electron theory are compared with measurements in the high and low electron density regime. The unified theory calculations cover the entire line profile from the line center to the static wing and the simpler one-electron theory calculations provide the line intensities only in the line wings.

Key words: Classical path; hydrogen lines; line wings; one-electron theory; Stark broadening; unified theory.

* This research was supported in part by the Advanced Research Projects Agency of the Department of Defense, monitored by Army Research Office-Durham under Contract No. DA-31-124-ARO-D-139.

I. INTRODUCTION

For the first few Balmer lines of hydrogen, recent papers (Gerardo and Hill, 1966; Bacon and Edwards, 1968; Kepple and Griem, 1968; Birkeland, Oss and Braun, 1969) have demonstrated fairly good agreement between measurements in high electron density plasmas ($n_e > 10^{16} cm^{-3}$) and improved calculations of the so called "modified impact theory". The experimental and theoretical half-widths differ less than about 10%. However, measurements of the Lyman-α wings (Boldt and W. Cooper, 1964; Elton and Griem, 1964) and low electron density measurements ($n_e \cong 10^{13} cm^{-3}$) of the higher Balmer and Paschen lines (Ferguson and Schlüter, 1963; Vidal, 1964; Vidal, 1965) have revealed parts of the hydrogen line profile, for which the modified impact theory appears to break down. For the higher series members better agreement has been obtained with quasi-static calculations (Vidal, 1965). The reason the current impact theories break down is that these theories correct the completed collision assumption by means of the Lewis cutoff (Lewis, 1961) which is only correct to second order. With this cutoff it was possible to extend the range of validity for the impact theory beyond the plasma frequency. However, in the distant wings, where the electron broadening becomes quasistatic, the second order perturbation treatment with the Lewis cutoff breaks down because the time development operator must then be evaluated to all orders. Attempts to correct the second order theory have been made already (Griem, 1965; Shen and J. Cooper, 1969), but these theories still make the completed collision assumption by replacing the time development operator by the corresponding S-matrix, and so it has to be emphasized that in conjunction with the Lewis cutoff these theories would only be correct to second order. The impact theory in its present form is intrinsicly not able to describe the static wing and the transition region to the line center where dynamic effects

cannot be neglected. To overcome this problem, several semiempirical procedures (Griem, 1962; Griem, 1967a; F. Edmonds, Schlüter and Wells, 1967) have been suggested to generate a smooth transition from the modified impact theory to the static wing.

Recently the classical path methods in line broadening have been reinvestigated in two review papers (E. Smith, Vidal and J. Cooper, 1969a, 1969b), which are from now on referred to as papers I and II. The purpose of I and II was to state clearly the different approximations which are required to obtain the classical path theories of line broadening and to find out where these theories are susceptible to improvements. In a manner similar to the Mozer-Baranger treatment of electric microfield distribution functions (Baranger and Mozer, 1959, 1960), it was shown that the general thermal average can be expanded in two ways, one of which leads to the familiar impact theory describing the line center (Baranger, 1958, 1962; Griem, Kolb and Shen, 1959, 1962). The other expansion represents a generalized version of the one electron theory (J. Cooper, 1966), which holds in the line wings. It is also shown that there is generally a considerable domain of overlap between the modified impact theory and the one electron theory. Based on these results, a "unified theory" was then developed (E. Smith, J. Cooper and Vidal, 1969), henceforth referred to as paper III, which presents the first line shape expression which is valid from the line center out to the static line wing including the problematic transition region. The line shape obtained by the unified theory has the form

$$I(\omega) = \frac{1}{\pi} \sum \mathrm{Im} \left\{ \vec{d} \quad \frac{1}{\Delta\omega - \mathfrak{L}(\Delta\omega)} \vec{d} \right\} , \qquad (I.1)$$

where d, $\Delta\omega$ and $\mathfrak{L}(\Delta\omega)$ are operators. In paper III it was shown that the familiar impact theories, which hold in the line center, may be obtained by making a Markoff approximation in the unified theory, while the one electron theory describing the line wings is just a wing expansion of the unified theory. Consequently the crucial problem for any line broadening calculation is to evaluate the matrix elements of $\mathfrak{L}(\Delta\omega)$, which is essentially the Fourier transform of the thermal average (see Eq. (46) and (47) of paper III). This will be done in detail in this paper for the general case of upper and lower state interactions.

In the following Sec. II we start with a brief summary of the basic relations which are required for the classical path approach pursued here. We then generalize the results of the unified theory to include lower state interaction (Sec. IV) after introducing a more compact tetradic notation (Sec. III). From this general result we turn to the specific problem of hydrogen by discussing briefly the no quenching assumption (Sec. V) and deriving the thermal average $\mathfrak{F}^{(1)}(t)$ (see Eq. (47) of paper III) for the general case of upper and lower state interaction (Sec. VI). We next investigate the multipole expansion of the classical interaction potential in the time development operator (Sec. VII). The thermal average $\mathfrak{F}^{(1)}(t)$ is then evaluated in two steps by first performing a spherical average (Sec. VIII) and then an average over the collision parameters: some reference time t_o, impact parameter ρ and velocity v (Sec. IX). Appendix A gives the computer program which we used in calculating the thermal average for dipole interactions including lower state interactions. The large time limit of the thermal average, which leads to the familiar impact theories in the line center, is investigated in detail in Appendix B for different cutoff procedures and compared with the results in the literature. In

Sec. X, a method is developed for performing the Fourier transformation of the thermal average and it leads us to the crucial function for any classical path theory of Stark broadening. This function is finally applied in Sec. XI to the one electron theory, which forms the basis for the asymptotic wing expansion, and in Sec. XII to the unified theory, which describes the whole line profile from the line center to the static wing. Numerical results are given for the hydrogen line profiles as measured by Boldt and W. Cooper, 1964; Elton and Griem, 1964, and Vidal, 1964, 1965. The computer program for the unified theory calculations and the asymptatic wing expansion is given and explained in Appendix C.

II. BASIC RELATIONS

In this section we will briefly outline the basic relations which are used in our classical path treatment of line broadening.

As discussed in Sec. 2 of paper I, we are considering a system containing a single radiator and a gas of electrons and ions. We will make the usual quasi-static approximation for the ions by regarding their electric field $\vec{\mathcal{E}}_i$ as being constant during the times of interest $\simeq 1/\Delta\omega$. This approximation is usually very good because the region where ion dynamics are important is normally well inside the half width of the line except for a few cases such as the n-α lines of hydrogen (Griem, 1967b). The complete line profile $I(\omega)$ is then given by the microfield average (see Eq. (3) of paper II)

$$I(\omega) = \int_0^\infty P(\mathcal{E}_i)\, I(\omega, \mathcal{E}_i)\, d\mathcal{E}_i \qquad \text{(II. 1)}$$

where the normalized distribution function $P(\mathcal{E}_i)$ is the low frequency component of the fluctuating electric microfields. Due to shielding effects $P(\mathcal{E}_i)$ depends on the shielding parameter r_o/D where r_o and D are the mean particle distance and the Debye length (for electrons only) respectively.

With the static ion approximation we have reduced the problem to a calculation of the electron broadening of a radiator in a static electric field $\mathcal{E}_i$. The resulting line profile $I(\omega, \mathcal{E}_i)$ is then simply averaged over all possible ion fields to give the complete line profile $I(\omega)$. The static ion field will be used to define the z-axis for the radiator and the ion-radiator interaction will be taken to be the dipole interaction $eZ\mathcal{E}_i$ where $-eZ$ denotes the Z-component of the radiators dipole moment.

If the unperturbed radiator is described by a Hamiltonian H_a, we may then define a Hamiltonian for a radiator in the static field $\mathcal{E}_i$ by

$$H_o = H_a + eZ\mathcal{E}_i \tag{II. 2}$$

The complete Hamiltonian for the system is then given by

$$H = H_o + V_e(\vec{R}, \vec{x}, \vec{v}, t) \tag{II. 3}$$

where V_e denotes the electron radiator interaction. In this equation, $\vec{x}$ and $\vec{v}$ are 3N vectors $\vec{x} = (\vec{x}_1, \vec{x}_2, \cdots, \vec{x}_N)$, $\vec{v} = (\vec{v}_1, \vec{v}_2, \cdots, \vec{v}_N)$, which denote the positions and velocities of the N electrons and $\vec{R}$ denotes some internal radiator coordinates. For one-electron atoms, $\vec{R}$ is the position of the "orbital" electron relative to the nucleus. The interaction V_e will be regarded as a sum of binary interactions,

$$V_e(\vec{R}, \vec{x}, \vec{v}, t) = \sum_j V_1(\vec{R}, \vec{x}_j, \vec{v}_j, t) \tag{II. 4}$$

where V_1 denotes the interaction between the radiator and a single electron. As is well known the line shape $I(\omega, \mathcal{E}_i)$ may be given by the Fourier transform of an autocorrelation function C(t) (Baranger, 1962)

$$I(\omega, \mathcal{E}_i) = \frac{1}{\pi} \mathrm{Re} \int_o^\infty e^{i\omega t} C(t)\, dt \tag{II. 5}$$

In the classical path approximation, the correlation function for electric dipole radiation is given by

$$C(t) = Tr_a \left\{ d \langle T_a^\dagger (t)\, d\, T_a(t) \rangle_{av} \rho_a \right\} , \qquad \text{(II. 6)}$$

where $\vec{d}$ and ρ_a denote the dipole moment and the density matrix for the radiator. The thermal average denoted by the subscript av represents the average over electron states (see Eq. (47) of paper I):

$$\langle T_a^\dagger(t)\, d\, T_a(t) \rangle_{av} = \int d\vec{x} d\vec{v}\, P(\vec{x}) W(\vec{v})\, T_a^\dagger(\vec{R}, \vec{x}, \vec{v}, t)\, d\, T_a(\vec{R}, \vec{x}, \vec{v}, t) \qquad \text{(II. 7)}$$

where $P(\vec{x})$ and $W(\vec{v})$ are the position and velocity distribution functions for the electron perturbers (defined by Eqs.(37) to (40) in paper II). The time development operator for the system $T_a(\vec{R}, \vec{x}, \vec{v}, t)$ is the solution of the differential equation

$$i\hbar \frac{\partial}{\partial t} T_a(t) = \left[H_o + V_e(t) \right] T_a(t) \qquad \text{(II. 8)}$$

and it may be written in an interaction representation defined by

$$T_a(\vec{R}, \vec{x}, \vec{v}, t) = \exp(-itH_o/\hbar)\, U_a(\vec{R}, \vec{x}, \vec{v}, t) \qquad \text{(II. 9)}$$

where

$$i\hbar \frac{\partial}{\partial t} U_a(t) = \tilde{V}_e(t)\, U_a(t) \qquad \text{(II. 10)}$$

and

$$\tilde{V}_e(t) = \exp(itH_o/\hbar) V_e(t) \exp(-itH_o/\hbar) . \qquad \text{(II. 11)}$$

It should be noted that $\tilde{V}_e(t)$ is identical with $\tilde{V}_e(t)$ in paper II except that we have not yet made the no quenching assumption which removes the unperturbed part H_a in the Hamiltonian H_o in Eq. (II. 11). Using the time ordering operator $\mathcal{O}$, $U_a(t)$ may be written in the form

$$U_a(\vec{R}, \vec{x}, \vec{v}, t) = \mathcal{O} \exp\left\{ -\frac{i}{\hbar} \int_o^t \tilde{V}_e(\vec{R}, \vec{x}, \vec{v}, t') \, dt' \right\} . \qquad \text{(II. 12)}$$

To evaluate the trace over atomic states in Eq. (II. 6), it is convenient to use the H_o eigenstates $|a\rangle$, $|b\rangle$, $\cdots$ with the eigenvalues E_a, E_b, $\cdots$. Hence, using $U_a(t)$ we have

$$C(t) = \sum_{abcd} \langle a|d|b\rangle \langle c|\dot{d}|d\rangle e^{-i\omega_{dc}t} \qquad \text{(II. 13)}$$
$$\left[\langle b|U_a^{\dagger}(t)|c\rangle \langle d|U_a(t)|a\rangle \right]_{av} \langle a|\rho_a|a\rangle$$

where

$$\omega_{dc} = (E_d - E_c)/\hbar \qquad \text{(II. 14)}$$

In paper II and III, the correlation function C(t) was evaluated for the case of no lower state interactions in order to keep the mathematics as simple as possible because one of the $U_a(t)$ operators in Eq. (II. 13) may then be replaced by a unit operator. In this paper we will give a more general evaluation of C(t) which includes lower state interactions. For this purpose we introduce in the next section a more compact tetradic notation. Furthermore, it should be noted already at this stage that we will interchange the sequence of approximations

with respect to paper II by deriving the generalized unified theory before making the no quenching approximation. This makes the results of the unified theory also useful for situations where the no quenching approximation cannot be made like, for example, microwave lines.

III. THE TETRADIC NOTATION

The purpose of the tetradic notation which we shall use is to write the product of the $U_a(t)$ operators in Eq. (II. 13) in terms of a single operator. To do this we first consider the product of the matrix elements $\langle\alpha|A|\alpha'\rangle$ and $\langle\beta|B|\beta'\rangle$ where A and B may be any arbitrary operator. This product may be written in terms of the direct product $A\otimes B$ according to

$$\langle\alpha|A|\alpha'\rangle\langle\beta|B|\beta'\rangle \equiv \langle\alpha\beta|A\otimes B|\alpha'\beta'\rangle, \qquad \text{(III. 1)}$$

where the product states $|\alpha\beta\rangle = |\alpha\rangle|\beta\rangle$ are essentially the same as the states of Barangers "doubled atom"(Baranger, 1962). This direct product, $A\otimes B$, is a simple form of tetradic operator. If one of the operators A or B happens to be a unit operator I, we may conveniently denote this fact by means of superscripts ℓ and r according to

$$\langle\alpha\beta|A\otimes I|\alpha'\beta'\rangle = \langle\alpha\beta|A^{\ell}|\alpha'\beta'\rangle = \langle\alpha|A|\alpha'\rangle\,\delta_{\beta\beta'}, \qquad \text{(III. 2)}$$

$$\langle\alpha\beta|I\otimes B|\alpha'\beta'\rangle = \langle\alpha\beta|B^{r}|\alpha'\beta'\rangle = \langle\beta|B|\beta'\rangle\,\delta_{\alpha\alpha'}, \quad . \qquad \text{(III. 3)}$$

That is, a superscript ℓ denotes a "left" operator which operates only on the "left" subspace (in this case the $|\alpha\rangle$, $|\alpha'\rangle$ subspace) and a superscript r denotes a "right" operator which operates on the "right"

subspace. It is thus clear that any "left" operator will commute with any "right" operator:

$$[A^{\ell}, B^{r}] = 0. \tag{III. 4}$$

With this notation, the thermal average in Eq. (II. 13) can now be written in the more compact form

(III. 5)

$$\left[\langle b|U_a^{\dagger}(t)|c\rangle\ \langle d|U_a(t)|a\rangle\right]_{av} = \left[\langle c|U_a^{*}(t)|b\rangle\ \langle d|U_a(t)|a\rangle\right]_{av}$$

$$= \left[\langle cd|\ U_a^{\ell *}(t)\ U_a^{r}|ba\rangle\right]_{av}$$

$$= \langle cd|\left[U_a^{\ell *}(t)\ U_a^{r}(t)\right]_{av}|ba\rangle\ .$$

We have chosen to write $\langle b|U_a^{\dagger}(t)|c\rangle$ as $\langle c|U_a^{*}(t)|b\rangle$ simply for convenience in the derivation given in later sections. Noting the definition of $U_a(t)$ given in Eq. (II. 12), we define operators $\tilde{V}_e^{\ell}(\vec{R}, \vec{x}, \vec{v}, t)$ and $\tilde{V}_e^{r}(\vec{R}, \vec{x}, \vec{v}, t)$ so that

$$U_a^{\ell}(\vec{R}, \vec{x}, \vec{v}, t) = \mathcal{O} \exp\left\{-\frac{i}{\hbar}\int_o^t \tilde{V}_e^{\ell}(\vec{R}, \vec{x}, \vec{v}, t')\, dt'\right\} \tag{III. 6}$$

$$U_a^{r}(\vec{R}, \vec{x}, \vec{v}, t) = \mathcal{O} \exp\left\{-\frac{i}{\hbar}\int_o^t \tilde{V}_e^{r}(\vec{R}, \vec{x}, \vec{v}, t')\, dt'\right\}.$$

Since any "left" operator commutes with any "right" operator, we have

$$U_a^{\ell *}(\vec{R}, \vec{x}, \vec{v}, t)\ U_a^{r}(\vec{R}, \vec{x}, \vec{v}, t) = \mathcal{O} \exp\left\{-\frac{i}{\hbar}\int_o^t \tilde{\mathcal{V}}_e(\vec{R}, \vec{x}, \vec{v}, t')dt'\right\}$$

$$\equiv \mathcal{U}(\vec{R}, \vec{x}, \vec{v}, t) \tag{III. 7}$$

where

$$\tilde{\mathcal{V}}_e(\vec{R}, \vec{x}, \vec{v}, t) = \tilde{V}_e^r(\vec{R}, \vec{x}, \vec{v}, t) - \tilde{V}_e^{\ell *}(\vec{R}, \vec{x}, \vec{v}, t). \qquad \text{(III. 8)}$$

We have now succeeded in replacing the two $U_a(t)$ operators by a more general tetradic operator $\mathcal{U}(t)$ which operates in both "left" and "right" subspaces. Eq. (III. 5) thus becomes

$$\left[\langle b| U_a^\dagger(t)|c\rangle \langle d| U_a(t)|a\rangle\right]_{av} = \langle cd|\left[\mathcal{U}(t)\right]_{av}|ba\rangle. \qquad \text{(III. 9)}$$

It is important to realize that the tetradic operator $\mathcal{U}(t)$ is formally the same as the operator $U_a(t)$; that is, it satisfies the same type of differential equation

$$i\hbar \frac{\partial}{\partial t}\mathcal{U}(\vec{R}, \vec{x}, \vec{v}, t) = \tilde{\mathcal{V}}_e(\vec{R}, \vec{x}, \vec{v}, t)\mathcal{U}(\vec{R}, \vec{x}, \vec{v}, t) . \qquad \text{(III. 10)}$$

This means that all of the line broadening formalism which has been developed for $U_a(t)$, will be directly applicable to $\mathcal{U}(t)$.

To make the formal correspondence more complete we use the operators H_o^ℓ, H_o^r, $V_e^\ell(\vec{R}, \vec{x}, \vec{v}, t)$ and $V_e^r(\vec{R}, \vec{x}, \vec{v}, t)$ to define the tetradics $\mathcal{K}_o$ and $\mathcal{V}_e(\vec{R}, \vec{x}, \vec{v}, t)$ according to

$$\mathcal{K}_o = H_o^r - H_o^\ell \qquad \text{(III. 11)}$$

$$\mathcal{V}_e(\vec{R}, \vec{x}, \vec{v}, t) = V_e^r(\vec{R}, \vec{x}, \vec{v}, t) - V_e^{\ell *}(\vec{R}, \vec{x}, \vec{v}, t) . \qquad \text{(III. 12)}$$

Since any left operator commutes with any right operator we have

$$\tilde{V}_e^r(t) = \exp\left\{ itH_o^r/\hbar \right\} V_e^r(t) \exp\left\{ -itH_o^r/\hbar \right\} \qquad \text{(III. 13)}$$

$$= \exp\left\{ it\mathcal{H}_o/\hbar \right\} V_e^r(t) \exp\left\{ -it\mathcal{H}_o/\hbar \right\}$$

Hence

$$\tilde{\mathcal{V}}_e(\vec{R}, \vec{x}, \vec{v}, t) = \exp\left\{ it\mathcal{H}_o/\hbar \right\} \mathcal{V}_e(\vec{R}, \vec{x}, \vec{v}, t) \exp\left\{ -it\mathcal{H}_o/\hbar \right\} \qquad \text{(III. 14)}$$

which is formally the same as Eq. (II. 11). It is also obvious that both $\mathcal{V}_e$ and $\tilde{\mathcal{V}}_e$ will be given by a sum over binary interactions $\mathcal{V}_1$ or $\tilde{\mathcal{V}}_1$ just as in Eq. (II. 4).

$$\mathcal{V}_e(\vec{R}, \vec{x}, \vec{v}, t) = \sum_j \mathcal{V}_1(\vec{R}, \vec{x}_j, \vec{v}_j, t) \qquad \text{(III. 15)}$$

$$\mathcal{V}_1(\vec{R}, \vec{x}_j, \vec{v}_j, t) = V_1^r(\vec{R}, \vec{x}_j, \vec{v}_j, t) - V_1^{\ell *}(\vec{R}, \vec{x}_j, \vec{v}_j, t) \qquad \text{(III. 16)}$$

The formal similarity between the operators H_o, $V_e(t)$, $\tilde{V}_e(t)$, $U_a(t)$, etc. and the tetradic operators $\mathcal{H}_o$, $\mathcal{V}_e(t)$, $\tilde{\mathcal{V}}_e(t)$, $\mathcal{U}(t)$, etc. will greatly simplify the treatment of the thermal average for the general case of upper and lower state interactions.

IV. THE GENERALIZED UNIFIED THEORY

Using the tetradic operators as defined in the previous section we have for the correlation function

$$C(t) = \sum_{abcd} \langle a|\vec{d}|b\rangle \langle c|\vec{d}|d\rangle e^{-i\omega_{dc}t} \langle a|\rho_a|a\rangle \langle cd|\overline{\mathfrak{F}}(t)|ba\rangle \qquad \text{(IV.1)}$$

where $\overline{\mathfrak{F}}(t)$ denotes the thermal average of $\mathcal{H}(\vec{R}, \vec{x}, \vec{v}, t)$:

$$\overline{\mathfrak{F}}(t) = [\mathcal{H}(t)]_{av} = \int d\vec{x}\, d\vec{v}\, P(\vec{x}) W(\vec{v}) \mathcal{H}(\vec{R}, \vec{x}, \vec{v}, t) \quad . \qquad \text{(IV.2)}$$

This tetradic operator $\overline{\mathfrak{F}}(t)$ is formally identical to the operator F(t) defined in Sec. (2. A) of paper III. It would also be formally identical to the F(t) defined by Eq. (19) of paper II if we would make the no quenching approximation at this point. To preserve generality, however, the no quenching approximation will be deferred until a later section when we specify the $|a\rangle, |b\rangle, \cdots$ eigenstates to be H_o eigenstates for hydrogen.

Following the formalism developed in Sec. 2 of paper III, we define an operator $\mathfrak{F}(\vec{R}, \vec{x}, \vec{v}, t)$ by

$$\mathfrak{F}(\vec{R},\vec{x},\vec{v}, t) = P(\vec{x})\, W(\vec{v})\, \mathcal{U}(\vec{R}, \vec{x}, \vec{v}, t) \qquad \text{(IV. 3)}$$

so that

$$\overline{\mathfrak{F}}(t) = \int d\vec{x}\, d\vec{v}\, \mathfrak{F}(\vec{R}, \vec{x}, \vec{v}, t) \qquad \text{(IV. 4)}$$

(cf. Eqs. (11) and (12) of paper III). From Eq. (III. 10) we see that

$$i\hbar \frac{\partial}{\partial t}\, \mathfrak{F}\,(\vec{R}, \vec{x}, \vec{v}, t) = \tilde{\mathcal{V}}_e(\vec{R}, \vec{x}, \vec{v}, t)\, \mathfrak{F}(\vec{R}, \vec{x}, \vec{v}, t) \qquad \text{(IV. 5)}$$

which is formally the same as Eq. (13) in paper III. We next introduce a projection operator $\mathcal{P}$ which is identically the same as the operator $\mathcal{P}$ defined by Eq. (14) of paper III (the fact that $\mathcal{P}$ now operates on tetradics does not change its definition). That is, for <u>any</u> function of electron variables $f(\vec{x}, \vec{v})$ we have

$$\mathcal{P}f(\vec{x}, \vec{v}) = P(\vec{x})\, W(\vec{v}) \int d\vec{x}'\, d\vec{v}'\, f\,(\vec{x}', \vec{v}') \quad . \qquad \text{(IV. 6)}$$

This relation holds whether f is a matrix, tetradic or any other type of operator. With this operator we can follow the derivation in Sec. (2. B) of paper III replacing H_o, V_e, $\tilde{V}_e$ etc. by $\mathcal{H}_o$, $\mathcal{V}_e$, $\tilde{\mathcal{V}}_e$, etc. As a result (cf. Eq. (27) in paper III) we have

$$\frac{\partial}{\partial t}\,\overline{\mathcal{F}}(t) = -\hbar^{-2}\int_o^t \exp\,(it'\mathcal{H}_o/\hbar)\left[\widetilde{\mathcal{V}}_e\,(t-t')\,\mathcal{G}\,(t-t')\,\widetilde{\mathcal{V}}_e(0)\right]_{av}$$

$$\exp\,(-it'\mathcal{H}_o/\hbar)\,\overline{\mathcal{F}}(t')\,dt' \qquad \text{(IV. 7)}$$

where

$$\mathcal{G}(\vec{R},\vec{x},\vec{v},t-t') = \mathcal{O}\exp\left\{-\frac{i}{\hbar}\int_o^{t-t'}(1-\mathcal{P})\,\widetilde{\mathcal{V}}_e\,(\vec{R},\vec{x},\vec{v},t'')\,dt''\right\}. \qquad \text{(IV. 8)}$$

Returning to Eqs. (II. 5) and (IV. 1) we see that the quantity of interest is not $\overline{\mathcal{F}}(t)$ but rather its Fourier transform.

$$\langle cd|\mathcal{J}(\omega)|ba\rangle = \int_o^\infty e^{i\omega t}e^{-i\omega}\,dc^t\,\langle cd|\overline{\mathcal{F}}(t)|ba\rangle\,dt$$

$$= \int_o^\infty e^{i\omega t}\langle cd|\exp\,(-it\mathcal{H}_o/\hbar)\,\overline{\mathcal{F}}(t)|ba\rangle\,dt$$

$$= \int_o^\infty e^{i\omega t}\,\langle cd|\widetilde{\mathcal{F}}(t)|ba\rangle\,dt \qquad \text{(IV. 9)}$$

where

$$\widetilde{\mathcal{F}}(t) = \exp\,(-it\mathcal{H}_o/\hbar)\,\overline{\mathcal{F}}(t)\,. \qquad \text{(IV. 10)}$$

From Eq. (IV. 7) we see that

$$\frac{\partial}{\partial t}\,\widetilde{\mathcal{F}}\,(t) = -(i\mathcal{H}_o/\hbar)\,\widetilde{\mathcal{F}}(t) - \hbar^{-2}\int_o^t \exp\,(-i(t-t')\,\mathcal{H}_o/\hbar)$$

$$\left[\widetilde{\mathcal{V}}_e(t-t')\,\mathcal{G}\,(t-t')\,\widetilde{\mathcal{V}}_e(0)\right]_{av}\;\widetilde{\mathcal{F}}(t')\,dt'. \qquad \text{(IV. 11)}$$

Solving this equation by Fourier transforms gives

$$\mathcal{J}(\omega) = i\;\left[\Delta\omega_{op} - \mathcal{L}(\Delta\omega_{op})\right]^{-1} \qquad \text{(IV. 12)}$$

where

$$\mathfrak{L}(\Delta\omega_{op}) = -i\hbar^{-2}\int_o^\infty \exp(it\Delta\omega_{op})\left[\tilde{\mathcal{V}}_e(t)\mathcal{G}(t)\tilde{\mathcal{V}}_e(0)\right]_{av} dt \qquad (IV.13)$$

and $\Delta\omega_{op}$ is an operator defined by

$$\Delta\omega_{op} = \omega - \mathcal{H}_o/\hbar = \omega - (H_o^r - H_o^\ell)/\hbar \ . \qquad (IV.14)$$

With these results, the line shape given in Eq. (II.5) becomes (cf Eq. (I.1))

$$I(\omega,\mathcal{E}_i) = \frac{1}{\pi}\,\mathrm{Im}\sum_{abcd}\langle a|\vec{d}|b\rangle\langle c|\vec{d}|d\rangle\langle a|\rho_a|a\rangle \langle cd|\left[\Delta\omega_{op} - \mathfrak{L}(\Delta\omega_{op})\right]^{-1}|ba\rangle \ . \qquad (IV.15)$$

We next simplify $\mathfrak{L}(\Delta\omega_{op})$ by means of the impact approximation (see Sec. (3.2) of paper II). Basically this approximation assumes that the average collision is weak, that strong collisions do not overlap in time and that a weak collision overlapping a strong one is negligible in comparison (weak collisions are those interactions for which a low order perturbation expansion in $\mathcal{V}_e$ provides a good approximation to $\mathcal{U}$ or $\mathcal{G}$; for strong collisions the full exponential must be retained). It should be emphasized again that we make a distinction between the impact approximation and the impact theory. The latter contains the impact approximation as well as other approximations like the completed collision assumption which will not be made here. We also assume that the electron perturbers may be replaced by statistically independent quasi particles (e.g., shielded electrons). In Sec. (3) and Appendix B of paper III, it is shown that these approximations

reduce $\mathcal{L}(\Delta\omega_{op})$ to

$$\mathcal{L}(\Delta\omega_{op}) = -i\Delta\omega_{op}\int_0^t e^{it\Delta\omega_{op}}\,\bar{\mathfrak{F}}^{(1)}(t)\,dt\,\Delta\omega_{op} \qquad \text{(IV.16)}$$

where

$$\bar{\mathfrak{F}}^{(1)}(t) = n_e\int d\vec{x}_1\,d\vec{v}_1\,W(\vec{v}_1)\left[\mathcal{V}_1(\vec{R},\vec{x}_1,\vec{v}_1,t) - 1\right] \qquad \text{(IV.17)}$$

and

$$\mathcal{V}_1(\vec{R},\vec{x}_1,\vec{v}_1,t) = \mathcal{O}\exp\left\{-\frac{i}{\hbar}\int_0^t \tilde{\mathcal{V}}_1(\vec{R},\vec{x}_1,\vec{v}_1,t')dt'\right\} \qquad \text{(IV.18)}$$

and n_e denotes the electron density.

Equations (IV.15) through (IV.18) give the line profile of the generalized unified theory. To obtain the impact theory we simply replace $\mathcal{L}(\Delta\omega_{op})$ by $\mathcal{L}(0)$ and as discussed in Sec. 4 of paper III, we have the familiar result (cf. Eq. (44) of Baranger, 1962).

$$\mathcal{L}(0) = i\int(S_1^{\ell *}\,S_1^{r} - 1)\,d\nu \qquad \text{(IV.19)}$$

where S_1 denotes an S-matrix for a binary (completed) collision and $\int d\nu$ denotes the integral over collision variables, as defined in the Appendix of paper II.

$$\int d\nu \equiv n_e\int_0^\infty dv\,vf(v)\int d\rho\,2\pi\rho\int d\Omega \qquad \text{(IV.20)}$$

In comparing Eq. (IV.19) with Barangers result it is important to note that Barangers operators S_i and S_f operate only on "initial" and "final" states respectively, whereas our operators S_1^{ℓ} and S_1^{r} operate on all

possible H_o eigenstates. This difference occurs because we have not made the no quenching assumption yet.

The other limit of the one electron theory is obtained by making a wing expansion of the unified theory; that is, the operator $[\Delta\omega_{op} - \mathcal{L}(\Delta\omega_{op})]^{-1}$ is expanded in powers of $[\mathcal{L}(\Delta\omega_{op})/\Delta\omega_{op}]$. To lowest order this gives

$$[\Delta\omega_{op} - \mathcal{L}(\Delta\omega_{op})]^{-1} = \frac{1}{\Delta\omega_{op}} + \frac{1}{\Delta\omega_{op}} \mathcal{L}(\Delta\omega_{op}) \frac{1}{\Delta\omega_{op}} + \cdots\cdots$$

$$= \frac{1}{\Delta\omega_{op}} - i\int_o^t e^{it\Delta\omega_{op}} \bar{\mathfrak{F}}^{(1)}(t)\, dt + \cdots \quad . \qquad \text{(IV.21)}$$

The first term, $1/\Delta\omega_{op}$, gives a delta function when one takes the imaginary part required by Eq. (IV.15). To get this delta function we approximate radiation damping effects by using $(\Delta\omega_{op} + i\varepsilon)$ in place of $\Delta\omega_{op}$ (see Sec. (3. A) of Smith and Hooper, 1967); the imaginary part of $1/(\Delta\omega_{op} + i\varepsilon)$ is just $-\pi\delta(\Delta\omega_{op})$ when $\varepsilon \to 0$. When this delta function term is averaged over ion fields according to Eq. (II.1) it will produce the line broadening due to the static ions alone (see Sec. 5 of paper II). The influence of the electrons as well as electron-ion coupling is contained in the second term of Eq. (IV.21). Hence one is interested in the matrix elements of the Fourier transform of $\bar{\mathfrak{F}}^{(1)}(t)$, which is also the quantity of interest in the unified theory (see Eq. (IV.16)). The primary difference between calculations made by the unified and one-electron theories is therefore the matrix inversion of $[\Delta\omega_{op} - \mathcal{L}(\Delta\omega_{op})]$ which is required by the unified theory but not by the one electron theory. Since the matrix elements of the Fourier transform of $\bar{\mathfrak{F}}^{(1)}(t)$ play such a central role in any classical path theory (including the impact theory), the evaluation of these matrix elements for hydrogen will be discussed in detail in the following sections.

V. THE NO-QUENCHING APPROXIMATION FOR HYDROGEN

In the preceding section we have derived the thermal average $\bar{\mathcal{F}}(t)$ and its Fourier transform $\mathcal{J}(\omega)$ for the general case of upper and lower state interaction. In order to evaluate $I(\omega, \varepsilon_i)$ in Eq. (IV.15) we have to consider the complete trace over all H_o eigenstates $|a\rangle$, $|b\rangle$, $\cdots$. However, in looking at the Eqs. (IV.9), (IV.18) and (III.14) one realizes that due to the exponential factors only a few of all the possible matrix elements will contribute significantly to the final line profile at a particular frequency ω. That is, we can neglect those matrix elements for which the argument of the exponential factor is so large that it gives rise to rapid oscillations within the range of the time integral. Hence, if one treats well isolated lines, only those matrix elements of $U_1(t)$ between either "initial" or "final" states have to be considered. We may therefore state the no-quenching approximation as

$$\mathcal{U}_1(t) = U_1^{i*}(t)\, U_1^{f}(t) \tag{V.1}$$

where U_1 now no longer operates on the complete "left" or "right" subspace, but only on "initial" or "final" states (see also Sec. 2.2 and 7.2 of paper II).

Further approximations cannot easily be generalized and depend on the particular problem investigated. We now apply our general results to the problem of hydrogen. In this case the no-quenching assumption states that we need to consider only those matrix elements of $U_1(t)$ and $\tilde{V}_1(\vec{R}, \vec{x}_1, \vec{v}_1, t)$ which are diagonal in the principal quantum number n. As shown already in paper II this is a good approximation as long as the lines investigated are well separated. For calculating the line wings it is furthermore required that there is no appreciable overlap

with wings of adjacent lines in the region of interest. The same is true also in any reliable measurement of line wings.

To show this we can proceed as in Secs. 2.2 and 7.2 of paper II with the difference that now we are dealing with the operator $H_o = H_a + eZ\mathcal{E}_i$ rather than just H_a. Since H_a does not commute with Z we introduce a projection operator P_n (see Sec. 2.2 of paper II) which picks out the part of an operator which is diagonal in n. Using this operator we split H_o into a part which is diagonal in n

$$H_{on} = H_a + eP_n Z\mathcal{E}_i \tag{V.2}$$

and a part which is not diagonal in n

$$H_{off} = e(1-P_n)\, Z\mathcal{E}_i. \tag{V.3}$$

H_a now commutes with $P_n Z$ because both operators are diagonal in parabolic coordinates. We therefore specify their eigenstates completely by the principal quantum number n, the magnetic quantum number m and the quantum number q which is defined to be

$$q = n_1 - n_2 \; ; \tag{V.4}$$

n_1 and n_2 are the usual parabolic quantum numbers which obey the relation

$$n = n_1 + n_2 + |m| + 1 \; . \tag{V.5}$$

Knowing the solution of the eigenvalue problem

$$H_{on}|nqm\rangle = E_{nqm}|nqm\rangle \qquad (V.6)$$

with

$$E_{nqm} = E_n + eZ_{nq}\mathcal{E}_i \qquad (V.7)$$

we see from a second order perturbation approach (cf. Chap. 16 of Merzbacher, 1961) that the energy correction

$$\Delta E^{(2)}_{nqm} = \sum_{n' \neq n} \frac{|\langle nqm|H_{off}|n'q'm'\rangle|^2}{E_{nqm} - E_{n'q'm'}} \qquad (V.8)$$

can always be neglected as long as the ion fields do not become too large. This is again equivalent to stating that the lines have to be well separated.

As a result one is left with the eigenvalues E_a, E_b, $\cdots\cdots$ of the Hamiltonian H_{on} whose eigenstates $|a\rangle$, $|b\rangle$, $\cdots|d\rangle$ are the parabolic states $|nqm\rangle$. This allows us to rewrite the autocorrelation function C(t) in Eq. (IV.1) for hydrogen in the form:

$$C(t,\mathcal{E}_i) = \sum \langle nq_a m_a|\vec{d}|n'q'_a m'_a\rangle\langle n'q'_b m'_b|\vec{d}|nq_b m_b\rangle$$

$$\exp\left\{-\frac{i}{\hbar}\left[E_n - E_{n'} + e(Z_{nq_b} - Z_{n'q'_b})\mathcal{E}_i\right]t\right\}\langle nq_a m_a|\rho_a|nq_a m_a\rangle$$

$$\langle n'q'_b m'_b\,;\, nq_b m_b|\overline{\mathfrak{F}(t)}|n'q'_a m'_a\,;\, nq_a m_a\rangle \qquad (V.9)$$

where quantum numbers which refer to the lower state are distinguished from the upper state quantum numbers by a prime.

The matrix elements of $P_n Z$ are given by (see Bethe and Salpeter, 1957)

$$\langle nqm| Z |nqm\rangle = Z_{nq} = \frac{3}{2} nqa_o \qquad (V.10)$$

with $a_o = \hbar^2/(me^2)$ being the Bohr radius. As a further definition the ion field $\mathcal{E}_i$ will be normalized to the Holtsmark field strength $\mathcal{E}_o$

$$\mathcal{E}_i = \beta \cdot \mathcal{E}_o \qquad (V.11)$$

where

$$\mathcal{E}_o' = \left(\frac{4\pi}{3}\right)^{\frac{2}{3}} e\, n_e^{\frac{2}{3}} . \qquad (V.12)$$

This yields

$$\frac{e}{\hbar}\left(Z_{nq_b} - Z_{n'q_b'}\right)\mathcal{E}_i = \Delta\omega_i(n, q_b, n', q_b') \cdot \beta \qquad (V.13)$$

with

$$\Delta\omega_i(n, q_b, n', q_b') = \left(\frac{4\pi}{3}\right)^{\frac{2}{3}} \cdot \frac{3}{2} \left(nq_b - n'q_b'\right) \frac{\hbar}{m} n_e^{\frac{2}{3}} . \qquad (V.14)$$

$\Delta\omega_i$ is now the frequency shift of a particular Stark component characterized by the quantum numbers n, q_b, n' and q_b' due to the Holtsmark field strength $\mathcal{E}_o$. Introducing the frequency shift $\Delta\omega = \omega - \omega_{nn'}$, where the frequency of the unperturbed line $\omega_{nn'}$, is given by

$$\omega_{nn'} = (E_n - E_{n'})/\hbar \qquad (V.15)$$

the line profile $I(\Delta\omega, \beta)$ can be written in the form

$$I(\Delta\omega, \beta) = \frac{Re}{\pi} \sum \langle nq_a m_a | \vec{d} | n'q_a'm_a' \rangle \langle n'q_b'm_b' | \vec{d} | nq_b m_b \rangle \tag{V.16}$$

$$\langle nq_a m_a | \rho_a | nq_a m_a \rangle \langle n'q_b'm_b'; nq_b m_b | \mathcal{J}(\omega) | n'q_a'm_a'; nq_a m_a \rangle$$

where

$$\langle n'q_b'm_b'; nq_b m_b | \mathcal{J}(\omega) | n'q_a'm_a'; nq_a m_a \rangle = \tag{V.17}$$

$$\int_o^\infty dt \exp\left\{ i(\Delta\omega - \Delta\omega_i\beta)t \right\} \langle n'q_b'm_b'; nq_b m_b | \overline{\mathfrak{F}}(t) | n'q_a'm_a'; nq_a m_a \rangle \ .$$

Performing the ion field average according to Eq. (II.1) will then give us the desired line profile once we know the thermal average $\overline{\mathfrak{F}}(t)$.

VI. THE THERMAL AVERAGE $\overline{\mathfrak{F}}^{(1)}(t)$ FOR HYDROGEN

In Sec. IV. we saw that the crucial problem in any classical path theory of line broadening is the evaluation of the matrix elements of $\overline{\mathfrak{F}}^{(1)}(t)$. With the no-quenching approximation for hydrogen a typical matrix element in parabolic states is given by

$$\langle n'q_b'm_b'; nq_b m_b | \overline{\mathfrak{F}}^{(1)}(t) | n'q_a'm_a'; nq_a m_a \rangle = \tag{VI.1}$$

$$n_e \int d\vec{x}_1 \, d\vec{v}_1 \, W(\vec{v}_1) \quad \langle n'q_b'm_b' ; nq_b m_b | \mathcal{O}\!\!\!\!\mathcal{J}_1(t) - 1 | n'q_a'm_a'; nq_a m_a \rangle$$

To simplify the evaluation we transform to the natural collision variables ρ, v and t_o which denote the impact parameter, electron velocity and some reference time of the collision (see the appendix of paper II). The orientation of the collision axes with respect to the radius vector $\vec{R}$ of the orbital electron is specified by the three Euler angles

represented by Ω. Furthermore we assume a spherically symmetric distribution of perturbing electrons; this is a good approximation as long as the impact parameters are not too small. The velocity distribution function W(v) is related to the Maxwell distribution function f(v) by

$$f(v) = 4\pi v^2 W(v). \tag{VI. 2}$$

With the preceding definitions Eq. (VI. 1) can be rewritten as

$$\langle n'q_b'm'_b;\, nq_b m_b | \bar{\mathfrak{F}}^{(1)}(t) | n'q_a'm_a';\, nq_a m_a \rangle = \tag{VI. 3}$$
$$\frac{n_e}{4\pi}\int d\Omega \int dv\, vf(v) \int d\rho\, \rho \int dt_o \langle n'q_b'm_b';nq_b m_b | \mathfrak{U}_1(t)-1 | n'q_a'm_a';\, nq_a m_a \rangle$$

Next we have to know the matrix elements of the time development operator $\mathfrak{U}_1(t)$ defined by Eq. (IV. 18). This requires the matrix elements of the interaction potential $\tilde{\mathfrak{V}}_1(t)$. In order to save some writing we consider for the moment only $U_1(t)$ and $\tilde{V}_1(t)$ which after making the no-quenching assumption may be the "initial" or "final" part of the corresponding tetradic operators (see Eq. (V. 1)). A typical matrix element of $\tilde{V}_1(t)$ is given by

$$\langle nq_c m_c | \tilde{V}_1(t) | nq_d m_d \rangle = \exp\left\{ i\frac{e}{\hbar}(Z_{nq_c} - Z_{nq_d})\mathcal{E}_i t \right\} \langle nq_c m_c | V_1(t) | nq_d m_d \rangle. \tag{VI. 4}$$

With the no-quenching assumption the unperturbed energy eigenvalues E_n have cancelled. At this stage we now make another simplification by dropping the exponential in the latter equation; this has been done

in all previous Stark broadening calculations but it is rarely stated explicitly. This will be a good approximation in the line wings where the times of interest $1/\Delta\omega$ are small and $\Delta\omega$ is much larger than the average ion field splitting. In the line center, however, the argument of the exponential can easily be on the order of unity or larger in which case $\tilde{V}_1(t)$ effectively vanishes due to rapid oscillations of the exponentials. This effect was first noted by Van Regemorter, 1964, who shows that this effectively introduces another cut off which may easily be smaller than the usual Debye or Lewis cutoffs. This additional cutoff has been included in recent calculations(Kepple and Griem, 1968). However, as discussed in Sec. XII it turns out that its influence on the final line profile is in most cases negligible.

Neglecting the ion field exponentials in Eq. (VI. 4). the time development operator U_1 is now given by

$$U_1 = \mathcal{T} \exp \left\{ - \frac{i}{\hbar} \int_o^t P_n V_1(t')\, dt' \right\} \qquad \text{(VI. 5)}$$

where the time ordering is still required because $P_n V_1(t)$ need not commute with $P_n V_1(t')$. In paper II it was shown that this time ordering is negligible for weak collisions (to second order) as well as quasi-static collisions (i. e., in the distant line wings). Time ordering is not negligible for strong collisions; however, when the thermal average is performed, the errors due to neglecting time ordering are expected to be small. The reason for this is that the time development operator

$$U_1 = \exp \left\{ - \frac{i}{\hbar} \int_o^t P_n V_1(t')\, dt' \right\} \qquad \text{(VI. 6)}$$

still retains its unitarity (cf. Sec. 8 of paper II).

VII. THE MULTIPOLE EXPANSION OF THE CLASSICAL INTERACTION POTENTIAL

Before evaluating the thermal average $\overline{\mathcal{F}^{(1)}}(t)$ we briefly consider the classical interaction potential $V_1(t)$ due to a single electron. If the perturber does not "penetrate" the radiator, $V_1(t)$ is given by the well known multipole expansion

$$V_1(t) = e^2 \sum_{k=1}^{\infty} \frac{|\vec{R}|^k}{[r(t)]^{k+1}} \cdot P_k \left[\cos \theta(t)\right] \qquad \text{(VII. 1)}$$

where $|\vec{R}|$ is the distance of the orbital electron from the nucleus, $r(t)$ is the instantaneous distance of the perturbing electron, the P_k are Legendre polynomials and $\theta(t)$ is the instantaneous angle between $\vec{R}$ and $\vec{r}(t)$.

In most cases it is sufficient to consider only the dipole (k=1) term. However, to account for some asymmetries of a line, it may be necessary to keep some of the higher multipole terms as well. In any case, one can show that this multipole expansion is terminated after some finite number of terms due to symmetries of the radiator.

To show this we specify the angular positions of $\vec{R}$ and $\vec{r}(t)$ by θ_1, φ_1 and θ_2, φ_2 respectively and we apply the spherical harmonic addition theorem (Eq. (4.6.7) of Edmonds, 1960)

$$P_k(\cos\theta) = \sum_{p=-k}^{+k} (-1)^p C_p^k(\theta_1, \varphi_1) \cdot C_{-p}^k(\theta_2, \varphi_2) \qquad \text{(VII. 2)}$$

where

$$\cos\theta = \cos\theta_1 \cos\theta_2 + \sin\theta_1 \sin\theta_2 \cos(\varphi_1 - \varphi_2). \qquad \text{(VII. 3)}$$

We may simplify the mathematics without loosing generality by choosing a coordinate system in which $\varphi_2 = 0$. Using the relation

$$C^k_{-p}(\theta_2, \varphi_2 = 0) = (-1)^p \cdot C^k_p(\theta_2, \varphi_2 = 0) \qquad \text{(VII. 4)}$$

one then obtains

$$P_k(\cos\theta) = C^k_o(\theta_1, \varphi_1) C^k_o(\theta_2) + \cdot \sum_{p=1}^{k} (-1)^p C^k_p(\theta_2, \varphi_2 = 0) \left[C^k_{-p}(\theta_1, \varphi_1) + (-1)^p C^k_p(\theta_1, \varphi_1) \right] \qquad \text{(VII. 5)}$$

which gives for the interaction potential

$$V_1(t) = e^2 \sum_{k=1}^{\infty} \frac{|\vec{R}|^k}{[r(t)]^{k+1}} \left[C^k_o \cdot P_k(\cos\theta_2(t)) + \sum_{p=1}^{k} \sqrt{\frac{(k-p)!}{(k+p)!}} P^p_k(\cos\theta_2(t)) \left\{ C^k_{-p} + (-1)^p C^k_p \right\} \right]. \qquad \text{(VII. 6)}$$

The dipole case (k=1) gives the well known result

$$V_d(t) = \frac{e^2 |\vec{R}|}{r^2(t)} \left[C^1_o \cos\theta_2(t) + \frac{1}{\sqrt{2}} \left\{ C^1_{-1} - C^1_1 \right\} \sin\theta_2(t) \right]$$

$$= \frac{e^2}{r^2(t)} \left[\vec{Z} \cdot \cos\theta_2(t) + \vec{X} \sin\theta_2(t) \right] \qquad \text{(VII. 7)}$$

The y-component vanished because $\varphi_2 = 0$. Similarily one can write down the higher order multipole terms. The necessary matrix elements of C^k_p are given by

$$\langle \ell' m' | C^k_p | \ell m \rangle = (-1)^{m'} \sqrt{(2\ell'+1)(2\ell+1)} \begin{pmatrix} \ell' & k & \ell \\ -m' & p & m \end{pmatrix} \begin{pmatrix} \ell' & k & \ell \\ 0 & 0 & 0 \end{pmatrix}. \qquad \text{(VII. 8)}$$

From the last 3j-symbol we see that these matrix elements exist only if ℓ, k, ℓ' satisfy the triangle condition and their sum is an even integer. Therefore it turns out that, within the no-quenching assumption where one needs the matrix elements of $P_n V_1(t)$, only a finite number of multipole terms exist. The summation index k in equation (VII. 6) has to obey the condition

$$1 \leq k \leq 2\,(n-1)\ . \qquad \text{(VII. 9)}$$

As an example we see that a calculation of the upper state interaction of Lyman α requires only the dipole and quadrupole terms. This condition also illustrates the well known fact that there is no ground state interaction for the Lyman series.

VIII. THE SPHERICAL AVERAGE OF THE TIME DEVELOPMENT OPERATOR $\mathcal{U}_1(t)$

In our evaluation of the thermal average $\bar{\mathfrak{F}}^{(1)}(t)$, defined in Eq. (VI. 3), we first perform the spherical average represented by the integral over the Euler angles Ω, because it greatly simplifies the remaining integrals over t_o, ρ and v. This is due to the spherical symmetry of the time development operator $U_1(t)$ defined in Eq. (VI. 6). It should be noted that this symmetry was achieved by dropping the ion field exponentials in Eq. (VI. 4), thus replacing $\tilde{V}_1(t)$ by $V_1(t)$. We will perform this average by means of a rotation technique used by J. Cooper, 1967, and Baranger, 1958, for S-matrices. Although we are working with the more general time development operators $U_1(t)$ or $\mathcal{U}_1(t)$, the rotation technique is the same.

In terms of the collision variables ρ, v, t_o and Ω, the dipole interaction between the radiator and a perturber is given by

$$V_d(t) = e^2 \vec{R} \left[\vec{\rho} + \vec{v}\,(t+t_o)\right] / \left[\rho^2 + v^2 (t+t_o)^2\right]^{\frac{3}{2}} \qquad \text{(VIII. 1)}$$

(see the appendix of paper II). The three Euler angles denoted by Ω describe the orientation of the collision frame relative to the atomic frame. It is therefore convenient to perform a rotation of the atomic axis through the angles Ω in such a way that $\vec{R}$ points in the same direction as $\vec{\rho}$ and the x axis of the rotated atomic frame points in the same direction as $\vec{v}$. In this rotated frame, the interaction potential takes the form

$$V_c(t) = e^2 \left[Z\rho + Xv\,(t+t_o) \right] / \left[\rho^2 + v^2 (t+t_o)^2 \right]^{\frac{3}{2}} \qquad \text{(VIII. 2)}$$

This rotation transforms the time development operator U_1 into a new operator U_{1c}, where U_1 and U_{1c} are related to one another by

$$U_1 = \mathfrak{D}^{-1}(\Omega)\, U_{1c}\, \mathfrak{D}(\Omega) \qquad \text{(VIII. 3)}$$

where $\mathfrak{D}(\Omega)$ is a rotation operator (see Chap. 4 of Edmonds, 1960). The time development operator in the rotated frame, U_{1c}, is given by

$$U_{1c} = \exp \left\{ -\frac{i}{\hbar} \int_o^t P_n V_c(t')\, dt' \right\} . \qquad \text{(VIII. 4)}$$

To make the form of U_{1c} more explicit, we perform the integral over t' and we obtain

$$U_{1c} = \exp \left\{ -\frac{i}{\hbar} \frac{e^2}{\rho v} \left[P_n ZA(t, t_o, \rho, v) - P_n XB(t, t_o, \rho, v) \right] \right\} \qquad \text{(VIII. 5)}$$

where

$$A(t, t_o, \rho, v) = \frac{(v/\rho)(t_o+t)}{\sqrt{1+(v/\rho)^2 (t_o+t)^2}} - \frac{(vt_o/\rho)}{\sqrt{1+(vt_o/\rho)^2}} \qquad \text{(VIII. 6)}$$

and

$$B(t, t_o, \rho, v) = \frac{1}{\sqrt{1+(v/\rho)^2(t_o+t)^2}} - \frac{1}{\sqrt{1+(vt_o/\rho)^2}} . \qquad \text{(VIII. 7)}$$

Substituting Eq. (VIII. 3) into Eq. (VI. 3) we see that the integral over Ω in Eq. (VI. 3) involves only the matrix elements of four rotation operators. Since it is convenient to use spherical states $|n\ell m\rangle$ when taking matrix elements of $\mathcal{D}(\Omega)$, we make use of the unitary transformation from parabolic to spherical states discussed by Hughes, 1967.

$$|nqm\rangle = \sum_{\ell m'} |n\ell m'\rangle\langle n\ell m'|nqm\rangle \qquad \text{(VIII. 8)}$$

$$\langle n\ell m'|nqm\rangle = \delta_{mm'}(-1)^{\frac{1}{2}(1+m-q-n)}\sqrt{2\ell+1}\begin{pmatrix} \frac{n-1}{2} & \frac{n-1}{2} & \ell \\ \frac{m-q}{2} & \frac{m+q}{2} & -m \end{pmatrix}$$

using 3j-symbols and the definitions in the Eqs. (V. 4) and (V. 5). (An error in the phase factor has been pointed out by H. Pfennig, private communication). Noting that $\mathcal{D}(\Omega)$ is diagonal in the angular momentum ℓ, the Ω integral in Eq. (VI. 3) may now be written

$$\int \langle n'q_b'm_b'; nq_bm_b|\mathcal{U}_1(t)|n'q_a'm_a'; nq_am_a\rangle \, d\Omega =$$

$$\sum \int d\Omega \Big[\langle n'q_a'm_a'|n'\ell_a'm_a'\rangle \, \mathcal{D}^{(\ell_a')-1}_{m_a'm_c'} \langle n'\ell_a'm_c'|U_{1c}^{\dagger}|n'\ell_b'm_d'\rangle \qquad \text{(VIII. 9)}$$

$$\mathcal{D}^{(\ell_b')}_{m_d'm_b'} \langle n'\ell_b'm_b'|n'q_b'm_b'\rangle\Big]\Big[\langle nq_bm_b|n\ell_bm_b\rangle$$

$$\mathcal{D}^{(\ell_b)-1}_{m_bm_d} \langle n\ell_bm_d|U_{1c}|n\ell_am_c\rangle \, \mathcal{D}^{(\ell_a)}_{m_cm_a} \langle n\ell_am_a|nq_am_a\rangle\Big]$$

where the summation $\sum$ denotes sums over $\ell_a, \ell_a', \ell_b, \ell_b', m_c, m_c', m_d$ and m_d'. The Ω dependence of the integrand in Eq. (VIII. 9) is contained entirely in the four rotation operators $\mathcal{D}(\Omega)$. Using Eqs. (4.3.2) and (4.6.1) of Edmonds, 1960, we obtain the identity

$$\int \mathcal{D}^{(\ell_a')-1}_{m_a' m_c'} \mathcal{D}^{(\ell_b')}_{m_d' m_b'} \mathcal{D}^{(\ell_b)-1}_{m_b m_d} \mathcal{D}^{(\ell_a)}_{m_c m_a} \, d\Omega =$$

$$8\pi^2 \sum_{L, M, M'} (-1)^{m_c' - m_a' + m_d - m_b + M - M'} (2L+1)$$

$$\begin{pmatrix} \ell_a' & \ell_a & L \\ -m_c' & m_c & M' \end{pmatrix} \begin{pmatrix} \ell_a' & \ell_a & L \\ -m_a' & m_a & M \end{pmatrix} \begin{pmatrix} \ell_b' & \ell_b & L \\ -m_d' & m_d & M' \end{pmatrix} \begin{pmatrix} \ell_b' & \ell_b & L \\ -m_b' & m_b & M \end{pmatrix}. \qquad \text{(VIII. 10)}$$

Hence Eq. (VIII. 9) becomes

$$\int \langle n' q_b' m_b'; n q_b m_b | \mathcal{U}_1(t) | n' q_a' m_a'; n q_a m_a \rangle \, d\Omega =$$

$$\sum \langle n' q_a' m_a' | n' \ell_a' m_a' \rangle \langle n' \ell_b' m_b' | n' q_b' m_b' \rangle \langle n q_b m_b | n \ell_b m_b \rangle \langle n \ell_a m_a | n q_a m_a \rangle$$

$$8\pi^2 \sum_{L, M, M'} (-1)^{m_c' - m_a' + m_d - m_b + M - M'} (2L+1)$$

$$\begin{pmatrix} \ell_a' & \ell_a & L \\ -m_c' & m_c & M' \end{pmatrix} \begin{pmatrix} \ell_a' & \ell_a & L \\ -m_a' & m_a & M \end{pmatrix} \begin{pmatrix} \ell_b' & \ell_b & L \\ -m_d' & m_d & M' \end{pmatrix} \begin{pmatrix} \ell_b' & \ell_b & L \\ -m_b' & m_b & M \end{pmatrix}$$

$$\langle n' \ell_b' m_d'; n \ell_b m_d | \mathcal{U}_{1c}(t) | n' \ell_a' m_c'; n \ell_a m_c \rangle \qquad \text{(VIII. 11)}$$

This result is spherically symmetric; that is, any further rotations of the atomic coordinate system leave this expression unchanged. One may verify this rotational invariance by rotating U_{1c} through some arbitrary angle Ω' so that $U_{1c} = \mathcal{D}^{-1}(\Omega')\, U'_{1c}\, \mathcal{D}(\Omega')$. Taking matrix elements of the new rotation operators and making use of the orthogonality properties of the 3j-symbols one sees that the right hand side of Eq. (VIII. 11) did not change. Since we are free to perform further rotations on U_{1c} without altering Eq. (VIII. 11), it is convenient to rotate the X-Y plane through an angle $\epsilon = \text{arctg}\,(B/A)$ where A and B are given by Eqs. (VIII. 6) and (VIII. 7). This rotation transforms U_{1c} into an operator $\overline{U}_1$ given by

$$\overline{U}_1 = \exp\left\{-\frac{i}{\hbar} e^2 P_n Z\, g(t, t_o, \rho, v)\right\} \qquad \text{(VIII. 12)}$$

where

$$g(t, t_o, \rho, v) = \frac{1}{\rho v}\sqrt{A^2 + B^2} \qquad \text{(VIII. 13)}$$

$$= \frac{\sqrt{2}}{\rho v}\left[1 - \frac{1 + (v/\rho)^2 t_o\,(t_o + t)}{\sqrt{1 + (v/\rho)^2 (t_o + t)^2}\,\sqrt{1 + (v t_o/\rho)^2}}\right]^{\frac{1}{2}}$$

The operator $\overline{U}_1$ has the important property that it is diagonal in parabolic states (because it contains only $P_n Z$). Hence a typical matrix element of U_1 is given by

$$\langle nqm|\, \overline{U}_1(t)\,|nqm\rangle = \exp\left\{-i\frac{3}{2} nq \frac{\hbar}{m} g\,(t, t_o, \rho, v)\right\}. \qquad \text{(VIII. 14)}$$

We also realize that one and the same rotation through the angle $\epsilon = \text{arctg}\,(B/A)$ diagonalizes simultaneously both time development operators

acting on initial and final states respectively. As a result a typical matrix element of the corresponding tetradic operator $\overline{\mathcal{U}}_1(t)$ is given by

$$\langle n'q'm';nqm|\overline{\mathcal{U}}_1(t)|n'q'm';nqm\rangle = \exp\left\{-i\frac{3}{2}(nq-n'q')\frac{\hbar}{m}g(t,t_o\rho,v)\right\} \tag{VIII.15}$$

Substituting this identity into Eq. (VIII. 11) the spherical average of the time development operator $\mathcal{U}_1(t)$ finally becomes

$$\int\langle n'q_b'm_b';\ nq_bm_b|\mathcal{U}_1(t)|n'q_a'm_a';\ nq_am_a\rangle\,d\Omega =$$

$$\sum\langle n'q_a'm_a'|n'\ell_a'm_a'\rangle\langle n'\ell_a'm_c'|n'q_c'm_c'\rangle\langle n'q_c'm_c'|n'\ell_b'm_c'\rangle\langle n'\ell_b'm_b'|n'q_b'm_b'\rangle$$

$$\langle nq_am_a|n\ell_am_a\rangle\langle n\ell_am_c|nq_cm_c\rangle\langle nq_cm_c|n\ell_bm_c\rangle\langle n\ell_bm_b|nq_bm_b\rangle$$

$$8\pi^2(-1)^{-m_a-m_b}(2L+1)\begin{pmatrix}\ell_a' & \ell_a & L\\ -m_c' & m_c & M'\end{pmatrix}\begin{pmatrix}\ell_a' & \ell_a & L\\ -m_a' & m_a & M\end{pmatrix}\begin{pmatrix}\ell_b' & \ell_b & L\\ -m_c' & m_c & M'\end{pmatrix}\begin{pmatrix}\ell_b' & \ell_b & L\\ -m_b' & m_b & M\end{pmatrix}$$

$$\exp\left\{-i\frac{3}{2}(nq_c-n'q_c')\frac{\hbar}{m}\,g\,(t,t_o,\rho,v)\right\} \tag{VIII.16}$$

where the unitary transformations are given by Eq. (VIII. 8). This result greatly simplifies if there is no lower state interaction (e. g., Lyman lines), in which case one obtains

$$\int\langle nq_bm_b|U_1(t)|nq_am_a\rangle\,d\Omega = \sum\langle nq_bm_b|n\ell_am_a\rangle\langle n\ell_am_a|nq_am_a\rangle\delta_{m_am_b}$$

$$\left[\langle n\ell_am_c|nq_cm_c\rangle\right]^2\frac{8\pi^2}{2\ell_a+1}\exp\left\{-i\frac{3}{2}\,nq_c\,\frac{\hbar}{m}\,g(t,t_o,\rho,v)\right\} \tag{VIII.17}$$

This simplified relation may also be used for the higher series members of the Balmer, Paschen etc. series where lower state interactions contribute only a negligible amount of broadening to the final line profile.

IX. EVALUATION OF THE THERMAL AVERAGE $\overline{\mathfrak{F}}^{(1)}(t)$ FOR HYDROGEN

Having performed the spherical average over the Euler angles Ω we can rewrite Eq. (VI. 3) in the form

$$\langle n'q_b'm_b'; nq_bm_b|\overline{\mathfrak{F}}^{(1)}(t)|n'q_a'm_a'; nq_am_a\rangle = (-1)^{-m_a-m_b}\sum(2L+1)$$

$$\langle n'q_a'm_a'|n'\ell_a'm_a'\rangle\langle n'\ell_a'm_c'|n'q_c'm_c'\rangle\langle n'q_c'm_c'|n'\ell_b'm_c'\rangle\langle n'\ell_b'm_b'|n'q_b'm_b'\rangle$$

$$\langle nq_am_a|n\ell_am_a\rangle\langle n\ell_am_c|nq_cm_c\rangle\langle nq_cm_c|n\ell_bm_c\rangle\langle n\ell_bm_b|nq_bm_b\rangle$$

$$\begin{pmatrix}\ell_a' & \ell_a & L\\ -m_c' & m_c & M'\end{pmatrix}\begin{pmatrix}\ell_a' & \ell_a & L\\ -m_a' & m_a & M\end{pmatrix}\begin{pmatrix}\ell_b' & \ell_b & L\\ -m_c' & m_c & M'\end{pmatrix}\begin{pmatrix}\ell_b' & \ell_b & L\\ -m_b' & m_b & M\end{pmatrix}\overline{F}(t, n, q_c, n', q_c') \qquad (IX.1)$$

where

$$\overline{F}(t, n, q_c, n', q_c') = 2\pi n_e\int dv\, vf(v)\int d\rho\,\rho\int dt_o\ \Phi(t, t_o, \rho, v) \qquad (IX.2)$$

and

$$\Phi(t, t_o, \rho, v) = \exp\left\{-i\frac{3}{2}(nq_c - n'q_c')\frac{\hbar}{m}g(t, t_o, \rho, v)\right\} - 1. \qquad (IX.3)$$

Thus, the problem is now reduced to evaluating $\overline{F}(t)$, which will be done in this section. It is interesting to note the similarity between Eqs. (VIII. 13) and (IX. 2) and the ψ-function of Anderson and Talman, 1955, which is the crucial function in their classical adiabatic theory.

We first realize that due to the symmetry of the line profile we only have to evaluate the real part of $\Phi(t, t_o, \rho, v)$; that is, for every positive value of $(nq_c - n'q_c')$ there will be the corresponding negative value. Hence we are left with

$$\Phi(t, t_o, \rho, v) = \cos\left\{\frac{3}{2}(nq_c - n'q_c')\frac{\hbar}{m}g(t, t_o, \rho, v)\right\} - 1. \qquad (IX.4)$$

In performing the integrals over ρ and t_o in Eq. (IX. 2) we account for shielding by setting the interaction potential V and hence also Φ equal to zero whenever the distance of the perturbing electron is larger than the Debye length D. We also introduce a strong collision cutoff ρ_{min}. In principle we can let the impact parameter go to zero because the functions Φ and F(t) do not diverge for small impact parameters as they do in some second order theories. However, for numerical purposes this would result in very large computer times due to the growing fluctuations in the integral. For this reason we will choose ρ_{min} to be small enough so that when we are interested in large frequency perturbations $\Delta\omega$ where perturbers at small impact parameters are quasi-static, the rest of the integral from 0 to ρ_{min} may then be replaced by the static limit. In the dipole approximation this gives rise to the well known Holtsmark $\Delta\lambda^{-5/2}$-wing (see also Sec. X). According to the validity conditions of the classical path theories (see Paper I) the minimum impact parameter ρ_{min} will be of the order of

$$\rho_o = \lambda\!\!\!^{-} + n^2 a_o \qquad (IX.5)$$

where $\lambda\!\!\!^{-}$ is the De Broglie wavelength.

We now concentrate our attention on the integral

$$G(t, \rho, v) = \int dt_o \, \Phi (t, t_o, \rho, v). \qquad \text{(IX. 6)}$$

For convenience we consider the collision sphere as shown in Fig. 1. The perturbing electron moves along the classical straight line trajectory L and we are interested in the interaction from some time t_o to some time $t_o + t$. Due to the Debye cutoff the t_o- integral extends from -T to + T where

$$T = \frac{1}{v} \sqrt{D^2 - \rho^2} \qquad \text{(IX. 7)}$$

and the interaction potential vanishes if the electron is outside the sphere of radius D. The corresponding time integration limit τ due to the strong collision cutoff ρ_{min} is given by

$$\tau = \frac{1}{v} \sqrt{\rho_o^2 - \rho^2} \quad . \qquad \text{(IX. 8)}$$

Based on this model of the collision sphere we split the integral G into two parts

$$G(t, \rho, v) = U(\rho > \rho_o) \cdot G_a(t, \rho, v) + U(\rho_o > \rho) \cdot G_b(t, \rho, v) \qquad \text{(IX. 9)}$$

where the step function U is defined to be

$$U(a>b) = \begin{cases} 1 & \text{if} \quad a \geq b \\ 0 & \text{if} \quad a < b \end{cases} \qquad \text{(IX. 10)}$$

In order to evaluate $G_a(t, \rho, v)$ we have to distinguish the following four cases depending on whether the initial and final times of interaction are inside or outside the sphere.

Case I: $-T < t_o ; t_o + t < T$

$$g_1(t, t_o, \rho, v) = \frac{\sqrt{2}}{\rho \cdot v} \left[1 - \frac{1 + \frac{v^2}{\rho^2} t_o (t_o + t)}{\sqrt{\left[1 + \frac{v^2}{\rho^2} (t_o + t)^2\right]\left[1 + \frac{v^2}{\rho^2} t_o^2\right]}} \right]^{\frac{1}{2}} \qquad \text{(IX. 11a)}$$

This is the same general expression as given in Eq. (VIII. 13).

Case II: $-T < t_o ; T < t_o + t$

$$g_2(t, t_o, \rho, v) = \frac{\sqrt{2}}{\rho \cdot v} \left[1 - \frac{\frac{\rho}{D} + \frac{v}{\rho} t_o \sqrt{1 - \frac{\rho^2}{D^2}}}{\sqrt{1 + \frac{v^2}{\rho^2} t_o^2}} \right]^{\frac{1}{2}} \qquad \text{(IX. 11b)}$$

Case III: $t_o < -T ; t_o + t < T$

$$g_3(t, t_o, \rho, v) = \frac{\sqrt{2}}{\rho \cdot v} \left[1 - \frac{\frac{\rho}{D} - \frac{v}{\rho} (t_o + t) \sqrt{1 - \frac{\rho^2}{D^2}}}{\sqrt{1 + \frac{v^2}{\rho^2} (t_o + t)^2}} \right]^{\frac{1}{2}} \qquad \text{(IX. 11c)}$$

Case IV: $t_o < -T ; T < t_o + t$

$$g_4(t, t_o, \rho, v) = \frac{2}{\rho v} \sqrt{1 - \frac{\rho^2}{D^2}} \, . \qquad \text{(IX. 11d)}$$

After defining

$$\Phi_k(t, t_o, \rho, v) = \cos\left\{\frac{3}{2}(nq_c - n'q_c')\frac{\hbar}{m} g_k(t, t_o, \rho, v)\right\} - 1 \qquad \text{(IX. 12)}$$

the integral G_a is given by

$$G_a(t, \rho, v) = U(2T>t)\left\{\int_{-T}^{T-t}\Phi_1 dt_o + \int_{T-t}^{T}\Phi_2 dt_o + \int_{-T-t}^{-T}\Phi_3 dt_o\right\} \qquad \text{(IX. 13)}$$

$$+ U(t>2T)\left\{\int_{-T}^{T}\Phi_2 dt_o + \int_{-T-t}^{T-t}\Phi_3 dt_o + \int_{T-t}^{-T}\Phi_4 dt_o\right\}$$

where we have separated the cases where the time of interaction is longer or shorter than the time 2T required to cross the collision sphere.

In a similar manner we evaluate G_b distinguishing between the following cases:

Case I: $-T < t_o ; t_o + t < -\tau$

or $\tau < t_o ; t_o + t < T$

$$g(t, t_o, \rho, v) = g_1(t, t_o, \rho, v) \qquad \text{(IX. 14a)}$$

Case II: $\tau < t_o < T ; T < t_o + t$

$$g(t, t_o, \rho, v) = g_2(t, t_o, \rho, v) \qquad \text{(IX. 14b)}$$

Case III: $t_o < -T;\ -T < t_o + t < -\tau$

$$g(t, t_o, \rho, v) = g_3(t, t_o, \rho, v) \qquad \text{(IX. 14c)}$$

Collisions which enter the strong collision sphere are neglected because of the strong oscillations. This yields

$$G_b(t, \rho, v) = U(T-\tau>t)\left\{\int_{-T}^{-\tau-t}\Phi_1 dt_o + \int_{\tau}^{T-t}\Phi_1 dt_o + \int_{T-t}^{T}\Phi_2 dt_o + \int_{-T-t}^{-T}\Phi_3 dt_o\right\}$$
$$+ U(t>T-\tau)\left\{\int_{\tau}^{T}\Phi_2 dt_o + \int_{-T-t}^{-\tau-t}\Phi_3 dt_o\right\} \qquad \text{(IX. 15)}$$

where again interaction times longer or shorter than $(T-\tau)$ have been separated. In the expressions for G_a and G_b we realize after a change of variables that the corresponding integrals over Φ_2 and Φ_3 are identical. From the Eqs. (IX. 11a) and (IX. 12) it is also clear that Φ_1 is a symmetric function in $z = t_o + \frac{t}{2}$. Performing the Φ_4-integral one finally obtains

$$\tfrac{1}{\sigma}\cdot G_a(t, \rho, v) = U(2T>t)\left\{\int_{-t/2}^{T-t}\Phi_1 dt_o + \int_{T-t}^{T}\Phi_2\, dt_o\right\}$$
$$+ U(t>2T)\left\{\int_{-T}^{+T}\Phi_2 dt_o + \left(\frac{t}{2} - T\right)\cdot\Phi_4\right\} \qquad \text{(IX. 16a)}$$

and

$$\tfrac{1}{\sigma}\cdot G_b(t, \rho, v) = U(T-\tau>t)\left\{\int_{\tau}^{T-t}\Phi_1 dt_o + \int_{T-t}^{T}\Phi_2 dt_o\right\}$$
$$+ U(t>T-\tau)\left\{\int_{\tau}^{T}\Phi_2 dt_o\right\} . \qquad \text{(IX. 16b)}$$

We now introduce the following dimensionless variables

$$x = \frac{\rho}{D} \text{ and } x_o = \frac{\rho_o}{D} \quad \text{with } D = \sqrt{\frac{kT}{4\pi n_e e^2}} \quad ,$$

$$s = \tilde{\omega}_p t \quad \text{with } \tilde{\omega}_p = \sqrt{2}\cdot\omega_p = \sqrt{\frac{8\pi n_e e^2}{m}} \quad ,$$

$$y = t_{o/T} \tag{IX.17}$$

$$u = \frac{v}{v_{av}} \quad \text{with } v_{av} = \sqrt{\frac{2kT}{m}}$$

and the following abbreviations

$$R = \frac{t}{T} = \frac{u \cdot s}{\sqrt{1-x^2}}$$

$$P = \frac{\tau}{T} = \frac{\sqrt{x_o^2 - x^2}}{\sqrt{1-x^2}} \quad . \tag{IX.18}$$

With these definitions the preceding relations can be rewritten as

$$g_1(s, y, x, u) = \frac{\sqrt{2}}{xu} \cdot \left[1 - \frac{x^2 + (1-x^2)y\,(y+R)}{\sqrt{\left[x^2 + (1-x^2)y^2\right]\left[x^2 + (1-x^2)(y+R)^2\right]}} \right]^{\frac{1}{2}}$$

$$g_2(s, y, x, u) = \frac{\sqrt{2}}{xu} \cdot \left[1 - \frac{x^2 + y\,(1-x^2)}{\sqrt{x^2 + y^2\,(1-x^2)}} \right]^{\frac{1}{2}} \tag{IX.19}$$

$$g_4(s, y, x, u) = \frac{2}{xu} \cdot \sqrt{1-x^2}$$

and

$$\Phi_k(s, y, x, u) = \cos\left\{ C \cdot g_k(s, y, x, u) \right\} - 1 \qquad \text{(IX.20)}$$

where

$$C = C_1 \cdot C_2 \qquad \text{(IX.21a)}$$

and

$$C_1 = \frac{3}{2}\,(nq_c - n'q_c') \qquad \text{(IX.21b)}$$

$$C_2 = \frac{\hbar}{m \cdot D \cdot v_{av}} = \frac{\hbar\tilde{\omega}_p}{2kT} = 0.03043 \sqrt{\frac{Ncm^3}{10^{18}}} \cdot \frac{10^4\,K}{T}\,.$$

Similarly we have for the integrals over t_o

$$G_a(s, x, u) = U(2>R)\left\{ \int_{-R/2}^{1-R} \Phi_1\, dy + \int_{1-R}^{1} \Phi_2\, dy \right\} + U(R>2)\left\{ \int_{-1}^{+1} \Phi_2\, dy + \left(\frac{R}{2} - 1 \right) \Phi_4 \right\} \qquad \text{(IX.22a)}$$

and

$$G_b(s, x, u) = U(1>R+P)\left\{ \int_{P}^{1-R} \Phi_1\, dy + \int_{1-R}^{1} \Phi_2\, dy \right\} + U(R+P>1)\left\{ \int_{P}^{1} \Phi_2\, dy \right\} \qquad \text{(IX.22b)}$$

which leads to the thermal average

$$\bar{F}(s, n_e, T) = 2\pi n_e D^3 \int_o^\infty du\, \frac{4}{\sqrt{\pi}}\, u^2 \cdot e^{-u^2} \int_o^1 dx\, x\sqrt{1-x^2}\, 2 \cdot G(s, x, u) \qquad \text{(IX.23)}$$

with

$$G(s, x, u) = U(x>x_o) \cdot G_a(s, x, u) + U(x_o>x) \cdot G_b(s, x, u). \qquad \text{(IX. 24)}$$

These integrals have been evaluated numerically using the program (FORTRAN IV) discussed in Appendix A. This program calculates the thermal average F as a function of the normalized time s for the parameters $(nq_c - n'q'_c)$, n_e and T. The upper cutoff is given in units of the Debye length and the lower cutoff in units of the strong collision cutoff ρ_o of Eq. (IX. 5).

Before we discuss the methods for obtaining the Fourier transform of $\bar{F}(t)$ and the actual intensity profile, it is useful to derive the small and large time limit of $\bar{F}(t)$. The small time limit is determined by the integrals over Φ_1 and gives the asymptote of the thermal average for the static wing. The large time limit depends only on the Φ_4 integrals and yields the thermal average as required by the impact theory.

In the small time limit Φ_1 reduces to the form

$$\Phi_1(t, r)_{t\to 0} = \cos\left\{\frac{3}{2}(nq_c - n'q'_c)\frac{\hbar}{m}\frac{t}{r^2}\right\} - 1 \qquad \text{(IX. 25)}$$

where

$$r = \sqrt{\rho^2 + v^2 t_o^2} \quad . \qquad \text{(IX. 26)}$$

This expression depends only on the instantaneous distance r as expected in the static limit and the thermal average is therefore obtained immediately by the integral over r

$$\bar{F}(t)_{t\to 0} = 4\pi n_e \int_o^{r_c} r^2 \Phi_1(t, r)_{t\to 0}\, dr \quad . \qquad \text{(IX. 27)}$$

In the small time limit where $\frac{3}{2}(nq_c - n'q'_c)\frac{\hbar}{m}\cdot\frac{t}{r_c^2} \to 0$ we can then perform the integral with the result

$$\bar{F}(t)_{t\to 0} = -\frac{2}{3} n_e \left[3\pi(nq_c - n'q'_c)\frac{\hbar}{m} t\right]^{\frac{3}{2}} \qquad \text{(IX. 28)}$$

For the limit of large times of interaction we have to solve the integral

$$\bar{F}(t)_{t\to\infty} = 2\pi n_e \int_o^\infty dv\, vf(v) \int_{\rho_o}^D d\rho\, \rho\, t \cdot \Phi_4 \quad . \qquad \text{(IX. 29)}$$

For simplicity we set ρ_o equal to zero (for $\rho_o \neq 0$ see Appendix B). After a change of variables and a partial integration the integral can be rewritten as

$$\bar{F}(t)_{t\to\infty} = -2\pi n_e t D^2 v_{av} \int_o^\infty du \frac{4}{\sqrt{\pi}} u^2 e^{-u^2} C \int_o^\infty \frac{\sin\left(\frac{2C}{u} z\right)}{1 + z^2}\, dz \qquad \text{(IX. 30)}$$

The z-integral is known as Raabe's integral (see p. 144 of Bateman, 1953) and can be expressed in terms of exponential integrals. Furthermore, from Eq. (IX. 21) we realize that for most practical situations $C \ll 1$. Keeping only the leading term in C we have

$$\bar{F}(t)_{t\to\infty} = -4\sqrt{\pi} C^2 n_e D^2 v_{av} t \left[B - \ln(4C^2)\right] \qquad \text{(IX. 31)}$$

$$= -\left(\frac{3}{2}(nq_c - n'q'_c)\frac{\hbar}{m}\right)^2 n_e t \sqrt{\frac{8\pi m}{kT}} \left[B - \ln(4C^2)\right]$$

where

$$4C^2 = \frac{2\pi n_e}{m}\left(\frac{3(nq_c - n'q'_c)\hbar e}{kT}\right)^2 \quad \text{and} \quad B = 0.27 \qquad \text{(IX. 32)}$$

The large time limit of the thermal average in Eq. (IX. 31) is required for the calculation of the line center and all modern impact theories give the same result except for the additive constant B whose value depends on the particular cutoff procedure applied. Appendix B gives a summary of the different constants obtained in the literature which vary considerably. To what extent this uncertainty shows up in the final line profile depends on the value of the constant C. The influence will be small if $-\ln(4C^2)$ is considerably larger than the uncertainty in the additive constant B. Furthermore, the large time limit of the thermal average affects primarily the center of the line profile and its contribution vanishes when moving into the line wings.

Finally we show numerical results for $\overline{F}(t)$ as obtained by means of the program in Appendix A. Most of the calculations shown in this paper have been performed for the following electron density and temperature parameters.

case	$n_e[cm^{-3}]$	T_e [K]	experiment
A	$8.4 \cdot 10^{16}$	12200	G. Boldt and W. S. Cooper, 1964 (cascade arc)
B	$3.6 \cdot 10^{17}$	20400	R. C. Elton and H. R. Griem, 1964 (T-shock tube)
C	$1.3 \cdot 10^{13}$	1850	C. R. Vidal, 1964, 1965 (RF-discharge)

These parameters correspond to experiments which, as stated already in the introduction, have revealed the largest discrepancies between experiment and the modified impact theory. We will concentrate our attention on the high density case A and the low density case C, since case B is regarded as being less accurate because of lacking absolute intensity calibrations.

Figures 2 and 3 show the normalized thermal average $\overline{F}/\overline{F}_o$ as a function of the dimensionless variable $s = \tilde{\omega}_p . t$ for the cases A and C. Figure 3 shows the results for three different Stark components specified by the quantum numbers $n_k = nq_c - n'q'_c \cdot \overline{F}_o$ is the small time limit according to Eq. (IX.28) whose Fourier transform leads to the static wing. The dashed lines are obtained with a lower cutoff $\rho_{min} = \rho_o = \pi + n^2 a_o$. It can be seen that for case C the dashed curves get closer to the static limit $\overline{F}_o$ than for case A. In order to obtain the thermal average $\overline{F}$ for the limit $\rho_{min} \to 0$ the numerical calculations were finally performed with typically $\rho_{min} \simeq 0.01\ \rho_o$ so that $\overline{F}_{calc}$ and $\overline{F}_o$ differed less than about 0.1% over at least one order of magnitude in s. Far smaller values of s, where $\overline{F}_{calc}$ and $\overline{F}_o$ start to differ again, $\overline{F}_{calc}$ is then replaced by $\overline{F}_o$. In this manner we obtain the solid curves in Eqs. 2 and 3 which are used in the following.

It should be noted that these curves are calculated on the basis of the dipole approximation. It is clear that for impact parameters $\rho \lesssim n^2 a_o$ higher multipole terms have to be considered. Since the values s of interest are approximately given by $s \lesssim \tilde{\omega}_p / \Delta\omega$, one expects higher multipole terms to be less important the closer $\overline{F}_{calc}$ gets to $\overline{F}_o$ for $\rho_{min} = n^2 a_o$. This is consistent with the experimental fact that in case A an asymmetry of the line has been observed which cannot be explained within the dipole approximation, while in case C no asymmetry has been observed.

For large s Figs. 2 and 3 show the transition to $\overline{\overline{F}}_\infty$ as given in Eq. (IX. 31), which forms the basis for the familiar impact theories.

X. THE FOURIER TRANSFORM OF THE THERMAL AVERAGE

Having calculated the thermal average $\overline{\overline{F}}(t)$ we now focus our attention on the evaluation of its Fourier transform

$$i(\Delta\omega_R) = \frac{1}{\pi}\int_o^\infty \exp(i\Delta\omega_R s)\,\overline{\overline{F}}(s)\,ds \qquad (X.1)$$

as required by Eq. (V. 17) (see also Eq. (IV. 16))where the dimensionless variable

$$\Delta\omega_R = (\Delta\omega - \Delta\omega_i \cdot \beta)/\tilde{\omega}_p \qquad (X.2)$$

is the frequency separation from a particular Stark component (cf. Eq. (V. 14)) for an ion field strength β in units of the plasma frequency $\tilde{\omega}_p$.

The thermal average $\overline{\overline{F}}(s)$ does not immediately allow a straightforward Fourier transformation because for large s $\overline{\overline{F}}(s)$ is proportional to s according to Eq. (IX. 31), hence $i(\Delta\omega_R)$ diverges. This divergence is due to the fact that we neglected the finite lifetimes of the unperturbed states involved which naturally terminate the maximum time of interaction s. This may be taken care of by introducing a convergence factor $\exp(-\epsilon s)$ which can be obtained by replacing the delta function in the power spectrum of Eq. (3) in paper I by a narrow Lorentzian line with a natural width ϵ (E. Smith and Hooper, 1967). In the final line profile, however, natural line broadening is always negligible with respect to Stark broadening which allows us to set ϵ to zero without

affecting the shape of the profile. For this reason we will evaluate

$$i(\Delta\omega_R) = \lim_{\varepsilon \to 0} \frac{1}{\pi} \int_0^\infty e^{-\varepsilon s} e^{i\Delta\omega_R s} \bar{F}(s)\, ds \qquad (X.3)$$

$\bar{F}(s)$ is known numerically and there are many ways to perform the Fourier transform. In order to find the most convenient method we notice that according to Eqs. (IX.28) and (IX.31), $\bar{F}(s)$ has the following asymptotes

$$\text{for } s \to 0: \quad \bar{F}_o(s) = p_1 s^{3/2}$$

$$\text{and for } s \to \infty: \quad \bar{F}_\infty(s) = p_2 s\,, \qquad (X.4)$$

where

$$p_1 = -\frac{2}{3} n_e D^3 (2\pi C)^{3/2} \qquad (X.5)$$

and

$$p_2 = -4\sqrt{\pi}\, n_e D^3 C^2 \left[B - \ln(4C^2)\right]\,,$$

The transition from $\bar{F}_o$ to $\bar{F}_\infty$ is very smooth because the power in s changes only by 1/2 over the entire range. It has been found that $\bar{F}(s)$ may be approximated by a function $G(s)$ whose Fourier transform can be given analytically and whose parameters may be determined by a least square fit. The function $G(s)$ can be given in terms of the series

$$G(s) = \sum_k G_k(s)\,, \qquad (X.6)$$

where the number of terms in the series depends on the required

accuracy. As a first approximation Eq. (X. 4) suggests

$$G_1(s) = \frac{a_1 s^2}{\sqrt{s^2 + 2b_1 s}} \qquad (X.7)$$

with

$$a_1 = p_2 \qquad (X.8)$$

and

$$b_1 = \tfrac{1}{8}(p_2/p_1)^2$$

$G_1(s)$ has the small and large s behavior of $\overline{F}(s)$. It then turns out that

$$\text{for } s\to 0 \quad \overline{F}(s) - G_1(s) = p_3 s^{5/2}$$

$$\text{and for } s\to\infty \quad \overline{F}(s) - G_1(s) = p_4 \ , \qquad (X.9)$$

where p_3 and p_4 now have to be determined numerically. Consequently we take $G_2(s)$ to be

$$G_2(s) = \frac{a_2 s^5}{(s^2+2b_2 s)^{5/2}} \ . \qquad (X.10)$$

It then becomes apparent that $G_k(s)$ is given by

$$G_k(s) = \frac{a_k s^{3k-1}}{(s^2+2b_k s)^{2k-3/2}} \qquad (X.11)$$

with $a_k = p_{2k}$ and $b_k = \frac{1}{2}\,(p_{2k}/p_{2k-1})^{\frac{2}{4k-3}}$ (X.12)

such that one obtains

$$\text{for } s\to 0: \quad G(s) = \sum_{k=1}^{\infty} p_{2k-1}\, s^{k+\frac{1}{2}}$$

$$\text{and for } s\to\infty: \quad G(s) = \sum_{k=1}^{\infty} p_{2k}\cdot s^{2-k} \quad . \qquad \text{(X.13)}$$

In this manner the Fourier transform of any $G_k(s)$ can be expressed in terms of modified Bessel functions K_o and K_1. For all situations calculated it was found that $G_1(s)$ and $G_2(s)$ were sufficient to keep the deviation $\overline{F}(s)$-$G(s)$ smaller than 1% for all values of s. In some situations a fit better than 2% was obtained with $G_1(s)$ alone. As a further advantage it should be noted that this method tends to suppress "noise" introduced by the numerical evaluation of $\overline{F}(s)$.

In the following we evaluate the Fourier transform $i(k, \Delta\omega_R)$ of any $G_k(s)$ as defined by

$$i(k,\Delta\omega_R) = \lim_{\varepsilon\to 0} \frac{1}{\pi} \int_o^{\infty} e^{-\varepsilon s}\, e^{i\Delta\omega_R s}\, G_k(s)\, ds \qquad \text{(X.14)}$$

Their sum will then give us the desired Fourier transform $i(\Delta\omega_R)$. In particular we are interested in $i(k=1, \Delta\omega_R)$ and $i(k=2, \Delta\omega_R)$. We have

$$i_1(\wedge\omega_R) = i(k=1, \wedge\omega_R) = \lim_{\varepsilon\to 0} \frac{1}{\pi} \int_o^{\infty} e^{-\varepsilon s}\, e^{i\Delta\omega_R s}\, \frac{a_1 s^2}{\sqrt{s^2+2b_1 s}}\, ds$$

$$= a_1 \lim_{\varepsilon\to 0} \frac{1}{\pi} \frac{d^2}{d\varepsilon^2} \int_o^{\infty} \frac{e^{-\varepsilon s}\, e^{i\Delta\omega_R s}}{\sqrt{s^2+2b_1 s}}\, ds \qquad \text{(X.15)}$$

$$= a_1 \lim_{\varepsilon\to 0} \frac{1}{\pi} \frac{d^2}{d\varepsilon^2} \left\{ e^{b_1(\varepsilon - i\Delta\omega_R)}\, K_o\left[b_1(\varepsilon - i\wedge\omega_R)\right] \right\} \quad .$$

Introducing

$$Z_1 = b_1 \Delta\omega_R \tag{X.16}$$

one finally obtains

$$i_1(\Delta\omega_R) = a_1 \cdot b_1^2 \cdot e^{-iZ_1} \left\{ iH_o^{(1)}(Z_1) + H_1^{(1)}(Z_1) \left[1 - \frac{i}{2Z_1}\right]\right\}$$

$$= a_1 \cdot b_1^2 \ (\cos Z_1 - i \sin Z_1) \tag{X.17}$$

$$\left[\left(J_1(Z_1) - Y_o(Z_1) + \frac{Y_1(Z_1)}{2Z_1}\right) + i\left(J_o(Z_1) + Y_1(Z_1) - \frac{J_1(Z_1)}{2Z_1}\right)\right]$$

where $H_o^{(1)}$ and $H_1^{(1)}$ are Hankel functions and J_o, J_1, Y_o and Y_1 Bessel functions. These functions like all the other functions used in this report are consistent with the definitions as given, for example, by the NBS Handbook of Mathematical Functions (Abramowitz, 1969). For large arguments Z_1 it is also useful to have the asymptotic expansion

$$i_1(\Delta\omega_R) = -\frac{3}{8} \frac{a_1 \cdot b_1^2}{\sqrt{\pi Z_1}} \cdot \frac{1}{Z_1^2} \left\{1 + i + \frac{5}{8Z_1}(1-i) - \frac{3 \cdot 5 \cdot 7}{2 \cdot 8^2 Z_1^2}(1+i)\right.$$

$$\left. - \frac{9 \cdot 25 \cdot 7}{2 \cdot 8^3 Z_1^3}(1-i) + \frac{9 \cdot 25 \cdot 49 \cdot 11}{8^5 Z_1^4}(1+i) + - - \cdots \right\} \tag{X.18}$$

$$= -\frac{3}{8}\sqrt{\frac{2}{\pi}} p_1 \Delta\omega_R^{-5/2} \left\{1 + i + \frac{5}{4}\left(\frac{p_1}{p_2}\right)^2 \frac{(1-i)}{\Delta\omega_R} - \frac{105}{32}\left(\frac{p_1}{p_2}\right)^2 \frac{(1+i)}{\Delta\omega_R^2} - + + \cdots\right\}$$

Using Eq. (X.5) for p_1 the latter relation gives us exactly the Holtsmark $\Delta\lambda^{-5/2}$ wing for all Stark components

$$i_H(\Delta\omega_R) = \pi n_e D^3 C^{3/2} \cdot \Delta\omega_R^{-5/2} \quad . \tag{X.19}$$

In a similar way one derives

$$i_2(\Delta\omega_R) = i(k=2, \Delta\omega_R) = \lim_{\varepsilon\to 0} \frac{1}{\pi} \int_o^\infty e^{-\varepsilon s} e^{i\Delta\omega_R s} \frac{a_2 s^5}{(s^2+2b_2 s)^{5/2}} \, ds$$

$$= -\frac{a_2}{3} \lim_{\varepsilon\to 0} \frac{1}{\pi} \frac{d^3}{d\varepsilon^3} \frac{d^2}{db_2^2} \int_o^\infty \frac{e^{-\varepsilon s} e^{i\Delta\omega_R s}}{\sqrt{s^2 + 2b_2 s}} \, ds \quad . \tag{X.20}$$

With

$$Z_2 = b_2 \Delta\omega_R \tag{X.21}$$

one finally obtains

$$i_2(\Delta\omega_R) = \frac{a_2 b_2}{6} \cdot e^{-iZ_2} \left\{ H_o^{(1)}(Z_2)(i16Z_2^2 - 36Z_2 - i15) + H_1^{(1)}(Z_2)(16Z_2^2 + i28Z_2 - 3) \right\}$$

$$= \frac{a_2 b_2}{6} (\cos Z_2 - i \sin Z_2) \tag{X.22}$$

$$\left\{ \left[-36Z_2 J_o(Z_2) + J_1(Z_2)(16Z_2^2 - 3) - Y_o(Z_2)(16Z_2^2 - 15) - 28Z_2 Y_1(Z_2) \right] + i \left[J_o(Z_2)(16Z_2^2 - 15) + 28Z_2 J_1(Z_2) - 36Z_2 Y_o(Z_2) + Y_1(Z_2)(16Z_2^2 - 3) \right] \right\} .$$

The asymptotic expansion for large Z_2 is given by

$$i_2(\Delta\omega_R) = \frac{15}{64}\frac{a_2 b_2}{\sqrt{\pi}} Z_2^{-\frac{7}{2}}\left(1-i-\frac{35}{8Z_2}(1+i)-\frac{35\cdot 63}{128 Z_2^2}(1-i)+\cdots\right). \tag{X.23}$$

If one requires an even better fit of G(s) to $\bar{F}(s)$ the general transform $i(k, \Delta\omega_R)$ as defined in Eq. (X.14) is given by

$$i(k, \Delta\omega_R)$$

$$= \frac{4^{k-1}(2k-2)!}{(4k-4)!} a_k \lim_{\epsilon\to 0} \frac{1}{\pi}(-1)^{k+1}\frac{d^{k+1}}{d^{k+1}\epsilon}\frac{d^{2k-2}}{d^{2k-2}b_k}\left\{e^{b_k(\epsilon - i\Delta\omega_R)} K_o\left[b_k(\epsilon - i\Delta\omega_R)\right]\right\}. \tag{X.24}$$

Finally we want to show that this technique always gives the static wing according to Eq. (X.19) for large $\Delta\omega$. For this purpose one has to perform the Fourier transform of the small time limit of G(s) as given in Eq. (X.13).

$$i_\infty(\Delta\omega_R) = \lim_{\Delta\omega_R\to\infty} i(\Delta\omega_R) = \sum_{k=1}^{\infty} p_{2k-1} \lim_{\epsilon\to 0}\frac{1}{\pi}\int_o^\infty e^{-\epsilon s} e^{i\Delta\omega_R s} s^{k+\frac{1}{2}} ds$$

$$= \frac{1}{\sqrt{\pi}}\sum_{k=1}^{\infty}\frac{(2k+1)!}{2^{2k+1}k!} p_{2k-1}\exp\left[i\frac{\pi}{2}\left(\frac{3}{2}+k\right)\right]\Delta\omega_R^{-(k+\frac{3}{2})} \tag{X.25}$$

$$= \frac{3}{8}\sqrt{\frac{2}{\pi}}\frac{1}{\Delta\omega_R^{5/2}}\left\{-p_1(1+i)+\frac{5}{2}\frac{p_3}{\Delta\omega_R}(1-i)+\frac{5\cdot 7}{4}\frac{p_5}{\Delta\omega_R^2}(1+i)\right.$$

$$\left. -\frac{5\cdot 7\cdot 9}{8}\frac{p_7}{\Delta\omega_R^3}(1-i)-+\cdots\right\}.$$

One recognizes that the first two terms are identical with the first terms in the Eqs. (X. 18) and (X. 23). Hence, we always obtain the static wing for large $\Delta\omega_R$.

Another important property of $i(\Delta\omega_R)$ is that for small $\Delta\omega_R$ its leading terms in the expansion are

$$i_o(\Delta\omega_R) = \lim_{\Delta\omega_R \to 0} i(\Delta\omega_R) = -\frac{a_1}{\pi}\,\frac{1}{\Delta\omega_R^2} - i\,\frac{(a_1 b_1 - a_2)}{\pi\Delta\omega_R} + \cdots\cdots \qquad (X.26)$$

In this manner it smoothly goes over to the Lorentz profile of the unmodified impact theory.

Before discussing the numerical results of $i(\Delta\omega_R)$ we first list the constants a_k and b_k for the cases A, B and C as specified at the end of Sec. IX. a_1 and b_1 are determined from Eq. (X. 8), where p_1 is given by Eq. (X. 5) and p_2 is taken from the large time limit of the computed $\bar{F}(s)$. $p_{2\,\mathrm{comp.}}$ as calculated by the program of Appendix A may differ slightly from p_2 as defined in Eq. (X. 5), if C is not very much smaller than unity because $p_{2\,\mathrm{comp.}}$ is based on Eq. (A. 18), which is true for any value of C and goes over to Eq. (X. 5) for small C. a_2 and b_2 are determined numerically by a least squares fit. The maximum deviations from $\bar{F}(s)$ obtained with $G_1(s)$ alone and with $G_1(s) + G_2(s)$ are listed too.

Table 1. Numerical constants for the experimental cases, A, B, and C.

case	A $n_e = 8.4 \cdot 10^{16} cm^{-3}$ $T_e = 12200$ K $n_k = 2$	B $n_e = 3.6 \cdot 10^{17} cm^{-3}$ $T_t = 20400$ K $n_k = 2$	C $n_e = 1.3 \cdot 10^{13} cm^{-3}$ $T_e = 1850$ K $n_k = 3$	 $n_k = 16$	 $n_k = 90$
C	0.02169	0.02685	0.002669	0.01423	0.08006
p_1	-0.05124	-0.07373	-0.01050	-0.1293	-1.725
p_2	-0.03335	-0.04990	$-3.932 \cdot 10^{-3}$	-0.07696	-1.296
$a_1 = p_2$ comp.	-0.03340	-0.05003	$-3.932 \cdot 10^{-3}$	-0.07701	-1.323
b_1	0.2125	0.2303	0.07011	0.1773	0.2941
$\lvert(\bar{F}-G_1)/\bar{F}\rvert$	< 0.026	<0.034	<0.13	< 0.012	< 0.068
a_2	$-3.95 \cdot 10^{-3}$	$-6.57 \cdot 10^{-3}$	$2.38 \cdot 10^{-4}$	$-9.92 \cdot 10^{-3}$	- 0.355
b_2	0.539	0.449	0.0664	1.54	0.477
$\lvert(\bar{F}-G_1-G_2)/\bar{F}\rvert$	<0.004	<0.003	<0.009	< 0.013	< 0.013

In presenting the numerical results of $i(\Delta\omega_R)$ we concentrate on the real part which turns out to be the most important part. We have chosen two different normalizations. In Figs. 4 and 5, $i(\Delta\omega_R)$ is normalized with respect to the large frequency limit $i_\infty(\Delta\omega_R)$ to show the useful range of the static theory. The short vertical lines mark the position of the Weiskopf frequency

$$\Delta\omega_c = v_{av}^2 \Big/ \left(\frac{3}{2}(nq_c - n'q_c')\frac{\hbar}{m}\right) = \tilde{\omega}_p/C \qquad (X.27)$$

for a particular component $(nq_c - n'q_c')$ which according to classical arguments determines roughly the range of validity for the static theory (see p. 321 of Unsöld, 1955 and paper II). It should be pointed out that $\Delta\omega_c$ is usually defined in terms of an average Stark splitting. In both cases A and C $\Delta\omega_c$ describes the range of the static theory very well. If one allows for a deviation of about 10% at the most from the static asymptote, $\Delta\omega_c$ may be lowered effectively by more than an order of magnitude. A more detailed discussion is given later with the final line profile calculations.

The other normalization with respect to the small frequency limit $i_o(\Delta\omega_R)$ is shown in Figs. 6 and 7 for cases A and C again. These plots demonstrate the useful range of the unmodified impact theory, which is based on $i_o(\Delta\omega_R)$ and is expected to break down around the plasma frequency, as can be seen in Figs. 6 and 7. In order to extend the range of validity, the modified impact theory makes an impact parameter cutoff at $v/\Delta\omega$ (the Lewis cutoff) whenever this is smaller than the Debye length D; this cutoff accounts for the finite time of interaction to second order. More details are given in Appendix B. The corresponding function $i_{Lewis}(\Delta\omega_R)$ has been included in Figs. 6 and 7. Since the usual derivation of $i_{Lewis}(\Delta\omega_R)$ is based on the limit of very small C, one expects the best agreement between the Lewis result and our result, which considers the finite time of interaction to all orders, for the

situation with the smallest C. That this is in fact true can be seen from the low density case with $nq_c - n'q'_c = 3$. This component is plotted again in Fig. 8, in order to demonstrate the importance of $G_2(s)$ for those cases where the deviation of $G_1(s)$ from $\overline{F}(s)$ is large (Table I gives a maximum deviation of 13%).

Figures 6 and 7 also contain the static limit $i_\infty(\Delta\omega_R)$ (dashed lines) and the Weiskopf frequency $\Delta\omega_c$. It gives an idea how close the Lewis results get to the static limit. One notices that with increasing values of C the deviation of $i_{Lewis}(\Delta\omega_R)$ from the static limit becomes larger. In his line wing calculations (Griem, 1962, 1967a) Griem adjusts his "strong collision term" $E_{\beta\beta}$, in such a manner that the Lewis result is identical with the static limit at the Weiskopf frequency. In the Figs. 6 and 7 this means that the straight line representing $i_{Lewis}(\Delta\omega_R)$ is shifted to the right until it cuts $\Delta\omega_c$. We use here $\Delta\omega_c$ as defined in Eq. (X.27) for every individual component instead of the average value $\Delta\omega_c = kT/(\hbar n^2)$ used by Griem. Since the Lewis line would then lie appreciably above the curve $i(\Delta\omega_R)$ one realizes that this procedure definitely overestimates the electron broadening as already observed experimentally (Vidal, 1965; see also Pfennig, Trefftz and Vidal, 1966). A better method would have been to adjust $E_{\beta\beta}$, such that $i_{Lewis}(\Delta\omega_R)$ forms a tangent of the static limit. However, it is clear that any adjustment of $E_{\beta\beta}$, effectively changes the range of the unmodified impact theory and also defeats the purpose of the Lewis cutoff, namely to correct the completed collision assumption to second order.

Finally it ought to be emphasized again that except for the time ordering the Fourier transform of the thermal average $i(\Delta\omega_R)$ as presented here takes into account the finite time of interaction to all orders. Hence, for small $\Delta\omega_R$ it goes over to the impact theory limit and for large $\Delta\omega_R$ it gives the static limit without requiring a Lewis cutoff.

XI. THE ONE-ELECTRON LIMIT FOR HYDROGEN AND THE ASYMPTOTIC WING EXPANSION

Having obtained the Fourier transform of the thermal average $i(\Delta\omega_R)$ we are now prepared to calculate the actual line intensity by evaluating $I(\omega, \mathcal{E}_i)$ according to Eq. (IV. 15) and averaging it over all ion fields according to Eq. (II. 1). As explained in Sec. IV. this problem is greatly simplified in the one electron limit where no matrix inversion is required and the intensity $I(\Delta\omega)$ is given by

$$I(\Delta\omega) = I_i(\Delta\omega) + \int_0^\infty P(\beta)\, I(\Delta\omega, \beta)\, d\beta \quad . \tag{XI. 1}$$

$I_i(\Delta\omega)$ is the static ion contribution originating from the first term $1/\Delta\omega_{op}$ in Eq. (IV. 21) and $I(\Delta\omega, \beta)$ is given by

$$I(\Delta\omega, \beta) = \frac{Re}{\pi} \sum \langle n q_a m_a | d | n' q_a' m_a' \rangle \langle n' q_b' m_b' | d | n q_b m_b \rangle$$

$$\int dt \exp\left\{ i\Delta\omega_R t \right\} \langle n' q_b' m_b'; n q_b m_b | \bar{\mathfrak{F}}^{(1)}(t) | n' q_a' m_a'; n q_a m_a \rangle \tag{XI. 2}$$

using the definitions of Eqs. (V. 14) and (X. 2). The density matrix ρ_a is assumed to be constant over the relevant initial states. With Eq. (IX. 1) the last expression can be rewritten as

$$I(\Delta\omega, \beta) = \sum \langle n \ell_a m_a | d | n' \ell_a' m_a' \rangle \langle n' q_b' m_b' | n' \ell_c' m_b' \rangle \langle n' \ell_c' m_b' | d | n \ell_c m_b \rangle$$

$$\langle n \ell_c m_b | n q_b m_b \rangle \langle n' \ell_a' m_c' | n' q_c' m_c' \rangle \langle n' q_c' m_c' | n' \ell_b' m_c' \rangle \langle n' \ell_b' m_b' | n' q_b' m_b' \rangle$$

$$\langle n q_b m_b | n \ell_b m_b \rangle \langle n \ell_b m_c | n q_c m_c \rangle \langle n q_c m_c | n \ell_a m_c \rangle \, (-1)^{-m_a - m_b} (2L+1)$$

$$\begin{pmatrix} \ell_a' & \ell_a & L \\ -m_c' & m_c & M \end{pmatrix} \begin{pmatrix} \ell_a' & \ell_a & L \\ -m_a' & m_a & M \end{pmatrix} \begin{pmatrix} \ell_b' & \ell_b & L \\ -m_c' & m_c & M \end{pmatrix} \begin{pmatrix} \ell_b' & \ell_b & L \\ -m_b' & m_b & M \end{pmatrix} i(\Delta\omega_R, \beta, n, n', q_b, q_b', q_c, q_c') \tag{XI. 3}$$

where the dipole matrix elements have been transformed from parabolic to spherical states and the summation over intermediate states $|nq_a m_a\rangle$ and $|n'q_a' m_a'\rangle$ has been performed. We next apply the Wigner Eckart theorem (see Eq. (5.4.1) of Edmonds, 1960) to the dipole matrix elements and replace the reduced matrix elements by the corresponding radial matrix elements (see Bethe and Salpeter 1957).

$$\langle n\ell m|d_\mu|n'\ell'm'\rangle = (-1)^{-m}\sqrt{(2\ell+1)(2\ell'+1)}\begin{pmatrix}\ell & 1 & \ell'\\ -m & \mu & m'\end{pmatrix}\begin{pmatrix}\ell & 1 & \ell'\\ 0 & 0 & 0\end{pmatrix}\langle n\ell|r|n'\ell'\rangle \qquad \text{(XI. 4)}$$

Inserting this relation into Eq. (XI. 3) and using the orthogonality properties of the 3j-symbols we have

$$I(\Delta\omega,\beta) = \sum \langle n'q_b'm_b'|n'\ell_c'm_b'\rangle\langle n\ell_c m_b|nq_b m_b\rangle\langle n'\ell_a'm_c'|n'q_c'm_c'\rangle$$

$$\langle n'q_c'm_c'|n'\ell_b'm_c'\rangle\langle n'\ell_b'm_b'|n'q_b'm_b'\rangle\langle nq_b m_b|n\ell_b m_b\rangle\langle n\ell_b m_c|nq_c m_c\rangle$$

$$\langle nq_c m_c|n\ell_a m_c\rangle\left[(2\ell_a+1)(2\ell_a'+1)(2\ell_c+1)(2\ell_c'+1)\right]^{\frac{1}{2}}\langle n\ell_a|r|n'\ell_a'\rangle\langle n'\ell_c'|r|n\ell_c\rangle$$

$$\begin{pmatrix}\ell_a' & \ell_a & 1\\ 0 & 0 & 0\end{pmatrix}\begin{pmatrix}\ell_c' & \ell_c & 1\\ 0 & 0 & 0\end{pmatrix}\begin{pmatrix}\ell_a' & \ell_a & 1\\ -m_c' & m_c & M'\end{pmatrix}\begin{pmatrix}\ell_b' & \ell_b & 1\\ -m_c' & m_c & M'\end{pmatrix}\begin{pmatrix}\ell_b' & \ell_b & 1\\ -m_b' & m_b & M\end{pmatrix}\begin{pmatrix}\ell_c' & \ell_c & 1\\ -m_b' & m_b & M\end{pmatrix}$$

$$i(\Delta\omega_R,\beta,n,n',q_b,q_b',q_c,q_c') \qquad \text{(XI. 5)}$$

If we finally replace the unitary transformation by the corresponding 3j-symbols according to Eq. (VIII. 8) the result is

$$I(\Delta\omega, \beta) = \sum (2\ell_a+1)(2\ell_a'+1)(2\ell_b+1)(2\ell_b'+1)(2\ell_c+1)(2\ell_c'+1)$$

$$\begin{pmatrix} \ell_a' & \ell_a & 1 \\ 0 & 0 & 0 \end{pmatrix} \begin{pmatrix} \ell_c' & \ell_c & 1 \\ 0 & 0 & 0 \end{pmatrix} \begin{pmatrix} \ell_a' & \ell_a & 1 \\ -m_c' & m_c & M' \end{pmatrix} \begin{pmatrix} \ell_b' & \ell_b & 1 \\ -m_c' & m_c & M' \end{pmatrix} \begin{pmatrix} \ell_b' & \ell_b & 1 \\ -m_b' & m_b & M \end{pmatrix} \begin{pmatrix} \ell_c' & \ell_c & 1 \\ -m_b' & m_b & M \end{pmatrix}$$

$$\begin{pmatrix} \frac{n-1}{2} & \frac{n-1}{2} & \ell_b \\ \frac{m_b-q_b}{2} & \frac{m_b+q_b}{2} & -m_b \end{pmatrix} \begin{pmatrix} \frac{n-1}{2} & \frac{n-1}{2} & \ell_c \\ \frac{m_b-q_b}{2} & \frac{m_b+q_b}{2} & -m_b \end{pmatrix} \begin{pmatrix} \frac{n-1}{2} & \frac{n+1}{2} & \ell_a \\ \frac{m_c-q_c}{2} & \frac{m_c+q_c}{2} & -m_c \end{pmatrix}$$

$$\begin{pmatrix} \frac{n-1}{2} & \frac{n-1}{2} & \ell_b \\ \frac{m_c-q_c}{2} & \frac{m_c+q_c}{2} & -m_c \end{pmatrix} \begin{pmatrix} \frac{n'-1}{2} & \frac{n'-1}{2} & \ell_b' \\ \frac{m_b'-q_b'}{2} & \frac{m_b'+q_b'}{2} & -m_b' \end{pmatrix} \begin{pmatrix} \frac{n'-1}{2} & \frac{n'-1}{2} & \ell_c' \\ \frac{m_b'-q_b'}{2} & \frac{m_b'+q_b'}{2} & -m_b' \end{pmatrix}$$

$$\begin{pmatrix} \frac{n'-1}{2} & \frac{n'-1}{2} & \ell_a' \\ \frac{m_c'-q_c'}{2} & \frac{m_c'+q_c'}{2} & -m_c' \end{pmatrix} \begin{pmatrix} \frac{n'-1}{2} & \frac{n'-1}{2} & \ell_b' \\ \frac{m_c'-q_c'}{2} & \frac{m_c'+q_c'}{2} & -m_c' \end{pmatrix} \langle n\ell_a | r | n'\ell_a' \rangle \langle n'\ell_c' | r | n\ell_c \rangle$$

$$i(\Delta\omega_R, \beta, n, n', q_b, q_b', q_c, q_c') \qquad \text{(XI. 6)}$$

The preceding relations hold for the general case of upper and lower state interactions. They simplify considerably if there is no lower state interaction (e.g., Lyman lines). Then one obtains

$$I_u(\Delta\omega,\beta) = |\langle n1|r|10\rangle|^2 \sum_{\substack{m_b, m_c \\ q_b, q_c}} \begin{pmatrix} \frac{n-1}{2} & \frac{n-1}{2} & 1 \\ \frac{m_b-q_b}{2} & \frac{m_b+q_b}{2} & -m_b \end{pmatrix}^2 \begin{pmatrix} \frac{n-1}{2} & \frac{n-1}{2} & 1 \\ \frac{m_c-q_c}{2} & \frac{m_c+q_c}{2} & -m_c \end{pmatrix}^2 i_u(\Delta\omega_R, \beta, n, q_b, q_c) \qquad \text{(XI. 7)}$$

with

$$i_u(\Delta\omega_R, \beta, n, q_b, q_c) = i(\Delta\omega_R, \beta, n, n' = 1,\ q_b, q_b' = 0,\ q_c, q_c' = 0). \qquad \text{(XI. 8)}$$

Equation (XI. 7) may be further simplified by evaluating the 3j-symbols and summing over m_b and m_c with the result.

$$I_u(\Delta\omega,\beta) = \frac{|\langle n1|r|10\rangle|^2}{4(n^2-1)^2 n^2} \sum_{q_b=-(n-1)}^{n-1} \left[n^2 + (-1)^{q_b+n} (n^2 - 2q_b^2) \right]$$

$$\times \sum_{q_c=-(n-1)}^{n-1} \left[n^2 + (-1)^{q_c+n} (n^2 - 2q_c^2) \right] i_u(\Delta\omega_R, \beta, n, q_b, q_c) \qquad \text{(XI. 9)}$$

These simplified relations may also be used for the higher series members of the other series, whose transitions do not end on the ground state if lower state interactions contribute only a negligible amount of broadening to the final line profile.

The foregoing relations for the one electron limit essentially represent the asymptotic expression for the intensity in the line wings. If one is interested in frequency perturbations $\Delta\omega$ which are significantly larger than the average ion field splitting Eq. (XI. 1) can be simplified by replacing the ion field average of the electron contribution by the electron contribution for the average ion field β_{av}

$$I(\Delta\omega) = I_i(\Delta\omega) + I(\Delta\omega, \beta_{av}) \qquad \text{(XI. 10)}$$

with

$$\beta_{av} = \int_0^\infty \beta W(\beta)\, d\beta \,. \qquad \text{(XI. 11)}$$

If $\Delta\omega$ is very much larger than the average ion field splitting, then according to Eq. (X. 2) $\Delta\omega_R \simeq \Delta\omega/\tilde{\omega}_p$ and $I(\Delta\omega, \beta_{av})$ may be replaced by $I(\Delta\omega, \beta = 0)$.

$$I(\Delta\omega) = I_i(\Delta\omega) + I(\Delta\omega, \beta = 0) \qquad \text{(XI. 12)}$$

In the limit $\beta \to 0$ the Eqs. (XI. 5) to (XI. 9) simplify drastically because $i(\Delta\omega_R)$ depends no longer on the quantum numbers q_b and q_b' which specify the Stark components shifted by the quasistatic ion fields. This allows us to sum in Eq. (XI. 7) over q_b and m_b which gives us for the case of no lower state interaction

$$I_u(\Delta\omega, \beta=0) = |\langle nl|r|10\rangle|^2 \sum_{qm} \begin{pmatrix} \frac{n-1}{2} & \frac{n-1}{2} & 1 \\ \frac{m-q}{2} & \frac{m+q}{2} & m \end{pmatrix}^2 i_u(\Delta\omega, \beta=0, n, q)$$

(XI. 13)

$$= \frac{|\langle nl|r|10\rangle|^2}{2(n^2-1)\,n} \sum_{q=-(n-1)}^{(n-1)} \left(n^2+(-1)^{q+n}\,(n^2-2q^2)\right) i_u(\Delta\omega, \beta=0, n, q)$$

For the general case of upper and lower state interaction we can sum in Eq. (XI. 6) over q_b, q_b', m_b, m_b' and M and after applying Eq. (XI. 4) we finally sum over the intermediate spherical states to obtain

$$I(\Delta\omega, \beta=0) = \sum_{\substack{q, q' \\ m, m'}} |\langle nqm|d|n'q'm'\rangle|^2 \, i\,(\Delta\omega, \beta=0,\ n,\ n',\ q,\ q') \ . \tag{XI. 14}$$

How far into the line center the simplified relations (XI. 10) and (XI. 12) may be used, depends on the required accuracy. Numerical results, which compare the asymptotic wing expansions with the more rigorous unified theory calculations describing the entire line profile, are given at the end of the next section.

XII. THE UNIFIED THEORY FOR HYDROGEN

In those cases, where the entire line profile including the line center is required, the line intensities have to be calculated on the basis of the unified theory. It has to be pointed out that in principal even in calculating the distant line wings the unified theory has to be used whenever $\Delta\omega_R$ in Eqs. (X. 1) or (V. 17) is no longer large compared to unity. This will happen in the final integration over ion fields whenever β is close to

$$\beta_c = \Delta\omega/\Delta\omega_i\,(n,\ q_b,\ n,'\ q_b') \ . \tag{XII. 1}$$

However, it was shown in the last section, that for large $\Delta\omega$ one may use one of the asymptotic expansions in Eq. (XI. 10) and (XI. 12).

In the unified theory we have to evaluate the following expression

$$I(\Delta\omega, \beta) = \frac{\mathrm{Im}}{\pi} \sum \langle nq_a m_a | d | n'q_a' m_a' \rangle \langle n'q_b' m_b' | d | nq_b m_b \rangle \tag{XII. 2}$$

$$\langle n'q_b' m_b'; nq_b m_b | \left[\Lambda\omega_{op} - \mathcal{L}(\Delta\omega_{op}) \right]^{-1} | n'q_a' m_a'; nq_a m_a \rangle .$$

The matrix elements of $\Delta\omega_{op}$ as defined in Eq. (IV. 14) are diagonal in parabolic states and are given by

$$\langle n'q_a' m_a'; nq_a m_a | \Delta\omega_{op} | n'q_a' m_a'; nq_a m_a \rangle = \Delta\omega - \Delta\omega_i(n, q_a, n', q_a') \beta \tag{XII. 3}$$

where $\Delta\omega_i$ is defined in Eq. (V. 14). The matrix elements of $\mathcal{L}(\Delta\omega_{op})$ are given by

$$\langle n'q_b' m_b'; nq_b m_b | \mathcal{L}(\Delta\omega_{op}) | nq_a' m_a'; nq_a m_a \rangle =$$

$$-i\pi \cdot (-1)^{-m_a - m_b} \left[\Delta\omega - \Delta\omega_i(n, q_b, n', q_b') \beta \right]^2 \sum (2L + 1)$$

$$\langle n'q_a' m_a' | n'\ell_a' m_a' \rangle \langle n'\ell_a' m_c' | n'q_c' m_c' \rangle \langle n'q_c' m_c' | n'\ell_b' m_c' \rangle \langle n'\ell_b' m_b' | n'q_b' m_b' \rangle$$

$$\langle nq_a m_a | n\ell_a m_a \rangle \langle n\ell_a m_c | nq_c m_c \rangle \langle nq_c m_c | n\ell_b m_c \rangle \langle n\ell_b m_b | nq_b m_b \rangle$$

$$\begin{pmatrix} \ell_a' & \ell_a & L \\ -m_c' & m_c & M' \end{pmatrix} \begin{pmatrix} \ell_a' & \ell_a & L \\ -m_a' & m_a & M \end{pmatrix} \begin{pmatrix} \ell_b' & \ell_b & L \\ -m_c' & m_c & M' \end{pmatrix} \begin{pmatrix} \ell_b' & \ell_b & L \\ -m_b' & m_b & M \end{pmatrix} i\left(\Delta\omega_R, \beta, n, n', q_b, q_b', q_c, q \right. \tag{XII. 4}$$

Eqs. (IV.16), (IX.1) and (X.1). This relation simplifies significantly in case of no lower state interaction in which case we need the matrix elements

$$\langle nq_b m_b | \mathfrak{L}(\Delta\omega_{op}) | nq_a m_a \rangle = - i\pi \left[\Delta\omega - \Delta\omega_i(n, q_b)\, \beta \right]^2$$

$$\sum_{\ell_a, q_c, m_c} \frac{\delta_{m_a m_b}}{2\ell_a+1} \langle nq_b m_b | n\ell_a m_a \rangle \langle n\ell_a m_a | nq_a m_a \rangle \left[\langle n\ell_a m_c | nq_c m_c \rangle \right]^2$$

$$i_u(\Delta\omega_R, \beta, n, q_b, q_c) \ . \qquad \text{(XII. 5)}$$

Due to the delta function the matrix of the operator $\mathfrak{L}$ is then block diagonal in m, which reduces the size of the matrices to be inverted to n × n or (n-1) × (n-1) depending on the quantum numbers n and m. Furthermore, Eq. (XII.2) simplifies in case of no lower state interaction. After transforming the dipole matrix elements from parabolic to spherical states, applying the Wigner-Eckart theorem (see Eq. (XI.4)) and using Eq. (VIII.8) one obtains

$$I(\Delta\omega, \beta) = |\langle n1 | r | 10 \rangle|^2 \sum_{q_a, q_b, m} (-1)^{n+m-1-\frac{q_a+q_b}{2}} \begin{pmatrix} \frac{n-1}{2} & \frac{n-1}{2} & 1 \\ \frac{m-q_a}{2} & \frac{m+q_a}{2} & -m \end{pmatrix}$$

$$\begin{pmatrix} \frac{n-1}{2} & \frac{n-1}{2} & 1 \\ \frac{m-q_b}{2} & \frac{m+q_b}{2} & -m \end{pmatrix} \frac{\mathrm{Im}}{\pi} \langle nq_b m | \left[\Delta\omega_{op} - \mathfrak{L}(\Delta\omega_{op}) \right]^{-1} | nq_a m \rangle \ . \qquad \text{(XII. 6)}$$

In order to keep the mathematics simpler we concentrate in the following on the case of no lower state interaction, because it covers the experimental situations of case A and B and is also a good approximation to the higher Balmer lines of case C (see the list of references at the

end of Sec. IX). Including lower state interactions means at this stage only a more extensive summation over 3j-symbols because the crucial function $i(\Delta\omega_R, \beta)$, the Fourier transform of the thermal average, has already been evaluated for the general case of upper and lower state interactions.

Using the unitary transformation of Eq. (VIII. 8), Eq. (XII. 5) may be rewritten as

$$\langle nq_b m | \mathcal{L}(\Delta\omega_{op}) | nq_a m \rangle = - i\pi(-1)^{n+m-1-\frac{q_a+q_b}{2}}$$

$$\left[\Delta\omega - \Delta\omega_i(n, q_b)\,\beta\right] \sum_{\ell_a}^{2} (2\ell_a+1) \begin{pmatrix} \frac{n-1}{2} & \frac{n-1}{2} & \ell_a \\ \frac{m-q_a}{2} & \frac{m+q_a}{2} & -m \end{pmatrix} \begin{pmatrix} \frac{n-1}{2} & \frac{n-1}{2} & \ell_a \\ \frac{m-q_b}{2} & \frac{m+q_b}{2} & -m \end{pmatrix}$$

$$2 \sum_{q_c > 0} i_u(\Delta\omega_R, \beta, n, q_b, q_c) \sum_{m_c} \begin{pmatrix} \frac{n-1}{2} & \frac{n-1}{2} & \ell_a \\ \frac{m_c-q_c}{2} & \frac{m_c+q_c}{2} & -m_c \end{pmatrix}^2 \qquad \text{(XII. 7)}$$

where we have used the fact that $i_u(\Delta\omega_R, \beta, n, q_b, q_c) = i_u(\Delta\omega_R, \beta, n, q_b, -q_c)$ and that $i_u(\Delta\omega_R, \beta, n, q_b, q_c = 0) = 0$. We also realize that

$$\langle nq_b - m | \mathcal{L}(\Delta\omega_{op}) | nq_a - m \rangle = \langle nq_b m | \mathcal{L}(\Delta\omega_{op}) | nq_a m \rangle \qquad \text{(XII. 8)}$$

A computer program (FORTRAN IV), which evaluates $I(\Delta\omega, \beta)$ according to Eqs. (XII. 6) and (XII. 7) and also performs the final ion field average according to Eq. (II. 1) is presented in Appendix C. The ion microfield

distribution function employed is the one given by Hooper, 1968a, 1968b, which differs less than about 1% from the values determined independently by Pfennig and Trefftz, 1966.

For the experimental parameters of case C, Figs. 9 and 10 show numerical results of $I(\Delta\omega, \beta = 10)$ for $n = 6$ and $n = 10$. The fat vertical lines indicate the relative intensities and the positions of the Stark components for the static field (ion field) $\beta = 10$ and it demonstrates the electron broadening.

Figures 11 to 13 show the final line profiles $I(\Delta\omega)$ after performing the ion field average for the experimental cases A, B and C (see end of Sec. IX). As a first result it turns out that for numerical accuracies of about 2% it is in all 3 cases sufficient to consider only $G_1(t)$ meaning that $i(\Delta\omega_R, \beta, n, q_b, q_c)$ may be replaced by $i_1(\Delta\omega_R, \beta, n, q_b, q_c)$ as given in Eq. (X. 17). Although according to Table I, $G_1(t)$ may differ from $\overline{F}(t)$ for some components of case C by up to 13%, it turns out that after summing over all Stark components and averaging over ion fields this difference $\overline{F}(t) - G_1(t)$ is apparently smeared out over the entire line profile and affects the final line profile by not more than about 2%. This is very convenient for practical calculations, because it no longer requires an extensive evaluation of the thermal average anymore, but for most practical situations it is sufficient to calculate the line intensities directly on the basis of $G_1(t)$ whose specifying constants a_1 and b_1 are given immediately by the Eqs. (X. 8) and (X. 5).

This is even more true in view of the fact that the final line profile is partially affected by an uncertainty in the constant B as defined in Eq. (IX. 31) or (B. 19). As summarized in Table II of

Appendix B its actual value depends on the cutoff procedure applied, a problem, which has not yet been solved satisfactorily. The upper cutoff parameter $a = \rho_{max}/D$ (see Appendix B) and therefore also the limits on the integral $\int PV_c(t')\,dt'$ can in principal be decided within the frame work of the classical path theory (see also Chappell, J. Cooper and E. Smith, 1969). The lower cutoff parameter, however, which essentially replaces the dynamic strong collisions not amenable in a classical path theory, can only be determined conclusively from a quantum mechanical theory which is also able to handle strong collisions and which does not yet exist. The constant B adopted here is based on a lower cutoff parameter $\rho_{min} = \varkappa + \frac{3}{2} n^2 a_o$, which specifies approximately the region of validity for the classical path theories (see paper I). Numerical results based on other values for the constant B as used in the literature (see summary of Appendix B) are also included in Figs. 11 and 12 for the cases A and B. The largest value B = 1.27 is the one adopted in the recent calculations of Kepple and Griem, 1968, while the smallest value of B is obtained for $\rho_{min} = \varkappa + \frac{3}{2} n^2 a_o$ and choosing an upper cutoff of $\rho_{max} = 0.606D$ as proposed by Chappell, J. Cooper and E. Smith, 1969. For case C this variation of the constant B does not show up in Fig. 13 and amounts to an intensity change of at the most about 4%. These variations indicate the reliability of the classical path theories and demonstrate that for some cases the error estimates given in the literature are too optimistic. The effect on the final line profile due to the uncertainty of the constant B will be small if either according to Eq. (IX. 31)

$$-2 \ln (2C) \gg 1 \qquad \text{(XII. 9)}$$

or if (like for the higher series members) the number of Stark components is large which tends to smear out the influence of the constant B. It should be pointed out again that the unified theory is intrinsicly normalized independent of the value of the specifying constants of a particular line. Hence, any variation of the constant B does not affect the normalization of the line profile.

In comparing the numerical results for case C, with the experiment it has to be kept in mind that we are comparing the higher Balmer lines with calculations for the higher Lyman lines, because our final line profile calculations have not yet taken into account lower state interactions. This means that in a plot of the intensity versus the wavenumbers $\Delta\tilde{\nu}$, which is essentially an energy scale, the line profiles cannot be expected to coincide because of the difference in the Stark effect. This gives rise to different static wings as explained in detail by Vidal, 1965. Hence, we have to rescale the Lyman profiles preserving normalization in order to be able to compare the measured profiles of the Balmer lines with the calculated profiles of the Lyman lines. This means that in a plot of log I versus log $\Delta\tilde{\nu}$ we can compare the line shape of the corresponding lines directly. The agreement is remarkable. For the higher lines, $n \geq 8$, where Doppler broadening was shown to be negligible and where lower state interactions no longer affect the line shape noticeably, the agreement is better than 2% over the entire measured line profile, which for $n = 8$ extends over 3 orders of magnitude in intensity. In particular, the calculations show also the surprisingly large range of the $\Delta\omega^{-5/2}$- wing, which extends to 1/10 of the maximum intensity. This fact is not explainable by a purely static theory considering also shielding effects. For the lower lines the calculated profiles have to be folded into a Doppler profile in order to achieve similarly good agreement. For the lower line we

also expect in the line center some influence due to lower state interactions on the line shape, which is partially removed again by Doppler broadening.

A more detailed study of the $\Delta\omega^{-5/2}$-wings reveals some other interesting facts. In Fig. 13, the dashed lines indicate the asymptotic $\Delta\omega^{-5/2}$-wings; except for n = 5 and n = 6, what appears to be a $\Delta\omega^{-5/2}$-wing in the measurements and calculations is not the asymptotic Holtsmark $\Delta\omega^{-5/2}$-wing in the region of interest. If one extends the calculations to even larger frequencies $\Delta\omega$, all the wings will eventually coincide with their asymptotic limit. In the paper of Vidal, 1965, Table II gives a list of the electron densities, which were evaluated under the erroneous assumption that the measured $\Delta\omega^{-5/2}$-wing was the asymptotic Holtsmark wing; it was stated that for H_4 to H_{14} the electron densities coincide within ± 4%. A more careful analysis of the values, which have been plotted again in Fig. 14 reveals a systematic trend. For large and very small principal quantum numbers the electron density values rise above the average value, while the minimum value was obtained for n = 7. From Fig. 13, it now becomes apparent that the electron densities based on the asymptotic Holtsmark wing will go up for increasing n. For smaller n the quantum number dependence of the electron density is masked by Doppler broadening which raises the wings again and explains the increasing values of electron density for small n. Another important result can be seen from Fig. 13. For small principal quantum numbers the line intensities are much smaller than predicted by a quasistatic theory. This was observed first by Schlüter and Avila, 1966 and the effective electron densities for a quasistatic theory as a function of $\Delta\lambda$ show the qualitative behavior measured by them after unfolding the

Doppler broadening. This observation together with the measurements of Boldt and Cooper, 1964, suggested the semiemperical procedure proposed by Edmonds, Schlüter and Wells, 1967. A detailed quantitative comparison requires for the first series members a consideration of lower state interactions, which is in process.

For the parameters of case C, Kepple and Griem, 1968, have already calculated the lines H_6 and H_7. These calculations have been extended to H_{12} by Bengtson, Kepple and Tannich, 1969, using identically the same computer program. The results are plotted in Fig. 15 and comparing the line shape for the higher series members, for which lower state interaction becomes negligible, with our results in Fig. 13 one realizes a significant difference. In particular, their calculations do not reveal the $\Delta\lambda^{-5/2}$ decay in the near line wing for intensities smaller than about 1/10 of the maximum intensity at $\Delta\omega = 0$ which is discussed above. It should be pointed out that the ion field dependent cutoff, which has been introduced by Kepple and Griem, 1968, to account for the usually neglected exponential in Eq. (VI. 4) cannot be responsible for it. This has been tested in our calculations. One can understand this by realizing that for the higher series members the effect of dynamic broadening due to the electrons as described roughly by the constants p_2 in Eq. (X. 5) turns out to be much smaller than the half-width of the total line, which is essentially determined by quasistatic broadening.

As another interesting result, Fig. 16 shows a plot of a calculated Lyman-β profile for two different values of the constant B(B = 1.27 and B for $\rho_{min} = \lambda\!\!\!^{-} + \frac{3}{2} n^2 a_o$), which allows also some qualitative statements concerning H_β. We realize that changing B affects the very line center, where the profile shows the two humps and the near line wing, but it does not change the intensity around the halfwidth significantly,

which may be understood as an effect of the normalization. This is in agreement with experimental observations of Wende, 1967, which show that the calculations of Griem, Kolb and Shen, 1962 overestimate the near line wing. It also explains the good agreement of experimental and theoretical halfwidths in high density plasmas (see Gerardo and Hill, 1966) because the line intensity around the half width is rather insensitive to the exact value of B.

Finally in Fig. 17 to 19, we compare the unified theory calculations (solid curves) with calculations based on the one-electron theory in order to see how far into the line center the asymptotic wing expansions as given in Eq. (XI.10) or (XI.12) may be used. In all Figures the short vertical line indicates the position of the outermost, unperturbed Stark component for an average ion field β_{av}, which is given by $\Delta\omega = \beta_{av}\,\Delta\omega_i\,(n, q = n-1)$ where $\Delta\omega_i$ is defined in Eq. (V.14). The dashed lines correspond to the one-electron theory calculations for $\beta = 0$ according to Eq. (XI.12), while the dash-dotted lines give the results for $\beta=\beta_{av}$ according to Eq. (XI.10). First of all we realize that, as expected, the one-electron result for $\beta = \beta_{av}$ diverges when $\Delta\omega$ approaches $\beta_{av}\Delta\omega_i(n,\ q = n-1)$. However, in all three cases we see that for frequencies

$$\Delta\omega \gtrsim 5\ \beta_{av}\,\Delta\omega_i\,(n,\ q = n-1) \qquad \text{(XII.10)}$$

the one-electron theory calculations according to Eq. (XI.10) coincide with the unified theory calculations to within 1% and better. For slightly released accuracy requirements one may also apply the simpler one-electron theory calculations based on Eq. (XI.12) with $\beta = 0$. In particular we see that for small principal quantum numbers the useful range is very much larger than for the one-electron theory calculations

with $\beta = \beta_{av}$ because, for $\beta = 0$, the one-electron theory diverges only at $\Delta\omega = 0$. We also realize that for the line intensity range of practical interest both asymptotic wing expressions with $\beta = 0$ and $\beta = \beta_{av}$ become less useful with increasing principal quantum number.

APPENDIX A

PROGRAM FOR CALCULATING THE THERMAL AVERAGE $\bar{F}(t)$

This section gives a complete listing of the program which was used to calculate the thermal average $\bar{F}(t)$ as discussed in Sec. IX. In order to understand the program the following explanations may be of help.

1. Calculation of $\Phi_k(s, y, x, u)$

Function PHI(K,AY) calculates Φ_1, Φ_2, and Φ_4 as defined by the Eqs. (IX.17)-(IX.21). In order to assure sufficient numerical accuracy for computing $\Phi_k(s, y, x, u)$, series expansions have been applied whenever one of the different $g_k(s, y, x, u)$ becomes very small. The following expansions have been used abbreviating

$$r = \sqrt{\rho^2 + v^2 t_o^2}\,/D = x^2 + y^2(1-x^2)$$

$$a = \rho/\sqrt{\rho^2 + v^2 t_o^2} = x/r \qquad (A.1)$$

$$w = vt_o/\sqrt{\rho^2 + v^2 t_o^2} = \sqrt{1-x^2}\,y/r$$

and

$$\gamma = vt/\sqrt{\rho^2 + v^2 t_o^2} = us/r$$

(a) $g_1(s, y, x, u)$

$a < 0.01$ and $\gamma > 0$

$$g_1 = \frac{s}{r^2(1+\gamma)}\left\{1 + \frac{\gamma(4+\gamma)}{8(1+\gamma)^2}\,a^2 + \frac{\gamma(16+80\gamma+40\gamma^2+7\gamma^3)}{128(1+\gamma)^4}\,a^4\right.$$

$$+ \frac{(96+448\gamma+1024\gamma^2+1520\gamma^3+880\gamma^4+252\gamma^5+33\gamma^6)}{1024(1+\gamma)^6} a^6 + \ldots . \Bigg\}$$

(A. 2)

$a < 0.01$ and $\gamma < -2$

$$g_1 = \frac{2}{xu} \left\{ 1 - \frac{\gamma^2}{8(1-\gamma)^2} a^2 + \frac{\gamma^3(16-5\gamma)}{128(1-\gamma)^4} a^4 + \gamma \frac{(32-192\gamma+112\gamma^2-21\gamma^3)}{1024(1-\gamma)^6} a^6 + \ldots \right\}$$

(A. 3)

$\gamma < 0.01$

$$g_1 = \frac{s}{r^2} \left\{ 1 - w \cdot \gamma - (3-11w^2) \frac{\gamma^2}{8} + (9-17w^2) \cdot \frac{w\gamma^3}{8} \right.$$

$$\left. + (31-350w^2+447w^4) \frac{\gamma^4}{128} + \ldots \ldots \right\} \qquad \text{(A. 4)}$$

$\gamma > 100$

$$g_1 = \frac{\sqrt{2(1-w)}}{xu} \cdot \left\{ 1 - \frac{(1+w)}{2\gamma} \left[1 - \frac{5w-1}{4\gamma} - \frac{(3+4w-15w^2)}{8\gamma^2} \right. \right.$$

$$\left. \left. - \frac{(11-83w-59w^2+195w^3)}{64\gamma^3} - \ldots \ldots \right] \right\} \qquad \text{(A. 5)}$$

(b) $g_2(s, y, x, u)$

$(x/y)^2 < 0.0002$ and $y > 0$

$$g_2 = \frac{(1-y)}{y \cdot u} \left\{ 1 - \frac{(1+y)(3-y)}{8} \left(\frac{x}{y}\right)^2 + (31-42y+7y^2) \frac{(1+y)^2}{128} \left(\frac{x}{y}\right)^4 \right.$$

$$- (187-443y+297y^2-33y^3) \cdot \frac{(1+y)^3}{128} \left(\frac{x}{y}\right)^6 + \ldots .$$

(A. 6)

$(x/y)^2 < 0.0002$ and $y < 0$

$$g_2 = \frac{2}{xu} \left\{ 1 - \frac{(1-y)^2}{8} \left(\frac{x}{y}\right)^2 + (11+10y-5y^2) \cdot \frac{(1-y)^2}{128} \left(\frac{x}{y}\right)^4 - + \ldots \right\}$$

(A. 7)

$|1-y| < 3.10^{-3}$

$$g_2 = \frac{(1-y)\sqrt{1-x^2}}{u} \left\{ 1 + (1-x^2)(1-y) + (1-x^2)(1-\frac{11}{8}x^2)(1-y)^2 + (1-x^2)^2 (1-\frac{17}{8}x^2)(1-y)^3 + \cdots \right\}$$

(A. 8)

2. Calculation of G(s, x, u)

Function GN(AX, AXS) calculates G(s, x, u) as defined by the Eqs. (IX. 22) and (IX. 24). This integral has been solved by rewriting it in the following way.

$$G(s, x, u) = G_1(s, x, u) + G_2(s, x, u) + G_4(s, x, u) \qquad (A. 9)$$

The new integrals $G_k(s, x, u)$ are only functions of $\Phi_k(s, y, x, u)$ and turn out to be

$$G_1 = U(x > x_o)\, U(2 > R) \int_{-\frac{R}{2}}^{1-R} \Phi_1 \, dy + U(x_o > x)\, U(1 > R+P) \int_{P}^{1-R} \Phi_1 \, dy$$

(A. 10a)

$$G_1 = U(1-R > K)\int_K^{1-R} \Phi_1 \, dy \quad \text{with} \quad K = \begin{cases} P \text{ if } x < x_o \\ -\frac{R}{2} \text{ if } x > x_o \end{cases} \tag{A.10b}$$

$$G_2 = U(x > x_o)\left[U(2 > R)\int_{1-R}^{1} \Phi_2 dy + U(R > 2)\int_{-1}^{+1} \Phi_2 \, dy\right]$$
$$+ U(x_o > x)\left[U(1 > R+P)\int_{1-R}^{1} \Phi_2 dy + U(R+P > 1)\int_{P}^{1} \Phi_2 dy\right] \tag{A.11a}$$

$$G_2 = \int_B^1 \Phi_2 dy \text{ with } B = \text{MAX}(1-R, K) \text{ and } K = \begin{cases} -1 \text{ if } x > x_o \\ P \text{ if } x < x_o \end{cases} \tag{A.11b}$$

and

$$G_4 = U(x > x_o) \cdot U\left(\frac{R}{2} > 1\right) \cdot \left(\frac{R}{2} - 1\right) \Phi_4 \tag{A.12}$$

The first integral is split up at most into three parts

$$G_1 = \int_K^{-x} \Phi_1 dy + \int_{-x}^{+x} \Phi_1 dy + \int_x^{1-R} \Phi_1 dy \tag{A.13}$$

if every upper limit is larger than the lower limit using a different convenient change of variables in every part. The integration is performed in all cases by means of Weddle's rule (subroutine WEDDLE). The number of points besides the initial point is firstly taken to be 6 and is doubled in every iteration by calculating only the values in between the old values until the integral changes less than a preset relative value called DG.

3. Function GUS (AU) calculates the x-integral and is defined by

$$GUS(AU) = \frac{4}{\sqrt{\pi}} \, u^2 \cdot e^{-u^2} \, H(s, u) \qquad (A.14)$$

where

$$H(s, u) = 2 \int_0^1 x \sqrt{1-x^2} \, G(s, x, u) \, dx \qquad (A.15)$$

The integral is performed in two parts

$$H(s, u) = \int_0^{x_o^2} \sqrt{1-z} \, G(s, \sqrt{z}, u) \, dz + 2 \int_0^{-\ln(x_o)} e^{-2z} \sqrt{1-e^{-2z}} \, G(s, e^{-z}, u) \, dz \qquad (A.16)$$

by means of Weddle's rule again using a technique as described before for G(s, x, u). The new test parameter, which determines the number of iterations, is called ACC and is given in the main program. The old test parameter DG has been made a function of ACC, x and u in order to calculate those values of G(s, x, u) with the highest accuracy which give the largest contribution in the final velocity integral. For very small values of u· s the integral has been approximated by

$$H_a(s, u) = - C^2 \cdot s^2 \left[\frac{1}{x_o} - 1 \right] \qquad (A.17)$$

This limit does not lead to the static wing, as $\overline{F}(t)_{t \to 0}$ in Eq. (IX. 28) does because of the lower cutoff x_o . As explained in Sec. IX. this cut-off is necessary in order to avoid rapid fluctuations in the integrals which require more integration steps and longer computer time. For practical calculations x_o is chosen small enough so that over at least one order of magnitude in t the calculated $\overline{F}(t)$ comes as close as required to the asymptotic limit $\overline{F}(t)_{t \to 0}$.

For $us > 2$ the following relation is applied

$$2\int_0^1 x\sqrt{1-x^2}\, G_4(s,x,u)\, dx = -C\cdot s\int_0^\infty \frac{\sin(b\cdot z)}{1+z^2}\, dz + \frac{2}{3}(1-b\,K_1(b) + b^2 K_0(b)) \qquad (A.18)$$

where

$$b = \frac{2C}{u}$$

For simplicity x_o has been set to zero for this relation without affecting the final result noticably. For very large s Eq. (A.18) leads to Eq. (IX.31). However, Eq. (A.18) does not require C to be small as Eq. (IX.31) does. The Raabe integral is calculated by the function SNZ and the modified Bessel functions K_o and K_1 by the subroutine BESMOD.

4. The final thermal average $\overline{F}(s, n_k, n_e, T)$ as defined in Eq. (IX.23) is calculated in the main program FSTEST. The best results for the velocity integral have been obtained by Gauss's quadrature formula (function GLQUAD). The values FS in the program are given by

$$FS = \frac{1}{2\pi n_e D^3}\,\overline{F}(s, n_k, n_e, T)\ . \qquad (A.19)$$

The main program reads in the temperature T, the electron density n_e, the quantum number n_k, two cutoff parameters, which specify the lower and upper cutoff of the x-integral by

$$\rho_{min} = \text{STRONG}\cdot\rho_o$$
$$\rho_{max} = \text{CUT}\cdot D \qquad (A.20)$$

where ρ_o is given by Eq. (IX. 5). Finally the main program reads in the initial value of s for computing the thermal average and the number of values which proceed according to $s_{k+1} = s_k \cdot 10$. The program also gives the asymptotic thermal average leading to the static wing which is called GS and calculates the relative thermal average in units of this asymptotic value. Furthermore, the function KLOCK provides a means to test the computer time for every individual value of FS. The results are shown and discussed in Sec. IX.

```
      PROGRAM FSTEST
C     CALCULATION OF THE THERMAL AVERAGE FS
C     INTEGRAL FS OVER U IS TESTED FOR DIFFERENT L IN GAUSS QUADRATURE
      COMMON/PDS/S/PDCON/C1,C2,CON,BCON/PDRAD/BRAD/PDACC/ACC,DG,NGN
      COMMON/PDSTR/STRONG
      EXTERNAL GUS
  500 READ(60,100) TEMP,DENSTY,QNUM,Q,CUT,STRONG, SS, K
      IF(DENSTY.EQ.0.) CALL EXIT
      WRITE(61,104) TEMP, DENSTY, QNUM, Q, CUT, STRONG
      T = TEMP*1.E-4
      RELDEN = DENSTY*1.E-18
      C1 = 1.5 * Q * QNUM
      C2 = 0.03043 * SQRT(RELDEN)/(T * CUT)
      WRITE (61,105) C1,C2
      NK = QNUM * Q + 0.01
      CON = C1 * C2
      BCON = 1.414213562 * CON
      CT3 = CUT ** 3
      BRAD =       7.67E-3*SQRT(RELDEN/T)*QNUM**2*STRONG/CUT
      NUM = 0
      ACC = 3.E-4
    7 DO 1 I = 1,K
      NUM = NUM + 1
      SS = SS * 10.0
      S = SS / CUT
      FSOLD = 0.0
      GS = -1.671085516 * (CON*CUT*SS) ** 1.5
      GSAS = -(CON*SS)**2* (1.1283791671/(C2*STRONG) - 1.) * CUT
      PRINT 200,SS, GS, GSAS
      DO 20 L = 3,5
      LLL = KLOCK(0)
      FS = GLQUAD (GUS,0.0,5.0,L) * CT3
      FFGG = FS/GS
      DACC = ABS((FSOLD - FS)/FS)
      LLL = KLOCK(0) - LLL
      PRINT 300,  FS, FFGG, DACC, LLL
      IF(DACC.LT.ACC) GO TO 50
   20 FSOLD = FS
   50 PUNCH 400,SS, FS, DACC, NK, CUT, STRONG, DENSTY, TEMP, NUM
    1 CONTINUE
      GO TO 500
  100 FORMAT( 2E10.2, 4F10.1, E10.2, I5)
  104 FORMAT (1H1,* TEMPERATURE = *E14.5, 10X, * DENSITY = *E14.5//
     1    * QUANTUMNUMBERS     N = *F6.1,10X,*  (N1 - N2) = *F6.1//
     2    * DEBYE CUTOFF FACTOR = *F8.3,10X,* STRONG COLLISION FACTOR =
     3    F8.3)
  105 FORMAT  (//* C1 = * E14.6 , 10X * C2 = * E14.6)
  200 FORMAT (///* S = *E15.7,9X,* GS = *E17.9,9X,* GSAS = *E17.9/)
  300 FORMAT (* FS = *E17.9,* FS/GS = *E17.9,* DACC = *E17.9,
     1    * LLL = *I8/)
  400 FORMAT (E10.3, E15.7, E10.2, I5, F7.1, F7.3, 2E11.3, I4)
      END
C
C
```

```
C
      FUNCTION GUS(AU)
      COMMON/PDS/S/PDCON/C1,C2,CON,BCON/PDU/U/PDXM/XM1,XM2
      COMMON/PDRAD/BRAD/PDACC/ACC,DG,NGN/PDSTR/STRONG
      DIMENSION F(192), H(192)
      GUS = 0.0
      U = AU
      IF(S.EQ.0.0) RETURN
      XM1 = C2*STRONG/U
      IF(XM1.GE.1.) XM1 = 1. - 1.E-9
      XM2 = XM1 + BRAD
      IF(XM2.GE.1.)  XM2 = 1. - 1.E-9
      CONS = CON * S
      U2 = U * U
      FU = 2.2567583342 * U2 * EXPF(-U2)
      US = U * S
      IF((US/STRONG).GT.2.E-6) GO TO 5
      GUS = -CONS * CONS * (1./XM1 - 1.) * FU
      RETURN
    5 NGN = 0
      GD = 0.0
      IF(US.LT.2.) GO TO 8
      NGN = 1
      PA = 2. * CON/U
      XMM = XM2 * XM2
      SXM = SQRT(1. - XMM)
      CALL BESMOD (PA, FI0,FI1,FK0,FK1)
      GD = -CONS * SNZ(PA) + 2.*(1.+PA*(PA*FK0 - FK1))/3.
    8 GUOLD = 0.0
      G1OLD = 0.0
      G2OLD = 0.0
      N = 3
      DO 100 K = 1,6
      GUS = GD
      DG = ACC/FU
      N = 2 * N
      NN = 2
      IF(K.EQ.1)  NN = 1
      AN = N
      ANN = NN
      IF(K.EQ.1) GO TO 10
      DACC = ABS(DG1/GUOLD)
      IF(DACC.LT.ACC) GO TO 40
      GO TO 20
   10 F0 = GN(0.0,1.0)
      DQ1 = XM1 * XM1
   20 DQ0 = DQ1/AN
      DQ = DQ0 * ANN
      Q = DQ0 - DQ
      DO 30 J = 1,N,NN
      Q = Q + DQ
      X = SQRT(Q)
      XS = SQRT(1. - Q)
   30 F(J) = GN(X,XS) * XS
```

```
      CALL WEDDLE (DQO,N,F,GUS1,FO)
   40 GUS = GUS + GUS1
      IF(K.GE.6) GO TO 50
      DG1 = GUS1 - G1OLD
      G1OLD = GUS1
      IF(DG1.EQ.0.) GO TO 50
      DO 45 J = 1,N
      L = N + 1 - J
   45 F(2 * L) = F(L)
   50 IF(XM1.GE.0.999999999) GO TO 90
      IF(K.EQ.1) GO TO 60
      DACC = ABS(DG2/GUOLD)
      IF(DACC.LT.ACC) GO TO 80
      GO TO 65
   60 XO = SQRT(1. - DQ1)
      HO = GN(XM1,XO) * XO * DQ1
      DY1 = -LOGF(XM1)
   65 DYO = DY1/AN
      DY = DYO * ANN
      Y = -DY1 + DYO - DY
      N1 = N - 1
      DO 70 J = 1,N1,NN
      Y = Y + DY
      X = EXPF(Y)
      X2 = X * X
      XS = SQRT(1. - X2)
      DG = ACC/XS
   70 H(J) = GN(X,XS) * XS * X2
      H(N) = 0.0
      CALL WEDDLE (DYO,N,H,OUT,HO)
      GUS2 = 2.0 * OUT
   80 GUS = GUS + GUS2
      IF(K.GE.6) GO TO 90
      DG2 = GUS2 - G2OLD
      G2OLD = GUS2
      IF(DG2.EQ.0.) GO TO 90
      DO 85 J = 1,N
      L = N + 1 - J
   85 H(2 * L) = H(L)
   90 DACC = ABS((GUS - GUOLD)/GUS)
      IF(DACC.LT.ACC) GO TO 120
  100 GUOLD = GUS
  120 GUS = GUS * FU
      RETURN
      END
C
C
C
      FUNCTION GN(AX,AXS)
      COMMON/PDS/S/PDU/U/PDCON/C1,C2,CON,BCON/PDXD/X,XS,X2,DX2
      COMMON/PDACC/ACC,DG,NGN/PDXM/XM1,XM2
      DIMENSION  F(768), G(768), H(768), D(768)
      GN = 0.0
      X = AX
```

```
      XS = AXS
      X2 = X * X
      DX2 = 1. - X2
      GNOLD = 0.0
      G1OLD = 0.0
      G2OLD = 0.0
      G3OLD = 0.0
      G4OLD = 0.0
      R = U * S / XS
      R1 = 1. - R
      R2 = 0.5 * R
      P1 = -1.
      P2 = -1.
      N = 3
      DO 100 K = 1,8
      GN = 0.0
      N = 2 * N
      NN = 2
      IF(K.EQ.1) NN = 1
      AN = N
      ANN = NN
      QA = -R2
      IF(X.GE.XM1) GO TO 5
      IF(K.EQ.1) P1 = SQRT(XM1*XM1 - X2)/XS
      QA = P1
    5 IF(R1.LE.P1) GO TO 50
      QB = -X
      IF(R1.LT.-X) QB = R1
      IF(QA.GE.QB) GO TO 20
      IF(K.EQ.1) GO TO 7
      DGG = ABS(DG1/GNOLD)
      IF(DGG.LT.DG) GO TO 13
      GO TO 8
    7 DQ1 = (QB + R2) ** (1./3.)
    8 DQO = DQ1/AN
      DQ = DQO * ANN
      Q = DQO - DQ
      DO 10 J = 1,N,NN
      Q = Q + DQ
      Q2 = Q * Q
      Y = QB - Q * Q2
   10 F(J) = PHI(1,Y) * Q2
      CALL WEDDLE (DQO,N,F,OUT,0.0)
      G1 = 3.0 * OUT
   13 GN = G1
      IF(K.GE.8) GO TO 18
      DG1 = G1 - G1OLD
      G1OLD = G1
      IF(DG1.EQ.0.) GO TO 18
      DO 15 J = 1,N
      L = N + 1 - J
   15 F(2 * L) = F(L)
   18 QA = -X
   20 QB = X
```

```
      IF(R1.LE.X) QB = R1
      IF(QA.GE.QB) GO TO 35
      IF(K.EQ.1) GO TO 23
      DGG = ABS(DG2/GNOLD)
      IF(DGG.LT.DG) GO TO 31
      GO TO 25
   23 FO = PHI(1,QA)
      DY2 = QB - QA
   25 DYO = DY2/AN
      DY = DYO * ANN
      Y = QA + DYO - DY
      DO 30 J = 1,N,NN
      Y = Y + DY
   30 G(J) = PHI(1,Y)
      CALL WEDDLE (DYO,N,G,G2,FO)
   31 GN = GN + G2
      IF(K.GE.8) GO TO 33
      DG2 = G2 - G2OLD
      G2OLD = G2
      IF(DG2.EQ.0.) GO TO 33
      DO 32 J = 1,N
      L = N + 1 - J
   32 G(2 * L) = G(L)
   33 QA = X
   35 IF(QA.GE.R1) GO TO 50
      IF(K.EQ.1) GO TO 36
      DGG = ABS(DG3/GNOLD)
      IF(DGG.LT.DG) GO TO 42
      GO TO 37
   36 HO = PHI(1,R1) * R1 * R1
      QO = 1./R1
      DQ3 = 1./QA - QO
   37 DQO = DQ3/AN
      DQ = DQO * ANN
      Q = QO + DQO - DQ
      DO 40 J = 1,N,NN
      Q = Q + DQ
      Y = 1./Q
   40 H(J) = PHI(1,Y) * Y * Y
      CALL WEDDLE (DQO,N,H,G3,HO)
   42 GN = GN + G3
      IF(K.GE.8) GO TO 50
      DG3 = G3 -  G3OLD
      G3OLD = G3
      IF(DG3.EQ.0.) GO TO 50
      DO 45 J = 1,N
      L = N + 1 - J
   45 H(2 * L) = H(L)
   50 IF(R.LT.1.E-6) GO TO 80
      QA = R1
      IF(X.GE.XM2) GO TO 55
      IF(K.EQ.1) P2 = SQRT(XM2*XM2 - X2)/XS
   55 IF(R1.LT.P2) QA = P2
      IF(K.EQ.1) GO TO 57
```

```
      DGG = ABS(DG4/GNOLD)
      IF(DGG.LT.DG) GO TO 63
      GO TO 58
   57 DA = PHI(2,QA)
      DY4 = 1. - QA
   58 DYO = DY4/AN
      DY = DYO * ANN
      Y = QA + DYO - DY
      DO 60 J = 1,N,NN
      Y = Y + DY
   60 D(J) = PHI(2,Y)
      CALL WEDDLE (DYO,N,D,G4,DA)
   63 GN = GN + G4
      IF(K.GE.8) GO TO 70
      DG4 = G4 - G4OLD
      G4OLD = G4
      IF(DG4.EQ.0.) GO TO 70
      DO 65 J = 1,N
      L = N + 1 - J
   65 D(2 * L) = D(L)
   70 IF(R2.LE.1.) GO TO 80
      IF(K.EQ.1) G5 = (R2-1.)*PHI(4,Y)
      GN = GN + G5
   80 DGG = ABS((GN - GNOLD)/GN)
      IF(DGG.LT.DG) GO TO 120
  100 GNOLD = GN
  120 IF(NGN.EQ.1) GN = GN - G5
      RETURN
      END
C
C
C
      FUNCTION PHI(K,AY)
      COMMON/PDS/S/PDU/U/PDCON/C1,C2,CON,BCON/PDXD/X,XS,X2,DX2
      Y = AY
      PHI = 0.0
      FAC = 0.0
      IF(K.GT.2) GO TO 30
      RI = 1./SQRT(X2 + Y * Y * DX2)
      IF(K.GT.1) GO TO 10
      C = X * RI
      W = XS * Y * RI
      G = U * S * RI
      IF(C.GT.0.01) GO TO 3
      IF(Y.LT.0.)  G = -G
      AG = 1./ABS(1. + G)
      IF(AG.GT.2.) GO TO 70
      GI = (C * AG) ** 2
      IF(G.LT.-1.) GO TO 1
      FAC = CON * S * RI * RI * AG
      ARG = FAC * (1. + GI * G * 0.125 * (4. + G))
      IF(C.LT.1.E-3) GO TO 40
      AG =(((0.0546875*G+0.3125)*G+0.625)*G+0.125)*G*GI*GI
      GO TO 35
```

```
 1 FAC = 2.0 * CON/(X*U)
   ARG = FAC * (1. - GI * 0.125 * G * G)
   IF(C.LT.1.E-3) GO TO 40
   AG = -(0.125+0.0390625*G) * GI * GI * G**3
   GO TO 35
 3 IF(G.GT.0.01) GO TO 5
   FAC = CON * RI * RI * S
   W2 = W * W
   ARG = FAC * (((1.375*W2 - 0.375)*G - W)*G + 1.)
   IF(G.LT.3.E-4) GO TO 40
   AG = (3.4921875*W2-2.734375)*W2+0.2421875
   AG = (AG*G - (2.125*W2 - 1.125)*W) * G ** 3
   GO TO 35
 5 IF(G.LT.100.) GO TO 8
   FAC = BCON * SQRT(1. - W)/(X*U)
   GI = 1./G
   ARG = FAC * (((0.625*W-0.125)*GI-0.5)*GI*(1.+W)+1.)
   IF(GI.LT.3.E-4) GO TO 40
   AG=((1.5234375*W-0.4609375)*W-0.6484375)*W+0.0859375
   AG = (AG*GI+((0.25-0.9375*W)*W+0.1875))*(1.+W)*GI**3
   GO TO 35
 8 A = (1. + G*W)/SQRT(1. + G*(2.*W + G))
   GO TO 20
10 AG = ABS(Y)
   BY = ABS(1. - Y)
   IF(AG.LT.1.E-10) GO TO 15
   GI = (X/Y) ** 2
   IF(GI.GT.2.E-4) GO TO 15
   IF(Y.LT.0.) GO TO 13
   FAC = CON * BY / (AG * U)
   ARG = FAC * (1.-0.125*(1.+Y)*(3.-Y)*GI)
   IF(GI.LT.1.E-6) GO TO 40
   AG = ((0.0546875*Y-0.328125)*Y+0.2421875)*(GI*(1.+Y)) **2
   GO TO 35
13 FAC = 2.0 * CON/(X*U)
   ARG = FAC * (1.-0.125*GI*BY**2)
   IF(GI.LT.1.E-6) GO TO 40
   AG = ((2.-Y)*0.0390625*Y+0.0859375)*(GI*BY)**2
   GO TO 35
15 IF(BY.GT.3.E-3) GO TO 18
   IF(BY.LT.1.E-11) RETURN
   FAC = CON * XS * BY / U
   ARG = FAC * (1.+((1.-1.375*X2)*BY + 1.)*DX2*BY)
   IF(BY.LT.2.E-4) GO TO 40
   AG = (1. - 2.125*X2)*BY*(BY*DX2) ** 2
   GO TO 35
18 A = (X2 + Y * DX2) * RI
20 IF(A.GE.1.) RETURN
   ARG = BCON * SQRT(1. - A)/(X*U)
   GO TO 40
30 IF(X.EQ.0.) RETURN
   ARG = CON * 2.0 * XS / (X * U)
   GO TO 40
35 ARG = ARG + FAC * AG
```

```
   40 IF(ARG.LT.0.) GO TO 60
      IF(ARG.GT. 0.05) GO TO 50
      PHI = -(0.5 - ARG*ARG/24.)*ARG*ARG
      RETURN
   50 PHI = COS(ARG) - 1.0
      RETURN
   60 WRITE (61,100) ARG, FAC, K, X, U, Y, S
  100 FORMAT (* ERROR  NEGATIVE VALUE OF ARG IN PHI, ARG = *E17.9,
     1    * FAC = *E17.9/* K = *I1,* X = *E17.9,* U = *E17.9,
     2    * Y = *E17.9,* S = *E17.9)
      RETURN
   70 WRITE (61,200) G
  200 FORMAT (* PHI NOT ACCURATE ENOUGH , G = *E17.9)
      CALL EXIT
      END
C
C
C
      SUBROUTINE WEDDLE (DX, N, F, A, FO)
C     F IS THE FUNCTION TO BE INTEGRATED BY WEDDLES RULE
C     FO IS THE VALUE OF THE FUNCTION TO BE INTEGRATED AT SOME STARTING
C     POINT WHICH IS NOT INCLUDED IN THE INPUT ARRAY F
      DIMENSION F(N)
    1 A = 0.0
    2 K = N - 1
    3 DO 15 I = 1,6
    4 SUM = 0.0
    5 DO 6 J = I, K, 6
    6 SUM = SUM + F(J)
    7 GO TO (8, 10, 12, 10, 8, 14), I
    8 A = A + 5.0 * SUM
    9 GO TO 15
   10 A = A + SUM
   11 GO TO 15
   12 A = A + 6.0 * SUM
   13 GO TO 15
   14 A = A + 2.0 * SUM
   15 CONTINUE
   16 A = 0.3 * DX * (A + FO + F(N))
   17 RETURN
      END
C
C
C
      FUNCTION SNZ(X)
C     SNZ(X) CALCULATES RAABES INTEGRAL OVER SIN(X*Z)/(1.+Z*Z)  DZ
      DIMENSION AA(6), BB(4), CC(4)
      DATA((AA(I),I= 1,6) =  -0.57721566, 0.99999193, -0.24991055,
     1    0.05519968, -0.00976004, 0.00107857)
      DATA((BB(I),I= 1,4) =  8.5733287401, 18.0590169730, 8.6347608925,
     1    0.2677737343)
      DATA((CC(I),I= 1,4) =  9.5733223454, 25.6329561486,
     1   21.0996530827, 3.9584969228)
      SNZ = 0.
```

```
      IF(X.EQ.0.) RETURN
      A = ABS(X)
      IF(A.GT.40.) GO TO 100
      A2 = A * A
      EMA = EXPF(-A)
      IF(A.GT.0.2) GO TO 10
      EEA = ((((A2/72.+1.)*A2/42.+1.)*A2*0.05+1.)*A2/6.+1.)*A
      GO TO 20
   10 EEA = 0.5 * (EXPF(A) - EMA)
   20 IF(A.GT.1.) GO TO 30
      SUM = AA(1)
      Z = A
      DO 25 J = 2,6
      SUM = SUM + AA(J) * Z
   25 Z = Z * A
      EIT = SUM - LOGF(A)
      SNZ = EEA * EIT
      GO TO 40
   30 SUM = (((A+BB(1))*A+BB(2))*A+BB(3))*A+BB(4)
      SUMM = (((A+CC(1))*A+CC(2))*A+CC(3))*A+CC(4)
      EIT = SUM/(SUMM * A)
      SNZ = 0.5 * EIT * (1. - EXPF(-2.*A))
   40 PROD = A
      SUM = A
      DO 45 J = 1,200
      AJ = 2 * J + 1
      PROD = PROD * A2/(AJ*(AJ-1.))
      SUM = SUM + PROD/AJ
      PT = PROD * 1.E+10
      IF(SUM.GT.PT) GO TO 50
   45 CONTINUE
   50 PT = SNZ + SUM * EMA
      SNZ = SIGNF(PT,X)
      RETURN
  100 PROD = 1./X
      A2 = PROD * PROD
      SUM = PROD
      DO 110 J = 1,100
      AJ = 2 * J
      PROD = PROD * A2 * AJ * (AJ - 1.)
      SUM = SUM + PROD
      IF(AJ.GE.A) GO TO 150
      PT = ABS(PROD * 1.E+10)
      IF(ABS(SUM).GT.PT) GO TO 150
  110 CONTINUE
  150 SNZ = SUM
      RETURN
      END
C
C
C
      SUBROUTINE BESMOD(X,FI0,FI1,FK0,FK1)
C     BESMOD CALCULATES THE MODIFIED BESSELFUNCTIONS I0, I1, K0 AND K1
C     BY MEANS OF POLYNOMIAL APPROXIMATIONS AS GIVEN IN THE
```

```
C     NBS HANDBOOK OF MATHEMATICAL FUNCTIONS,  PAGE 378
      DIMENSION A(7),B(9),C(7),D(9),E(7),F(7),G(7),H(7)
      DATA ((A(I),I = 1,7) = 0.0045813, 0.0360768, 0.2659732,
     1   1.2067492, 3.0899424,  3.5156229, 1.0)
      DATA ((B(I),I = 1,9) = 0.00392377, -0.01647633, +0.02635537,
     1  -0.02057706, 0.00916281, -0.00157565, 0.00225319, 0.01328592,
     2   0.39894228)
      DATA ((C(I),I = 1,7) = 0.00032411, 0.00301532, 0.02658733,
     1   0.15084934, 0.51498869, 0.87890594, 0.5)
      DATA ((D(I),I = 1,9) = -0.00420059, 0.01787654, -0.02895312,
     1   0.02282967, -0.01031555, 0.00163801, -0.00362018,-0.03988024,
     2  0.39894228)
      DATA ((E(I),I = 1,7) = 7.4E-6, 1.075E-4, 0.00262698, 0.0348859,
     1   0.23069756, 0.4227842, -0.57721566)
      DATA ((F(I),I = 1,7) = 0.00053208, -0.00251540, 0.00587872,
     1   -0.01062446, 0.02189568, -0.07832358, 1.25331414)
      DATA ((G(I),I = 1,7) = -4.686E-5, -0.00110404, -0.01919402,
     1   -0.18156897, -0.67278579, 0.15443144, 1.0)
      DATA ((H(I),I = 1,7) = -0.00068245, 0.00325614, -0.00780353,
     1   0.01504268, -0.0365562, 0.23498619, 1.25331414)
      XS = 0.0
      XE = 0.0
      IF(X.LT.2.) GO TO 10
      XS = SQRT(X)
      XE = EXPF(X)
   10 IF(X.GT.3.75) GO TO 20
      Y = X/3.75
      Y2 = Y * Y
      FIO = (((((Y2*A(1)+A(2))*Y2+A(3))*Y2+A(4))*Y2+A(5))*Y2+A(6))*Y2+1.
      FI1 =(((((Y2*C(1)+C(2))*Y2+C(3))*Y2+C(4))*Y2+C(5))*Y2+C(6))*Y2+0.5
      FI1 = FI1 * X
      GO TO 40
   20 Y = 3.75/X
      FIO = B(1)
      FI1 = D(1)
      DO 30 K = 2,9
      FIO = FIO * Y + B(K)
   30 FI1 = FI1 * Y + D(K)
      XEX = XE/XS
      FIO = FIO * XEX
      FI1 = FI1 * XEX
   40 IF(X.GT.2.) GO TO 60
      Y = X/2.
      Y2 = Y * Y
      FKO = E(1)
      FK1 = G(1)
      DO 50 K = 2,7
      FKO = FKO * Y2 + E(K)
   50 FK1 = FK1 * Y2 + G(K)
      XEX = LOGF(Y)
      FKO = FKO - XEX * FIO
      FK1 = FK1/X + XEX * FI1
      RETURN
   60 Y = 2.0/X
```

```
      FKO = F(1)
      FK1 = H(1)
      DO 70 K = 2,7
      FKO = FKO * Y + F(K)
   70 FK1 = FK1 * Y + H(K)
      XEX = 1./(XS * XE)
      FKO = FKO * XEX.
      FK1 = FK1 * XEX
      RETURN
      END
C
C
C
      FUNCTION GLQUAD(F,A,B,L)
C     GAUSSIAN-LEGENDRE QUADRATURE OF F FROM A TO B WITH 4,6,10,20,
C     40 OR 80 NODES FOR L = 1, 2, 3, 4, 5, 6
      COMMON/GLQDAT/X1(2),W1(2),X2(3),W2(3),X3(5),W3(5),X4(10),W4(10),
     1   X5(20),W5(20),X6(40),W6(40)
      DATA  ((X1(I), I = 1,2) =  .8611363116, .3399810436)
      DATA  ((W1(I), I = 1,2) =  .3478548451, .6521451549)
      DATA  ((X2(I), I = 1,3) =  .9324695142, .6612093865, .2386191861
      DATA  ((W2(I), I = 1,3) =  .1713244924, .3607615730, .4679139346
      DATA  ((X3(I), I = 1,5) =
     1 .9739065285, .8650633667, .6794095683, .4333953941, .1488743390
      DATA  ((W3(I), I = 1,5) =
     1 .0666713443, .1494513491, .2190863625, .2692667193, .2955242247
      DATA  ((X4(I), I = 1,10) =
     1 .9931285992, .9639719273, .9122344283, .8391169718, .7463319065
     2 .6360536807, .5108670020, .3737060887, .2277858511, .0765265211
      DATA  ((W4(I), I = 1,10) =
     1 .0176140071, .0406014298, .0626720483, .0832767416, .1019301198
     2 .1181945320, .1316886384, .1420961093, .1491729865, .1527533871
      DATA  ((X5(I), I = 1,20) =
     1 .9982377097, .9907262387, .9772599500, .9579168192, .9328128083
     2 .9020988070, .8659595032, .8246122308, .7783056514, .7273182552
     3 .6719566846, .6125538897, .5494671251, .4830758017, .4137792044
     4 .3419940908, .2681521850, .1926975807, .1160840707, .0387724175
      DATA  ((W5(I), I = 1,20) =
     1 .0045212771, .0104982845, .0164210584, .0222458492, .0279370070
     2 .0334601953, .0387821680, .0438709082, .0486958076, .0532278470
     3 .0574397691, .0613062425, .0648040135, .0679120458, .0706116474
     4 .0728865824, .0747231691, .0761103619, .0770398182, .0775059480
      DATA  ((X6(I), I = 1,40) =
     1 .9995538227, .9976498644, .9942275410, .9892913025, .9828485727
     2 .9749091406, .9654850890, .9545907663, .9422427613, .9284598772
     3 .9132631026, .8966755794, .8787225677, .8594314067, .8388314736
     4 .8169541387, .7938327175, .7695024201, .7440002976, .7173651854
     5 .6896376443, .6608598990, .6310757730, .6003306228, .5686712681
     6 .5361459209, .5028041119, .4686966152, .4338753708, .3983934059
     7 .3623047535, .3256643707, .2885280549, .2509523584, .2129945029
     8 .1747122918, .1361640228, .0974083984, .0585044372, .0195113833
      DATA  ((W6(I), I = 1,40) =
     1 .0011449500, .0026635336, .0041803131, .0056909225, .0071929048
     2 .0086839453, .0101617660, .0116241141, .0130687616, .0144935080
```

```
   3 .0158961836, .0172746521, .0186268142, .0199506109, .0212440261,
   4 .0225050902, .0237318829, .0249225358, .0260752358, .0271882275,
   5 .0282598161, .0292883696, .0302723218, .0312101742, .0321004987,
   6 .0329419394, .0337332150, .0344731205, .0351605290, .0357943940,
   7 .0363737499, .0368977146, .0373654902, .0377763644, .0381297113,
   8 .0384249930, .0386617598, .0388396511, .0389583960, .0390178137)
     T0 = (A + B)/2.
     T1 = (B - A)/2.
     Y = 0.
     GO TO (1,2,3,4,5,6) L
   1 DO 10 K = 1,2
  10 Y=Y+W1(K)*(F(T0-T1*X1(K))+F(T0+T1*X1(K)))
     GO TO 100
   2 DO 20 K = 1,3
  20 Y=Y+W2(K)*(F(T0-T1*X2(K))+F(T0+T1*X2(K)))
     GO TO 100
   3 DO 30 K = 1,5
  30 Y=Y+W3(K)*(F(T0-T1*X3(K))+F(T0+T1*X3(K)))
     GO TO 100
   4 DO 40 K = 1,10
  40 Y=Y+W4(K)*(F(T0-T1*X4(K))+F(T0+T1*X4(K)))
     GO TO 100
   5 DO 50 K = 1,20
  50 Y=Y+W5(K)*(F(T0-T1*X5(K))+F(T0+T1*X5(K)))
     GO TO 100
   6 DO 60 K = 1,40
  60 Y=Y+W6(K)*(F(T0-T1*X6(K))+F(T0+T1*X6(K)))
 100 GLQUAD=Y*T1
     RETURN
     END
```

APPENDIX B

THE LARGE TIME LIMIT OF THE THERMAL AVERAGE $\overline{F}(t)$

In Eq. (IX. 31) the large time limit of the thermal average has been given, which is of the form

$$\overline{F}(t)_{t \to \infty} = At\,(B - \ell n\,(4C^2)). \tag{B.1}$$

This form has been obtained by most modern impact theories. The additive constant B varies depending on what type of cutoff has been used. In the following we derive the different constants B for the different cutoff procedures which have been used and compare them with the numbers given in the literature.

The various methods to evaluate $\overline{F}_\infty$, the large time limit of $\overline{F}(t, n_k, n_e, T)$, differ essentially in three respects, namely by the upper and lower limits of the ρ-integral and by the limits of the t'-integral in Eq. (VIII. 4). Based on the completed collision assumption (Baranger, 1962), the limits of the latter integral are usually extended from $-\infty$ to $+\infty$. This approach, however, is not quite consistent with the cutoff at the Debye length, which would rather require the integral to go from -T to + T as done in this report (T is defined by Eq. (IX. 7)). We therefore have to investigate the following integrals:

a.) for $\int_0^t PV_c(t')\,dt' \longrightarrow \int_{-T}^{+T} PV_c(t')\,dt'$ (case a)

$$\overline{F}_\infty^a = 2\pi n_e (a.D)^2 v_{av}\, t \int_0^\infty du\, \frac{4}{\sqrt{\pi}}\, u^3 e^{-u^2} \int_{x_{min}}^1 dx\, x \left[\cos\left(\frac{2C}{axu}\sqrt{1-x^2}\right) - 1\right] \tag{B.2}$$

and

$$\text{b.) for} \int_0^t PV_c(t')\,dt' \longrightarrow \int_{-\infty}^{+\infty} PV_c(t')\,dt' \qquad \text{(case b)}$$

$$\bar{F}_\infty^b = 2\pi n_e (a\cdot D)^2 v_{av} t \int_0^\infty du \frac{4}{\sqrt{\pi}} u^3 e^{-u^2} \int_{x_{min}}^1 dx\, x \left[\cos\left(\frac{2C}{axu}\right) - 1\right] \qquad \text{(B. 3)}$$

where

$$x_{min} = \rho_{min} / (a\cdot D)\,. \qquad \text{(B. 4)}$$

The factor $a = \rho_{max}/D$ is usually taken to be one and has in some papers (e.g., Griem et al. 1962) been varied to 1.1. or to 0.606 as proposed by W. R. Chappell, J. Cooper and E. Smith, 1969. As a lower cutoff we consider in particular the three cases of $\rho_{min} = 0$, $\rho_{min} = \lambda\!\!\!^{-}$ and $\rho_{min} = 3(nq - n'q')\lambda\!\!\!^{-} \simeq 2CD/u$ by setting

$$x_{min} = \frac{b}{a} \cdot \frac{2C}{u} \qquad \text{(B. 5)}$$

In the following we will set a=1. In order to recover the dependence on the upper cutoff parameter a, we only have to replace in all the following relations C by C/a.

First of all, one realizes that with $x_{min} \leq 1$ the lower limit on the u-integral is given by

$$u_o = b\cdot 2C\,. \qquad \text{(B. 6)}$$

Hence, we have to evaluate the following two integrals

$$I^a = \int_{u_o}^\infty du\, u^3 e^{-u^2} \int_{u_o/u}^1 dx\, x \left[\cos\left(\frac{2C}{xu}\sqrt{1-x^2}\right) - 1\right] \qquad \text{(B. 7)}$$

and

$$I^b = \int_{u_o}^{\infty} du\, u^3 e^{-u^2} \int_{u_o/u}^{1} dx\, x \left[\cos\left(\frac{2C}{xu}\right) - 1\right] . \qquad (B.8)$$

The second integral can be simplified after a change of variables and a partial integration to

$$I^b = \tfrac{1}{2} \int_{u_o}^{\infty} u e^{-u^2} \left[\cos\left(\frac{2C}{u}\right) - 1\right] du \qquad (B.9)$$

After expanding the cosine and another change of variables we have

$$I^b = \frac{u_o^2}{4} \sum_{k=1}^{\infty} \frac{(-1)^k}{(2k)!} \left(\frac{2C}{u_o}\right)^{2k} \int_1^{\infty} \frac{e^{-u_o^2 z}}{z^k} dz \qquad (B.10)$$

which can be expressed in terms of exponential integrals

$$I^b = -\frac{C^2}{2} E_1(u_o^2) + \frac{u_o^2}{4} \sum_{k=2}^{\infty} \frac{(-1)^k}{(2k)!} \left(\frac{2C}{u_o}\right)^{2k} E_k(u_o^2) . \qquad (B.11)$$

With the lower cutoff parameters stated above ($b \leq 1$) and typical densities and temperatures of interest one usually has $u_o < 0.1$ (see Eq. (IX.21)). Since for $k \geq 2$ $E_k(u_o^2) = 1/(k-1) + 0(u_o^2)$ one obtains to lowest order in u_o^2

$$I^b = \frac{C^2}{2} \left[-E_1(u_o^2) + 2 \sum_{k=2}^{\infty} \frac{(-1)^k}{(2k)!} \left(\frac{2C}{u_o}\right)^{2k-2} \frac{1}{k-1}\right] \qquad (B.12)$$

$$= \frac{C^2}{2}\left[-E_1(u_o^2) + 2\sum_{k=2}^{\infty}\left\{\frac{1}{(2k)!} + \frac{1}{(2k-1)!} - \frac{1}{(2k-2)(2k-2)!}\right\}\left(-\frac{4C^2}{u_o^2}\right)^{k-1}\right]$$

$$= \frac{C^2}{2}\left[-E_1(u_o^2) - 2\left(\frac{u_o}{2C}\right)^2 \left\{\cos\left(\frac{2C}{u_o}\right) + \tfrac{1}{2}\left(\frac{2C}{u_o}\right)^2 - 1\right\}\right.$$

$$+ 2\left(\frac{u_o}{2C}\right)\left\{ \sin\left(\frac{2C}{u_o}\right) - \left(\frac{2C}{u_o}\right)\right\} - 2\left\{ Ci\left(\frac{2C}{u_o}\right) - \gamma - \ell n\left(\frac{2C}{u_o}\right)\right\}\Bigg] ,$$

which yields

$$I^b = \frac{C^2}{2}\left[3(\gamma-1) + \ell n\,(4C^2) + 2K\left(\frac{1}{b}\right) + 0\,(u_o^2)\right] \qquad (B.13)$$

where K is defined as

$$K(z) = \frac{1-\cos z}{z^2} + \frac{\sin z}{z} - Ci(z) \qquad (B.14)$$

and Ci is the cosine integral. Eq. (B.13) was obtained already by Shen and Cooper, 1969. Their constant A is identical with our constant 2C.

The other integral I^a of Eq. (B.7) one can obtain by evaluating

$$\Delta I = \int_{u_o}^{\infty} du\; u^3 e^{-u^2} \int_{u_o/u}^{1} dx\, x \left[\cos\left(\frac{2C}{ux}\sqrt{1-x^2}\right) - \cos\left(\frac{2C}{ux}\right)\right] \qquad (B.15)$$

so that

$$I^a = I^b + \Delta I \ . \qquad (B.16)$$

If we again expand the cosine functions, ΔI can be given by

$$\Delta I = \sum_{k=1}^{\infty} \frac{(2C)^{2k}}{(2k)!} \sum_{j=o}^{k-1} \frac{k!\,(-1)^j}{j!(k-j)!} \int_{u_o}^{\infty} du\, u^{3-2k} e^{-u^2} \int_{u_o/u}^{1} x^{1-2j} dx \qquad (B.17)$$

$$= \frac{C^2}{2}\left[e^{-u_o^2} - u_o^2 E_1(u_o^2)\right]$$

$$+\frac{C^2}{2}\,2u_o^2\sum_{k=2}^{\infty}\frac{1}{(2k)!}\left(\frac{2C}{u_o}\right)^{2k-2}\left[E_{k-1}(u_o^2)-E_k(u_o^2)-k\int_1^{\infty}e^{-u_o^2 z}\frac{\ell nz}{z^{k-1}}\,dz\right]$$

$$-\frac{C^2}{2}\,4u_o^2\sum_{k=3}^{\infty}\frac{k!}{(2k)!}\left(\frac{2C}{u_o}\right)^{2k-2}\sum_{j=2}^{k-1}\frac{(-1)^j}{j!(k-j)!(2j-2)}\left[E_{k-1}(u_o^2)-E_{k-j}(u_o^2)\right. \tag{B.17}$$

which gives us to lowest order in u_o^2

$$\Delta I = \frac{C^2}{2}\left[1 + 0(u_o^2)\right] \tag{B.18}$$

This means that for the same lower cutoff case a.) and b.) as defined in the Eqs. (B.2) and (B.3) differ only by a constant 1 in their additive constants B. As a result we have

$$\overline{F}_{\infty} = -\left(\frac{3}{2}(nq-n'q')\frac{\hbar}{m}\right)^2 n_e\, t\sqrt{\frac{8\pi m'}{kT}}\left[B-\ell n\,(4C^2)\right] \tag{B.19}$$

where the constant B for the different cutoff parameters is compiled in the following Table 2.

Table 2. The constant B for different cutoff parameters.

	$\int_{-T}^{+T} PV_c(t')\,dt'$	$\int_{-\infty}^{+\infty} PV_c(t')\,dt'$
$\rho_{min} = 0$	0.27	1.27
$\rho_{min} = \chi$	0.23 → 0.27	1.23 → 1.27
$\rho_{min} = 3n_k\chi$	-1.66	- 0.66

In order to compare our results with the numbers given in the literature we rewrite Eq. (B.19) as

$$\overline{F}_{\infty} = - A \cdot t \cdot \left[B_o - \gamma - \ell n \, (y_{min}) \right] \qquad (B.20)$$

where y_{min} as introduced by Griem, Kolb and Shen (Griem et al., 1959) is given by

$$y_{min} = \frac{4\pi n_e}{3\,m} \left(\frac{e\hbar n^2}{kT} \right)^2 = \frac{2}{3} \left(\frac{n^2}{3(nq - n'q')} \right)^2 4C^2 . \qquad (B.21)$$

Consequently, B and B_o are related by the following relation

$$B_o = B + \gamma + \ell n \left[\frac{2}{3} \left(\frac{n^2}{n_k} \right)^2 \right] \quad . \qquad (B.22)$$

Comparing Eqs. (B.19) and (B.20) one notices that for a particular line the value of the square bracket as derived here depends on the quantum number n_k for that particular state. This is also true for the paper of Shen and Cooper, 1969, who consider our case (b) with infinite limits on the t'-integral. Otherwise the constants given in the literature are independent of n_k because the lower cutoff parameter is usually based on an average Stark splitting. If we set $nq - n'q' = n^2/2$, which corresponds approximately to the average Stark splitting and also gives the results for the Stark shifted component of Lyman-α, we have

$$B_o = B - 0.64 \quad . \qquad (B.23)$$

This yields directly for $n_k = n^2/2$ the B_o values corresponding to the B values in Table 2.

The following constants B_o have been given in the literature:

Griem, Kolb, Shen, 1959; (Eq. 29) :		$B_o = 0$
Griem, Kolb, Shen, 1962; (Eq. 2) :		$B_o = 1.0$
Griem, 1965 Kepple, Griem, 1968	(neglecting quadrupole term) :	$B_o = 0.58$
Shen, Cooper, 1969;		$B_o = 0.58$

Recently the time development operator (S-matrix) has been evaluated for Lyman-α including time ordering by solving the differential equations for the S-matrix elements (Bacon, 1969). Again the square bracket depends on $(nq-n'q')$ and the average value $B_o = 1.1$ considering only the dipole term. It should, however, be stressed that one should not overinterpret these numbers because within the classical path approximation there is always some uncertainty about the "correct" constant B because of the ambiguous lower cutoff. This is due to the fact that the classical path approximation breaks down roughly for $\rho \lesssim \lambda\!\!\!^{-}$ (for details see Paper I). For most cases this has no significant effect for the Stark broadening of hydrogen because the dynamic broadening is primarily due to weak collisions. More details are given with the discussion at the end of Chap. XII. The situation is quite different for the broadening of ionized lines where strong collisions are very important and where the uncertainty of the classical path approximation accounts for part of the still existing discrepancies between theory and experiment, which are large compared with the Stark broadening of hydrogen.

So far we have considered $\overline{\overline{F}}_\infty$, which is the basis of the unmodified impact theory. In order to extend the range of validity beyond the plasma frequency the modified impact theory introduces the Lewis cutoff by considering only those collisions for which the duration of a collision, which is typically ρ/v, is smaller than the time of interest being typically $1/\Delta\omega$. For this reason the modified impact theory introduces an upper cutoff

$$\rho_{max} = \text{MIN}\,(D,\ v_{av}/\Delta\omega) \qquad \text{(B.24)}$$

or

$$\rho_{max}/D = \text{MIN}\,(1,\ 1/\Delta\omega_R)$$

It should be noted at this stage that in the following relations we not only have to replace C by C/a but also $\Delta\omega_R$ by a $\Delta\omega_R$, in order to obtain the dependence on the upper cutoff parameter a. Considering the usually applied case (b) (Eq. (B.3)) we have to evaluate the following integral for $\Delta\omega_R > 1$

$$I_L^b = \int_{u_o\Delta\omega_R}^{\infty} du\, u^3 e^{-u^2} \int_{u_o/u}^{1/\Delta\omega_R} dx\, x\left[\cos\left(\frac{2C}{xu}\right) - 1\right] \qquad \text{(B.25)}$$

where the lower limit on the u-integral is determined by the condition $u_o/u \le 1/\Delta\omega_R$. After a change of variables and a partial integration one obtains similar to Eq. (B.9)

$$I_L^b = \frac{1}{2\Delta\omega_R^2} \int_{u_o\Delta\omega_R}^{\infty} u\, e^{-u^2}\left[\cos\left(\frac{2C\Delta\omega_R}{u}\right) - 1\right] du \qquad \text{(B.26)}$$

Expanding the cosine again and performing another change of variables the result is

$$I_L^b = \frac{u_o^2}{4} \sum_{k=1}^{\infty} \frac{(-1)^k}{(2k)!} \left(\frac{2C}{u_o}\right)^{2k} \int_1^{\infty} \frac{e^{-u_o^2\Delta\omega_R^2 z}}{z^k}\, dz \quad . \qquad \text{(B.27)}$$

This gives us then

$$I_L^b = -\frac{C^2}{2} E_1\left(u_o^2\Delta\omega_R^2\right) + \frac{u_o^2}{4} \sum_{k=2}^{\infty} \frac{(-1)^k}{(2k)!} \left(\frac{2C}{u_o}\right)^{2k} E_k\left(u_o^2\Delta\omega_R^2\right) \qquad \text{(B.28)}$$

Evaluating the exponential integrals E_k for small arguments only we finally have

$$I_L^b = \frac{C^2}{2}\left[-E_1\left(u_o^2 \Delta\omega_R^2\right) + E_1\left(u_o^2\right)\right] + I^b$$

$$= C^2 \ln \Delta\omega_R + I^b \qquad \text{(B.29)}$$

which gives us for $\Delta\omega_R > 1$ the log-dependence of the Φ_{ab}-matrix elements in the modified impact theory. A more appropriate way for applying the Lewis cutoff, which avoids the discontinuity at $\Delta\omega_R = 1$, is to take as an upper cutoff

$$\rho_{max} = \text{MIN}\,(D, v/\Delta\omega)$$

$$\text{or} \qquad \rho_{max}/D = \text{MIN}\,(1,\ u/\Delta\omega_R) \qquad \text{(B.30)}$$

which for case b leads to the following integral.

$$I_L^b = \int_{\sqrt{u_o \Delta\omega_R}}^{\Delta\omega_R} du\ u^3 e^{-u^2} \int_{u_o/u}^{u/\Delta\omega_R} dx\ x \left[\cos\left(\frac{2C}{xu}\right) - 1\right]$$

$$+ \int_{\Delta\omega_R}^{\infty} du\ u^3 e^{-u^2} \int_{u_o/u}^{1} dx\ x \left[\cos\left(\frac{2C}{xu}\right) - 1\right] \qquad \text{(B.31)}$$

These integrals are identical to

$$I_L^b = \int_{\sqrt{u_o \Delta\omega_R}}^{\infty} du\, u^3 e^{-u^2} \int_{u_o/u}^{u/\Delta\omega_R} dx\, x \left[\cos\left(\frac{2C}{xu}\right) - 1\right]$$

$$- \int_{\Delta\omega_R}^{\infty} du\, u^3 e^{-u^2} \int_{1}^{u/\Delta\omega_R} dx\, x \left[\cos\left(\frac{2C}{xu}\right) - 1\right] . \qquad \text{(B. 32)}$$

and after a partial integration we have

$$I_L^b = -\frac{1}{\Delta\omega_R^2} \int_{\sqrt{u_o \Delta\omega_R}}^{\infty} du\, u^3 e^{-u^2} \left[\cos\left(\frac{2C\Delta\omega_R}{u^2}\right) - 1\right]$$

$$- \frac{1}{\Delta\omega_R^2} \int_{\Delta\omega_R}^{\infty} du\, u^3 e^{-u^2} \left[\cos\left(\frac{2C\Delta\omega_R}{u^2}\right) - 1\right] \qquad \text{(B. 33)}$$

$$+ \tfrac{1}{2} \int_{\Delta\omega_R}^{\infty} du\, u e^{-u^2} \left[\cos\left(\frac{2C}{u}\right) - 1\right] .$$

Expanding the cosine functions, I_L^b can be evaluated in a similar manner as above with the result

$$I_L^b = -\frac{C^2}{2} \left[E_1(\Delta\omega_R^2) - 2 E_1(u_o \Delta\omega_R) \right]$$

$$+ 2C^2 \sum_{k=2}^{\infty} \frac{(-1)^k}{(2k)!} \left(\frac{2C}{u_o}\right)^{2k-2} E_{2k-1}(u_o \Delta\omega_R) \qquad \text{(B. 34)}$$

$$+ C^2 \sum_{k=2}^{\infty} \frac{(-1)^k}{(2k)!} \left(\frac{2C}{\Delta\omega_R}\right)^{2k-2} \left[E_k(\Delta\omega_R^2) - 2 E_{2k-1}(\Delta\omega_R^2) \right] .$$

For $\Delta\omega_R \lesssim 1$ with $2C \ll 1$ and $b \lesssim 1$ the latter result may be simplified to give

$$I_L^b = \frac{C^2}{2}\left[E_1(\Delta\omega_R^2) + \gamma + 2\,\ell n\,(\Delta\omega_R)\right] + I^b \qquad \text{(B.35)}$$

which for $\Delta\omega_R \to 0$ reduces down to $I_L^b = I^b$ and which has no discontinuity at $\Delta\omega_R = 1$. Furthermore, we see that for $\Delta\omega_R \to \infty$ Eq. (B.34) goes over to

$$I^b_{L,\,\Delta\omega_R\to\infty} = \frac{u_o}{2\Delta\omega_R}\, e^{-u_o\Delta\omega_R} \cos\left(\frac{2C}{u_o}\right) - \frac{e^{-\Delta\omega_R^2}}{4} \cos\left(\frac{2C}{\Delta\omega_R}\right) \qquad \text{(B.36)}$$

which does not lead to the static limit.

Similar results can be obtained for case a, which are not included because they are no longer required. The derivation for case b has been included, in order to obtain consistent relations which allow a comparison with the calculations done in this paper. The results for case b as given here differ slightly from the results in the literature which also vary from paper to paper depending on the average matrix elements used and on what lower cutoff and average velocity has been applied.

APPENDIX C

PROGRAM FOR CALCULATING THE FINAL LINE PROFILE $I(\Delta\omega)$

In the following a complete listing of the program is given which was used to calculate the final line profile $I(\Delta\omega)$ on the basis of the unified theory for the case of no lower state interactions.

1. The Fourier transform of the thermal average

The complex function FOUTR calculates essentially the Fourier transform of the thermal average as defined by

$$\text{FOUTR} = i\,\Delta\omega_R^2\, i_u\,(\Delta\omega_R, \beta, n, q_b, q_c) \qquad (C.1)$$

where

$$\text{DOM} = \Delta\omega_R = (\Delta\omega - \Delta\omega_i(n, q_b)\,\beta)/\tilde{\omega}_p. \qquad (C.2)$$

It uses the Eqs. (X.17) and (X.22) for calculating $i_1(\Delta\omega_R)$ and $i_2(\Delta\omega_R)$ respectively. The required Bessel functions J_o, J_1, Y_o and Y_1 are evaluated by the subroutine BSJY01. For large and small arguments $\Delta\omega_R$ these relations are replaced by their asymptotic expansions (X.18), (X.23) and (X.26). The specifying constants p_1, p_2, b_1, a_2 and b_2 (P1, P2, B1, A2, B2) are set in the function AIIM and are calculated once for all the Stark components in the main program STBRHY. The function FOUTR can be replaced by another short function FOUTR listed at the end of the program, which then makes the program calculate line profiles according to the modified impact theory.

2. Calculation of $I(\Delta\omega, \beta)$

The function AIIM calculates $I(\Delta\omega, \beta)$ as defined by Eq. (XII. 6). It establishes first of all the matrix of the $\mathfrak{L}$-operator according to Eq. (XII. 7) and calculates the array

$$\text{AMATR (NBN,, NAN)} = \delta_{q_a q_b} \Delta\omega_R \langle n q_b m | \mathfrak{L}(\Delta\omega_{op}) | n q_a m \rangle \quad \text{(C. 3)}$$

for the m values 0 and ±1. The required 3j-symbols are calculated once in the main program and their values are stored in three different arrays according to the following definitions

$$\text{SAR (NLA, NQC)} = (2\ell_a + 1) \sum_{m_c} \begin{pmatrix} \frac{n-1}{2} & \frac{n-1}{2} & \ell_a \\ \frac{m_c - q_c}{2} & \frac{m_c + q_c}{2} & -m_c \end{pmatrix}^2 \quad \text{(C. 4)}$$

where NLA = ℓ_a and NQC = q_c,

$$\text{SJQL (MCT, NBN, NLA)} = \begin{pmatrix} \frac{n-1}{2} & \frac{n-1}{2} & \ell_a \\ \frac{m-q_a}{2} & \frac{m+q_a}{2} & -m \end{pmatrix} \quad \text{(C. 5)}$$

and

$$\text{SSJJ (MCT, NBN, NAN)} = (-1)^{n+m-1-\frac{q_a+q_b}{2}} \begin{pmatrix} \frac{n-1}{2} & \frac{n-1}{2} & 1 \\ \frac{m-q_a}{2} & \frac{m+q_a}{2} & -m \end{pmatrix} \begin{pmatrix} \frac{n-1}{2} & \frac{n-1}{2} & 1 \\ \frac{m-q_b}{2} & \frac{m+q_b}{2} & -m \end{pmatrix} \quad \text{(C. 6)}$$

where MCT = m and NAN and NBN are numbering indices specifying the q_a and q_b. The matrix AMATR is then inverted by the subroutine CGAUSSEL, which is able to solve systems of linear, complex equations by Gaussian elimination. Multiplying the inverted matrix by the 3j-symbols according to Eq. (XII. 6) yields finally $I(\Delta\omega, \beta)$.

3. The final line profile $I(\Delta\omega)$

The main program STBRHY calculates the final line profile by performing the ion field average according to Eq. (II. 1). It first of all reads in the ion microfield distribution function for $0 < \beta \leq 30$ in steps of 0.1, which has been calculated in a separate program for the particular shielding parameter r_o/D. It then reads in the density n_e, the temperature T, the upper principal quantum number n, the wavelength λ, the average value of the static ion fields β_{av}, the initial value $\Delta\omega$, the logarithmic stepwidth, the total number of points, a parameter which specifies the number of ion field integration points and finally 6 numbers, which specify the G_2-function and hence $i_2(\Delta\omega_R)$ for all Stark components and which may in practically all cases be set to zero. These 6 numbers are obtained from the thermal average described in Appendix A.

The program then calculates the constants p_1, p_2, b_1, a_2 and b_2 for all Stark components and stores them in the array FPAR. p_1 is calculated according to Eq. (X. 5). p_2 is determined on the basis of Eq. (B. 19) where the constant B is given by

$$B = 0.27 - 2K\left(\frac{1}{b}\right) \quad . \qquad (C.7)$$

The K-function is defined in Eq. (B.14) and is calculated for a lower cutoff $\rho_{min} = \lambda\!\!\!^{-} + \frac{3}{2} n^2 a_o$ by setting

$$b = (\lambda\!\!\!^{-} + \frac{3}{2} n^2 a_o)/3n_k\lambda\!\!\!^{-} \qquad (C.8)$$

The necessary cosine integral is calculated by the function COSINT.

As a next step the main program evaluates all the required 3j-symbols by means of the function S3J, which in turn uses the function FCTRL to calculate all the necessary factorials. The numbers are stored in arrays according to the definitions in (C.4), (C.5) and (C.6).

In performing the ion field average the microfield distribution function is calculated by the function WFLD, which uses a 5 point interpolation on the values read in initially for $\beta < 30$ and otherwise uses the asymptotic expansion given by Hooper, 1968b. As a function of $\Delta\omega$ and β, which determine the shape of the ion field integrand, the ion field integral is subdivided in intervals, which are integrated separately by means of Weddle's rule (subroutine WEDDLE) using a convenient change of variables in every interval. Furthermore, the program calculates the asymptotic wing expansion according to Eq. (XI.12) and the unified theory for $\beta = 0$ and $\beta = \beta_{av}$ performing not the ion field integral. All three values are normalized with respect to the asymptotic $\Delta\omega^{-5/2}$-wing.

```
      PROGRAM STBRHY
C
C     PROGRAM FOR CALCULATING THE STARKBROADENING OF HYDROGEN ON THE
C     BASIS OF THE UNIFIED THEORY FOR NO LOWER STATE INTERACTION
      DIMENSION FF(1000), PFAC(6), SSJ(20), STRONG(20)
      COMPLEX FOUTR
      COMMON/FDAT/P1,P2,B1,A2,B2,PPFF
      COMMON/PSTR/NNN,NM1,BET,FPAR(6,20)
      COMMON/PSJD/SSJJ(2,20,20), SJQL(2,20,20), SAR(20,20)
      COMMON/PFW/FIELD(301)
      FIELD(1) = 0.0
      READ 100, (FIELD(I), I = 2,301)
  100 FORMAT (6E12.4)
  120 READ 150,DEN,TEMP,NNN,ALAM,BAV,GIN,DGG,NTOT,NFAC,(PFAC(I),I=1,6)
  150 FORMAT (2E10.2, I5, 4F10.2, 2I5/6F10.5)
      IF (EOF,60) 577, 170
  170 PRINT 180, DEN, TEMP, NNN, ALAM
  180 FORMAT (1H1,*  DENSITY = *E12.4* TEMPERATURE = *E12.4,
     1    *   QUANTUMNUMBER =*I2*   WAVELENGTH =*F8.2* ANGSTROM*//
     2    13X,*P1*18X,*P2*18X,*B1*18X,*A2*18X,*B2*17X,*STRONG*/)
      IF (NNN.LE.20) GO TO 200
      PRINT 190
  190 FORMAT (* PROGRAM NOT EXECUTED BECAUSE N IS LARGER THAN 20*)
  577 CALL EXIT
  200 SDEN = SQRT(DEN)
      FAC = 2064.936 * TEMP * SQRT(TEMP/DEN)
      NM1 = NNN - 1
      NEVODD = MOD(NNN,2)
      AN = NNN
      AN2 = AN * AN
      AN1M = 0.5 * (AN - 1.)
      CFAC = 4.5645E-7 * AN * SDEN/TEMP
      DEBROG = 2.1027E-6/SQRT(TEMP)
      RMIN = DEBROG + AN*AN*7.9376E-9
      DO 230 K = 1, NNN
      AK = K - 1
  230 SSJ(K)=(AN2+((-1.)**MOD(NM1+K,2))*(AN2-2.*AK*AK))/(2.*AN*(AN2-1.))
      BET = 5.6558E-5 * AN * DEN**(1./6.)
C
C     ARRAY FOR G-FUNCTION CONSTANTS
      ASY = 0.0
      DO 270 K = 1,NM1
      QC = K
      C = CFAC * QC
      P1 = -1.671086 * FAC * C * SQRT(C)
      BS  = 3. * AN * QC * DEBROG/RMIN
      STRONG(K) = 0.269-2.*(((1.-COSF(BS))/BS+SINF(BS))/BS-COSINT(BS))
      PPFF = -1.128379 * FAC * C * C
      P2 = PPFF * (STRONG(K) - 2.*LOGF(2.*C))
      FPAR(1,K) = P1
      FPAR(2,K) = P2
      FPAR(3,K) = 0.5 * (P2/P1)**2
      FIN = LOGF(AN*QC)
      FPAR(4,K) = P2 * ((PFAC(3)*FIN + PFAC(2)) * FIN + PFAC(1))
```

```
      FPAR(5,K) = (PFAC(6)*FIN + PFAC(5))*FIN + PFAC(4)
      FPAR(6,K) = PPFF
  270 ASY = ASY + 2. * FPAR(1,K) * SSJ(K+1)
      PRINT 240,((FPAR(K,I),K = 1,5),STRONG(I), I = 1,NM1)
  240 FORMAT (6E20.4)
      PRINT 280, FAC, CFAC, BET, ASY, DEBROG, NFAC
  280 FORMAT(/* FAC =*E12.4,* CFAC =*E12.4,* BET =*E12.4,* ASY =*E12.4
     1   * DEBROG =*E12.4,* INTEGRATIONFACTOR =*I2//
     2   5X*DOM*8X*DLAM*8X*ITOT*6X*IHOLTS*8X*ASY*10X*WING*7X*WHOLTS*7X
     3   *WSTAT*7X*WWOO*8X*WWBB*8X*WWNG*/)
      ADLFAC = 4.23538E-15 * SDEN * ALAM * ALAM
C
C     3JSYMBOL-ARRAYS SSJJ(MCT,NBN,NAN) AND SJQL(MCT,NBN,NLA)
      DO 650 MCT = 1,2
      AMA = MCT - 1
      NLIM = NNN + 1 - MCT
      NQB = -NLIM - 1
      DO 450 NBN = 1,NLIM
      NQB = NQB + 2
      QB = NQB
      FMB1 = (AMA - QB) * 0.5
      FMB2 = (AMA + QB) * 0.5
      DO 325 NLA = 1,NNN
      ALA = NLA - 1
  325 SJQL(MCT,NBN,NLA) = S3J(AN1M,AN1M,ALA,FMB1,FMB2,-AMA)
  450 CONTINUE
      DO 375 NBN = 1,NLIM
      DO 350 NAN = 1,NLIM
      AABB = (-1.)**MOD(NAN+NBN,2) * SJQL(MCT,NBN,2) * SJQL(MCT,NAN,2)
  350 SSJJ(MCT,NBN,NAN) = AABB
  375 CONTINUE
  650 CONTINUE
C
C     3JSYMBOL-ARRAY SAR(NLA,NQC)
      DO 780 NQC = 1,NM1
      QC = NQC
      DO 720 NLA = 1,NNN
      ALA = NLA - 1
      FBB = 0.
      DO 680 NMC = 1,NLA
      IF(NEVODD.NE.MOD(NMC+NQC,2)) GO TO 680
      AMC = NMC - 1
      FCF = 2.
      IF(NMC.EQ.1) FCF = 1.
      FMC1 = 0.5 * (AMC - QC)
      FMC2 = 0.5 * (AMC + QC)
      FBB = FBB + FCF * (S3J(AN1M,AN1M,ALA,FMC1,FMC2,-AMC))**2
  680 CONTINUE
  720 SAR(NLA,NQC) = FBB * (2.*ALA + 1.)
  780 CONTINUE
C
C     CALCULATION OF THE IONFIELD INTEGRAL
      NN6 = 6 * NFAC
      ANN6 = NN6
```

```
      N12 = 12 * NFAC
      AN12 = N12
      N30 = 30 * NFAC
      AN30 = N30
      G = GIN - DGG
      DO 950 MM = 1,NTOT
      G = G + DGG
      DOM = 10. ** G
      DLAM = ADLFAC * DOM
      WING52 = -0.2992067103 * ASY/(SQRT(DOM) * DOM * DOM)
      FHOLTS = 0.
      AWING = 0.
      DO 815 NQC = 1,NM1
      P1 = FPAR(1,NQC)
      P2 = FPAR(2,NQC)
      B1 = FPAR(3,NQC)
      A2 = FPAR(4,NQC)
      B2 = FPAR(5,NQC)
      PPFF = FPAR(6,NQC)
      AWING = AWING + SSJ(NQC+1)*AIMAG(FOUTR(DOM))*2./(DOM*DOM)
      QC = NQC
      BETFAC = BET * QC
      BCRIT = DOM/BETFAC
  815 FHOLTS = FHOLTS + SSJ(NQC + 1) * WFLD(BCRIT) / BETFAC
      AIRES = 0.
      IF(DOM.GT.(-3.*P2)) GO TO 840
      BCRIT = (DOM - P2)/((AN - 1.)*BET)
      DB = BCRIT/ANN6
      B = 0.
      DO 820 J = 1,NN6
      B = B + DB
  820 FF(J) = AIIM(DOM,B) * WFLD(B)
      CALL WEDDLE (DB,NN6,FF,AIII,0.)
      AIRES = AIII
      DY = 1./(BCRIT*AN30)
      Y = 0.
      DO 830 J = 1,N30
      Y = Y + DY
      B = 1./Y
  830 FF(J) = B * B * AIIM(DOM,B) * WFLD(B)
      CALL WEDDLE (DY,N30,FF,AIII,0.)
      AIRES = AIRES + AIII
      GO TO 980
  840 BCRCR = DOM/BET
      EPSPS = -P2/BET
      DO 957 NQ = 1,NM1
      ANQ = NQ
      BCR = BCRCR/ANQ
      EPS = EPSPS/ANQ
      IF(NQ.EQ.1) GO TO 907
      SL1 = 1./(GAM - BCR)
      GO TO 908
  907 SL1 = 0.
  908 SL2 = 1./EPS
```

```
      SL3 = 1./(BCR + EPS)
      SL4 = 1./(BCR - EPS)
      GAM = 0.5 * (BCR - EPS + (BCRCR + EPSPS)/(ANQ + 1.))
      IF(NQ.EQ.NM1) GAM = 0.5 * (BCR - EPS)
      SL5 = 1./(BCR - GAM)
      CRIT = SL2 - SL5
      Y = SL1
      IF(NQ.EQ.1) GO TO 913
      B = BCR + 1./Y
      FA = AIIM(DOM,B) * WFLD(B)/(Y * Y)
      GO TO 914
  913 FA = 0.
  914 DY = (SL2 - SL1)/ANN6
      DO 917 J = 1,NN6
      Y = Y + DY
      Y1 = 1./Y
      B = BCR + Y1
  917 FF(J) = Y1 * Y1 * AIIM(DOM,B) * WFLD(B)
      CALL WEDDLE (DY,NN6,FF,AIII,FA)
      AIRES = AIRES + AIII
      Y = SL3
      B = 1./Y
      FA = B * B * AIIM(DOM,B) * WFLD(B)
      DY = (SL4 - SL3)/ANN6
      DO 927 J = 1,NN6
      Y = Y + DY
      B = 1./Y
  927 FF(J) = B * B * AIIM(DOM,B) * WFLD(B)
      CALL WEDDLE (DY,NN6,FF,AIII,FA)
      AIRES = AIRES + AIII
      IF(CRIT.LE.0.) GO TO 977
      Y = SL5
      B = BCR - 1./Y
      FA = AIIM(DOM,B) * WFLD(B)/(Y * Y)
      DY = CRIT/AN12
      DO 937 J = 1,N12
      Y = Y + DY
      Y1 = 1./Y
      B = BCR - Y1
  937 FF(J) = Y1 * Y1 * AIIM(DOM,B) * WFLD(B)
      CALL WEDDLE (DY,N12,FF,AIII,FA)
  957 AIRES = AIRES + AIII
      IF(GAM.LT. 5.) GO TO 968
      Y = 1./GAM
      FA = GAM * GAM * AIIM(DOM,GAM) * WFLD(GAM)
      DY = (0.2 - Y)/AN12
      DO 967 J = 1,N12
      Y = Y + DY
      B = 1./Y
  967 FF(J) = B * B * AIIM(DOM,B) * WFLD(B)
      CALL WEDDLE (DY,N12,FF,AIII,FA)
      AIRES = AIRES + AIII
      SL4 = 0.2
      GO TO 977
```

```
 968   SL4 = 1./GAM
 977   B = 0.
       DB = 1./(SL4 * AN30)
       DO 947 J = 1,N30
       B = B + DB
 947   FF(J) = AIIM(DOM,B) * WFLD(B)
       CALL WEDDLE (DB,N30,FF,AIII,0.)
       AIRES = AIRES + AIII
 980   WING = AIRES/WING52
       WISTAT = AIRES/FHOLTS
       WINHOL = FHOLTS/WING52
       WWOO = (AIIM(DOM, 0.) + FHOLTS)/WING52
       WWBB = (AIIM(DOM,BAV) + FHOLTS)/WING52
       WWNG = (AWING + FHOLTS)/WING52
 950   PRINT 978,DOM,DLAM,AIRES,FHOLTS,WING52,WING,WINHOL,WISTAT,
      2   WWOO, WWBB, WWNG
 978   FORMAT (11E12.4)
       GO TO 120
       END
C
       FUNCTION AIIM(DOM,B)
C
C      CALCULATION OF I(DOM,B)
       COMPLEX DFTR(20),AMATR(20,40),FOUTR,AREF
       COMMON/FDAT/P1,P2,B1,A2,B2,PPFF
       COMMON/PSTR/NNN,NM1,BET,FPAR(6,20)
       COMMON/PSJD/SSJJ(2,20,20), SJQL(2,20,20), SAR(20,20)
       AIIM = 0.
       DO 800 MCT = 1,2
       AMCT = MCT
       NLIM = NNN + 1 - MCT
       NL22 = 2 * NLIM
       NQB = -NLIM - 1
       DO 750 NBN = 1,NLIM
       NQB = NQB + 2
       QB = NQB
       DOMRB = DOM - BET * QB * B
       DO 220 NQC = 1,NM1
       P1 = FPAR(1,NQC)
       P2 = FPAR(2,NQC)
       B1 = FPAR(3,NQC)
       A2 = FPAR(4,NQC)
       B2 = FPAR(5,NQC)
       PPFF = FPAR(6,NQC)
 220   DFTR(NQC) = FOUTR(DOMRB)
       DO 700 NAN = 1,NLIM
       AREF = (0.,0.)
       DO 600 NQC = 1,NM1
       FAA = 0.0
       DO 500 NLA = 1,NNN
 500   FAA = FAA + SJQL(MCT,NAN,NLA) * SJQL(MCT,NBN,NLA) * SAR(NLA,NQC)
 600   AREF = AREF + FAA * DFTR(NQC)
       AMATR(NBN,NAN + NLIM) = (0.,0.)
 700   AMATR(NBN,NAN) = 6.2831853072 * ((-1.)**MOD(NAN+NBN,2)) * AREF
```

```
      AMATR(NBN,NBN+NLIM) = (1.,0.)
  750 AMATR(NBN,NBN) = AMATR(NBN,NBN) + DOMRB
C     MATRIX INVERSION
      CALL CGAUSSEL(AMATR,20,NLIM,NL22,NRANK)
      DO 795 NBN = 1,NLIM
      DO 793 NAN = 1,NLIM
  793 AIIM = AIIM + AMCT*SSJJ(MCT,NBN,NAN)*AIMAG(AMATR(NBN,NAN+NLIM))
  795 CONTINUE
  800 CONTINUE
      AIIM =-AIIM * 0.3183099
      RETURN
      END
C
C     THE FOLLOWING FUNCTION FOUTR MAY BE REPLACED BY THE FUNCTION FOUTR
C     AT THE END OF THE LISTING TO OBTAIN THE MODIFIED IMPACTTHEORY
      FUNCTION FOUTR (DOM)
C
C     FOURIERTRANSFORM OF THERMAL AVERAGE FOR UNIFIED THEORY
      COMPLEX FOUTR
      COMMON/FDAT/P1,P2,B1,A2,B2,PPFF
      ARG = ABSF(DOM)
      Z = B1 * ARG
      IF (Z.LE.0.001) GO TO 600
      IF (Z.LE.40.) GO TO 300
      FAC1 = -0.2992067103 * P1/(SQRT(ARG) * ARG * ARG)
      CC = FAC1 * ((1. - 1.3125/Z)*0.625/Z + 1.)
      SS = FAC1 * ((-1.- 1.3125/Z)*0.625/Z + 1.)
      GO TO 500
  300 CALL BSJYO1 (Z, AJO, YO, AJ1, Y1)
      FAC1 = Y1/(2.*Z) + AJ1 - YO
      FAC2 = AJO + Y1 - AJ1/(2.*Z)
      CINE = COSF(Z)
      SINE = SINF(Z)
      CC = P2 * B1 * B1 * (CINE * FAC1 + SINE * FAC2)
      SS = P2 * B1 * B1 * (CINE * FAC2 - SINE * FAC1)
      IF (A2.EQ.0.) GO TO 500
      Z = B2 * ARG
      IF (Z.GT.10.) GO TO 400
      CALL BSJYO1 (Z, AJO, YO, AJ1, Y1)
      FAC1 = ((AJ1-YO)*16.*Z-36.*AJO-28.*Y1)*Z+15.*YO-3.*AJ1
      FAC2 = ((AJO+Y1)*16.*Z-36.*YO+28.*AJ1)*Z-15.*AJO-3.*Y1
      CINE = COSF(Z)
      SINE = SINF(Z)
      CC = CC + A2*B2*(CINE * FAC1 + SINE * FAC2)/6.
      SS = SS + A2*B2*(CINE * FAC2 - SINE * FAC1)/6.
      GO TO 500
  400 FAC1 = 0.1322319336 * A2 * B2 * Z**(-3.5)
      CC = CC + FAC1 * (1. - (3.9375/Z + 1.)*4.375/Z)
      SS = SS - FAC1 * (1. - (3.9375/Z - 1.)*4.375/Z)
  500 IF (DOM.LT.0.) SS = -SS
      FOUTR = ARG * ARG * CMPLX(-SS,CC)
      RETURN
  600 SS = (P2*B1 - A2) * DOM
      FOUTR = 0.3183099 * CMPLX(SS,-P2)
```

```
      RETURN
      END
C
      SUBROUTINE WEDDLE (DX, N, F, A, FO)
C
C     INTEGRATION SUBROUTINE
      DIMENSION F(N)
    1 A = 0.0
    2 K = N - 1
    3 DO 15 I = 1, 6
    4 SUM = 0.0
    5 DO 6 J = I, K, 6
    6 SUM = SUM + F(J)
    7 GO TO (8, 10, 12, 10, 8, 14), I
    8 A = A + 5.0 * SUM
    9 GO TO 15
   10 A = A + SUM
   11 GO TO 15
   12 A = A + 6.0 * SUM
   13 GO TO 15
   14 A = A + 2.0 * SUM
   15 CONTINUE
   16 A = 0.3 * DX * (A + FO + F(N))
   17 RETURN
      END
      FUNCTION WFLD(B)
C
C     CALCULATION OF THE ION MICROFIELD DISTRIBUTION FUNCTION USING A
C     5POINT INTERPOLATION FOR THE DATA READ INTO THE MAINPROGRAM
      COMMON/PFW/FIELD(301)
      WFLD = 0.0
      IF (B.LE.30.0) GO TO 200
      SBS = 1./(B * SQRT(B))
      WFLD = ((21.6 * SBS + 7.639) * SBS + 1.496) * SBS/B
      RETURN
  200 IF (B.LE.0.0) RETURN
      J = (B + 0.2) * 10.0
      L = J - 1
      IF (J.GT.2) L = J - 2
      IF (J.GT.3) L = J - 3
      IF (J.GT.300) L = 297
   70 LLL = L + 4
      DO 75 K = L,LLL
      AK = K - 1
      TERM = 1.0
      DO 74 M = L,LLL
      IF (K.EQ.M) GO TO 74
      AM = M - 1
      TERM = TERM * (10.*B - AM)/(AK - AM)
   74 CONTINUE
      TERM = TERM * FIELD(K)
   75 WFLD = WFLD + TERM
      RETURN
      END
```

```
C
      FUNCTION S3J (FJ1, FJ2, FJ3, FM1, FM2, FM3 )
C
C     CALCULATION OF 3J-SYMBOL
      S3J=0.0
      IF(ABS(FM1 + FM2 + FM3) .GT. 0.001) GO TO 153
      FM3=FM1+FM2
      A=FJ2+FJ3+FM1+.005
      B=FJ1-FM1+.005
      C=-FJ1+FJ2+FJ3+.005
      D=FJ3+FM3+.005
      E=FJ1-FJ2-FM3+.005
      F=FJ1-FJ2+FJ3+.005
      G=FJ1+FJ2-FJ3+.005
      H=FJ1+FJ2+FJ3+1.0+.005
      E2=FCTRL(B)*FCTRL(FJ1+FM1)*FCTRL(FJ2-FM2)*FCTRL(FJ2+FM2)
      IF (E2) 153,153,145
  145 E1=(FCTRL(C)*FCTRL(F)/FCTRL(H))*FCTRL(G)*FCTRL(D)*FCTRL(FJ3-FM3)
      IF (E1) 153, 153, 150
  150 E1=SQRT(E2)/SQRT(E1)
      I1=XMAX1F(0.0, -E+0.01)
      I2=XMIN1F(A, C, D)
      IF (I2-I1) 153, 151, 151
  151 DO 152 I=I1,I2
      FI=I
      E2=FCTRL(FI)*FCTRL(C-FI)*FCTRL(D-FI)/FCTRL(A-FI)
  152 S3J=S3J+(((-1.0)**XMODF(I,2))/E2)*FCTRL(B+FI)/FCTRL(E+FI)
      U=ABS(FJ1+FM2+FM3)+0.001
      S3J=S3J*((-1.0)**XMODF(XFIXF(U),2))/E1
      FM3=-FM3
  153 RETURN
      END
C
      FUNCTION FCTRL(A)
C
C     CALCULATION OF FACTORIALS REQUIRED BY FUNCTION S3J
      DIMENSION FCTI(20)
C
      DATA ((FCTI(I),I=1,20) =1.0,2.0,6.0,24.0,120.0,720.0,5040.0,
     1  40320.0,362880.0,3628800.0,39916800.0,479001600.0,
     2  6227020800.0,87178291200.0,1307674368000.0,
     3  2.0922789888E13, 3.55687428096E14, 6.402373705728E15,
     4  1.2164510040883 E17, 2.4329020081766 E18)
C
      IF(A) 50,60,70
   50 IF(A.GE.(-0.1) ) GO TO 60
      FCTRL = 0.0
      RETURN
   60 FCTRL = 1.0
      RETURN
   70 I = A + 0.1
      IF ( I .EQ. 0) GO TO 60
      IF (I-20) 140,140,130
  130 F=20.0
```

```
      FCTRL=FCTI(20)
      DO 131 J=21,I
      F=F+1.0
  131 FCTRL=FCTRL*F
      GO TO 150
  140 FCTRL=FCTI(I)
  150 RETURN
      END
C
      SUBROUTINE CGAUSSEL(C,NRD,NRR,NCC,NSF)
C
      DIMENSION C(NRD,NCC),L(128,2)
      TYPE COMPLEX C,DET,P,D,Q,R
      DATA (BITS = 1755 4000 0000 0000 B)
      CALL ROLLCALL(48HCGAUSSEL 6/5/68 1-BANK BITS=2**-18                )
      NR=NRR $ NC=NCC
      IF(NC.LT.NR.OR.NR.GT.128.OR.NR.LE.0) CALL Q8QERROR(0,9HBAD CALL.)
C     INITIALIZE.
      NSF=0
      NRM=NR-1 $ NRP=NR+1 $ D=(1.,0.) $ LSD=1
      DO 1 KR=1,NR
      L(KR,1)=KR
1     L(KR,2)=0
      CALL Q9EXUN(EXUN)
      IF(NR.EQ.1) GO TO 42
C     ELIMINATION PHASE.
      DO 41 KP=1,NRM
      KPP=KP+1 $ PM=0. $ MPN=0
C     SEARCH COLUMN KP FROM DIAGONAL DOWN, FOR MAX PIVOT.
      DO 2 KR=KP,NR
      LKR=L(KR,1)
      PT=CABS(C(LKR,KP))
      IF(PT.LE.PM) GO TO 2
      PM=PT $ MPN=KR $ LMP=LKR
2     CONTINUE
C     IF MAX PIVOT IS ZERO, MATRIX IS SINGULAR.
      IF(MPN.EQ.0) GO TO 9
      NSF=NSF+1
      IF(MPN.EQ.KP) GO TO 3
C     NEW ROW NUMBER KP HAS MAX PIVOT.
      LSD=-LSD
      L(KP,2)=L(MPN,1)=L(KP,1)
      L(KP,1)=LMP
C     ROW OPERATIONS TO ZERO COLUMN KP BELOW DIAGONAL.
3     MKP=L(KP,1)
      P=C(MKP,KP) $ D=D*P
      DO 41 KR=KPP,NR
      MKR=L(KR)
      Q=C(MKR,KP)/P
      IF(REAL(Q).EQ.0..AND.AIMAG(Q).EQ.0.) GO TO 41
C     SUBTRACT Q * PIVOT ROW FROM ROW KR.
      DO 4 LC=KPP,NC
      R=Q*C(MKP,LC)
      C(MKR,LC)=C(MKR,LC)-R
```

```
4       IF(CABS(C(MKR,LC)).LT.CABS(R)*BITS) C(MKR,LC)=(0.,0.)
41      CONTINUE
C       LOWER RIGHT HAND CORNER.
42      LNR=L(NR,1) $ P=C(LNR,NR)
        IF(REAL(P).EQ.0..AND.AIMAG(P).EQ.0.) GO TO 9
        NSF=NSF+1
        D=D*P*LSD
        IF(NR.EQ.NC) GO TO 8
C       BACK SOLUTION PHASE.
        DO 61 MC=NRP,NC
        C(LNR,MC)=C(LNR,MC)/P
        IF(NR.EQ.1) GO TO 61
        DO 6 LL=1,NRM
        KR=NR-LL $ MR=L(KR,1) $ KRP=KR+1
        DO 5 MS=KRP,NR
        LMS=L(MS,1)
        R=C(MR,MS)*C(LMS,MC)
        C(MR,MC)=C(MR,MC)-R
5       IF(CABS(C(MR,MC)).LT.CABS(R)*BITS) C(MR,MC)=(0.,0.)
6       C(MR,MC)=C(MR,MC)/C(MR,KR)
61      CONTINUE
C       SHUFFLE SOLUTION ROWS BACK TO NATURAL ORDER.
        DO 71 LL=1,NRM
        KR=NR-LL
        MKR=L(KR,2)
        IF(MKR.EQ.0) GO TO 71
        MKP=L(KR,1)
        DO 7 LC=NRP,NC
        Q=C(MKR,LC)
        C(MKR,LC)=C(MKP,LC)
7       C(MKP,LC)=Q
71      CONTINUE
C       NORMAL AND SINGULAR RETURNS.  GOOD SOLUTION COULD HAVE D=0.
8       C(1,1)=D $ GO TO 91
9       C(1,1)=(0.,0.)
91      CALL S9FAULT(EXUN) $ RETURN
        END
C
        SUBROUTINE BSJY01 (X, AJ0, Y0, AJ1, Y1)
C
C       CALCULATION OF THE BESSEL FUNCTIONS J0, Y0, J1, AND Y1 FOR AN
C       ARGUMENT X
        DIMENSION A(7), B(7), C(7), D(7), E(7), F(7), G(7), H(7)
        DATA ((A(I), I = 1,7) =  0.00021, -0.0039444, 0.0444479,
     1    -0.3163866, 1.2656208, -2.2499997, 1.0)
        DATA ((B(I), I = 1,7) = -0.00024846, 0.00427916, -0.04261214,
     1    0.25300117, -0.74350384, 0.60559366, 0.36746691)
        DATA ((C(I), I = 1,7) =  0.00014476, -0.00072805, 0.00137237,
     1    -0.00009512, -0.0055274, -0.00000077, 0.79788456)
        DATA ((D(I), I = 1,7) =  0.00013558, -0.00029333, -0.00054125,
     1    0.00262573, -0.00003954, -0.04166397, -0.78539816)
        DATA ((E(I), I = 1,7) =  0.00001109, -0.00031761, 0.00443319,
     1    -0.03954289, 0.21093573, -0.56249985, 0.5)
        DATA ((F(I), I = 1,7) =  0.0027873, -0.0400976, 0.3123951,
```

```
     1   -1.3164827, 2.1682709, 0.2212091, -0.6366198)
      DATA ((G(I), I = 1,7) = -0.00020033, 0.00113653, -0.00249511,
     1   0.00017105, 0.01659667, 0.00000156, 0.79788456)
      DATA ((H(I), I = 1,7) = -0.00029166, 0.00079824, 0.00074348,
     1   -0.00637879, 0.0000565, 0.12499612, -2.35619449)
      AX = ABSF(X)
      IF (AX.GT.0.0) GO TO 10
      AJO = 1.0
      YO = -1.E+030
      AJ1 = 0.0
      Y1 = -1.E+030
      RETURN
 10   IF (AX.GT.3.0) GO TO 50
      XX = (AX/3.0) ** 2
      AJO = A(1)
      YO = B(1)
      AJ1 = E(1)
      Y1 = F(1)
      DO 20 M = 2,7
      AJO = AJO * XX + A(M)
      YO = YO * XX + B(M)
      AJ1 = AJ1 * XX + E(M)
 20   Y1 = Y1 * XX + F(M)
      AJ1 = AJ1 * X
      ALF = 0.6366197724 * LOGF(0.5 * AX)
      YO = YO + ALF * AJO
      Y1 = Y1/X + ALF * AJ1
      RETURN
 50   X3 = 3.0/AX
      FO = C(1)
      THO = D(1)
      F1 = G(1)
      TH1 = H(1)
      DO 60 M = 2,7
      FO = FO * X3 + C(M)
      THO = THO * X3 + D(M)
      F1 = F1 * X3 + G(M)
 60   TH1 = TH1 * X3 + H(M)
      THO = THO + AX
      TH1 = TH1 + AX
      XS = 1./SQRT(AX)
      AJO= XS * FO * COSF(THO)
      YO = XS * FO * SINF(THO)
      AJ1= XS * F1 * COSF(TH1)
      Y1 = XS * F1 * SINF(TH1)
      RETURN
      END
C
      FUNCTION COSINT(X)
C
C     CALCULATION OF THE COSINE INTEGRAL
      TYPE DOUBLE Y2,PROD,SUM,PT,DK
      IF(X.LE.0.) GO TO 50
      X2 = X * X
```

```
      IF(X.GT.20.) GO TO 30
      Y2 = DBLE(X2)
      PROD = -Y2 * 0.5
      SUM = PROD * 0.5
      DO 10 K = 2,50
      DK = 2 * K
      PROD = -PROD * Y2/(DK*(DK - 1.))
      SUM = SUM + PROD/DK
      PT = ABS(PROD * 1.D+10)
      IF(ABS(SUM).GT.PT) GO TO 20
   10 CONTINUE
   20 SS = SNGL(SUM)
      COSINT = SS  + 0.5772156649 + LOGF(X)
      RETURN
   30 FA = 1.
      FB = 1.
      PO = 1.
      X2 = 1./X2
      DO 40 K = 1,10
      AK = 2 * K
      PO = -PO * AK * X2
      FA = FA + PO
      PO = PO * (AK + 1.)
      FB = FB + PO
      PA = ABS(PO * 1.E+10)
      IF(PA.LE.FB) GO TO 45
   40 CONTINUE
   45 FX = FA/X
      GX = FB * X2
      COSINT = FX * SIN(X) - GX * COS(X)
      RETURN
   50 WRITE (61,100) X
  100 FORMAT (* X LESS OR EQUAL TO ZERO, X = *E17.9)
      RETURN
      END
C
      FUNCTION FOUTR (DOM)
C
C     FOURIERTRANSFORM OF THERMAL AVERAGE FOR MODIFIED IMPACTTHEORY
      COMPLEX FOUTR
      COMMON/FDAT/P1,P2,B1,A2,B2,PPFF
      ARG = ABSF(DOM)
      CC = P2
      IF (ARG.GT.1.22474) CC = P2 - 2.*LOGF(ARG/1.22474)*PPFF
      FOUTR = 0.3183099 * CMPLX(0.,-CC)
      RETURN
      END
```

REFERENCES

F. Abramowitz and I. A. Stegun, Handbook of Mathematical Functions ed. by M. Abramowitz and I. Stegun (NBS Applied Mathematics Series 55, 1969).

P. W. Anderson and J. D. Talman, Proceedings of the Conf. on the Broadening of Spectral Lines, p. 29, Pittsburgh 1955, also Bell Telephone System Monograph 3117.

M. E. Bacon and D. F. Edwards, Phys. Rev. 170, 125 (1968).

M. Bacon, K. Y. Shen and J. Cooper, Phys. Rev., to be published.

M. Baranger, Phys. Rev. 111, 494 (1958); 112, 855 (1958).

M. Baranger and B. Mozer, Phys. Rev. 115, 521 (1959); 118, 626 (1960).

M. Baranger, Atomic and Molecular Processes p. 493, ed. D. R. Bates (New York, Academic Press 1962).

H. Bateman, Higher Transcendental Functions Vol. II (McGraw Hill, New York, 1953).

R. D. Bengtson, P. Kepple and J. D. Tannich, to be published.

A. Bethe and E. Salpeter, Quantum Mechanics of One-and Two-Electron Atoms (Springer Verlag, Berlin 1957).

J. W. Birkeland, J. P. Oss and W. G. Braun, Phys. Rev. 178, No. 1, 368 (1969).

G. Boldt and W. S. Cooper, Z. Naturforschung 19a, 968 (1964).

W. R. Chappell, J. Cooper and E. W. Smith, J.Q.S.R.T. 9, 149 (1969).

J. Cooper, Phys. Rev. Letters 17, 991 (1966).

J. Cooper, Rev. Mod. Phys. 39, 167 (1967).

A. R. Edmonds, Angular Momentum in Quantum Mechanics (Princeton University Press 1960).

F. N. Edmonds, H. Schlüter and D. C. Wells, Mem. Roy. Astr. Soc. 71, 271 (1967).

R. C. Elton and H. R. Griem, Phys. Rev. 135, A1550 (1964).

E. Ferguson and H. Schlüter, Ann. Phys. 22, 351 (1963).

J. B. Gerardo and R. A. Hill, Phys. Rev. Lett. 17, 623 (1966).

H. R. Griem, A. C. Kolb and K. Y. Shen, Phys. Rev. 116, 4 (1959).

H. R. Griem, Astrophys. J. 136, 422 (1962).

H. R. Griem, A. C. Kolb and K. Y. Shen, Astrophys. J. 135, 272 (1962).

H. R. Griem, Phys. Rev. 140, A1140 (1965).

H. R. Griem, Astrophys. J. 147, 1092, (1967).

H. R. Griem, Astrophys. J. 148, 547 (1967).

C. F. Hooper, Phys. Rev. 165, 215 (1968).

C. F. Hooper, Phys. Rev. 169, 193 (1968).

J. W. B. Hughes, Proc. Phys. Soc. 91, 810 (1967).

P. Kepple and H. R. Griem, Phys. Rev. 173, 317 (1968).

M. Lewis, Phys. Rev. 121, 501 (1961).

E. Merzbacher, Quantum Mechanics, Chap. 16 (J. Wiley, New York 1961).

H. Pfennig, E. Trefftz and C. R. Vidal, J. Q. S. R. T. 6, 557 (1966).

H. Pfennig and E. Trefftz, A. Naturforschung 21a, 697 (1966).

H. Pfennig, Z. Naturforschung 21a, 1648 (1966).

H. Schlüter and C. Avila, Astroph. J. 144, 785, 1966.

K. Y. Shen and J. Cooper, Astroph. J. 155, 37 (1969).

E. W. Smith and C. F. Hooper, Phys. Rev. 157, 126 (1967).

E. W. Smith, C. R. Vidal and J. Cooper, J. Res. Natl. Bur. Std. 73A, 389 (1969).

E. W. Smith, C. R. Vidal and J. Cooper, J. Res. Natl. Bur. Std. 73A, 405 (1969)

E. W. Smith, J. Cooper and C. R. Vidal, Phys. Rev. to be published.

A. Unsöld, Physik der Sternatmosphären (Springer Verlag, Berlin 1955).

H. Van Regemorter, Comptes Rendus 259, 3979 (1964).

C. R. Vidal, Z. Naturforschung 19a, 947 (1964).

C. R. Vidal, Proceedings of the 7th. Intern. Conf. on Phenomena in Ionized Gases, p. 168 Belgrade 1965.

B. Wende, Z. f. Angew, Physik 22, 181, 1967.

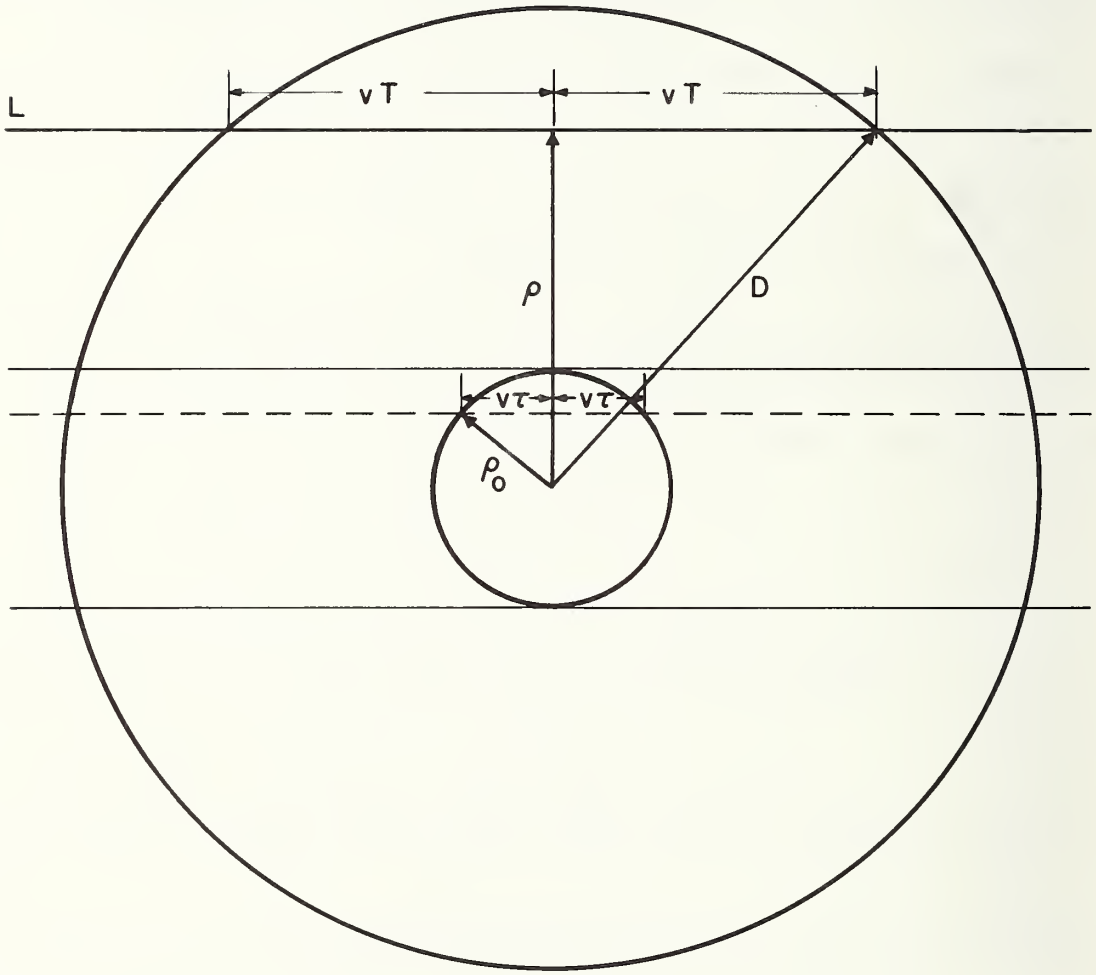

Figure 1. Schematic picture of the collision sphere showing the Debye sphere, a strong collision sphere and a straight line classical path trajectory.

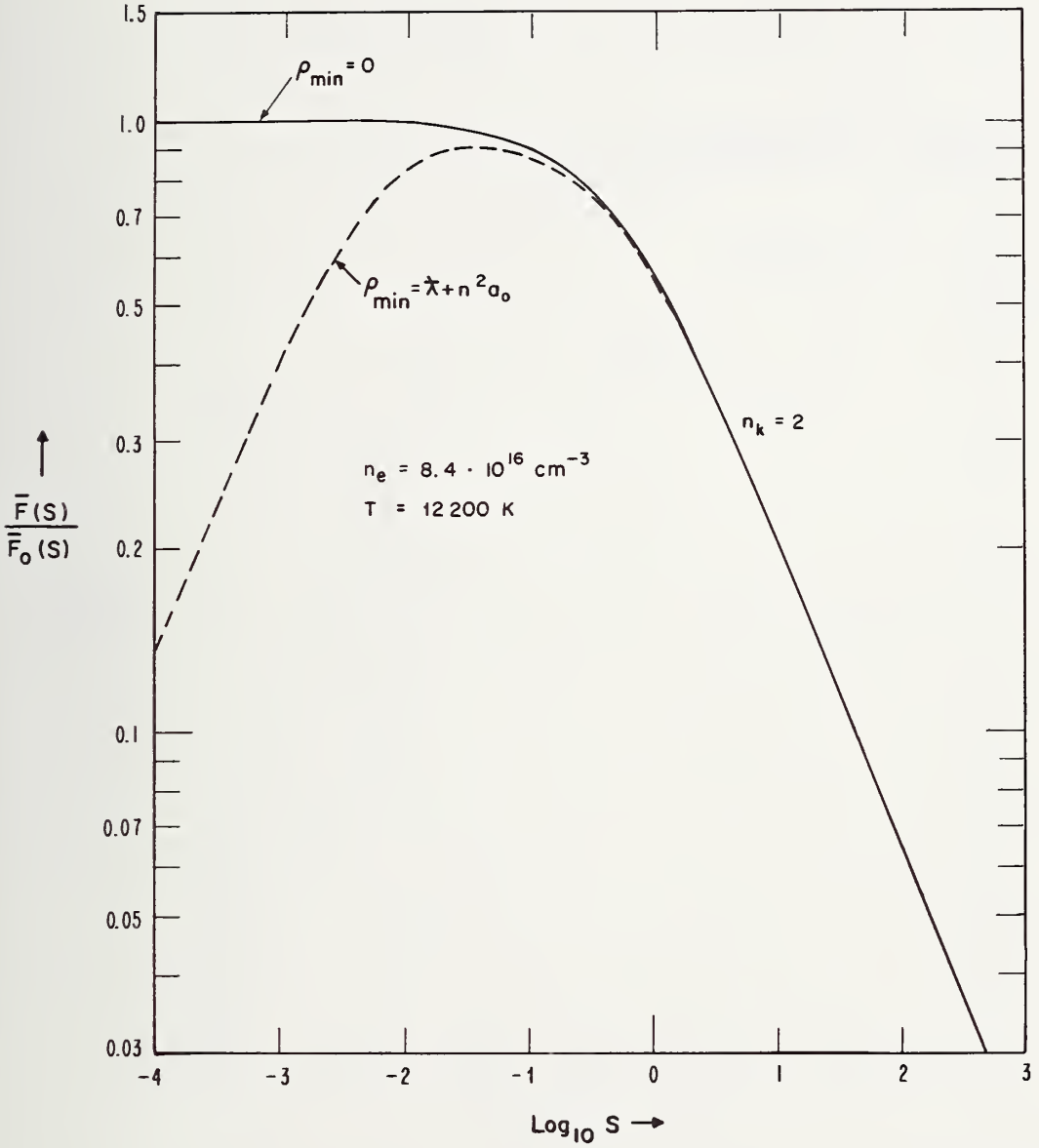

Figure 2. The thermal average $\bar{\bar{F}}$ of the time development operator normalized with respect to the static, small interaction time asymptote $\bar{\bar{F}}_o$ as a function of the normalized time $s = \tilde{\omega}_p \cdot t$. The two curves are obtained with two different lower cutoff parameters in the ρ-integral, $\rho_{min} = 0$ and $\rho_{min} = \pi + n^2 a_o$.

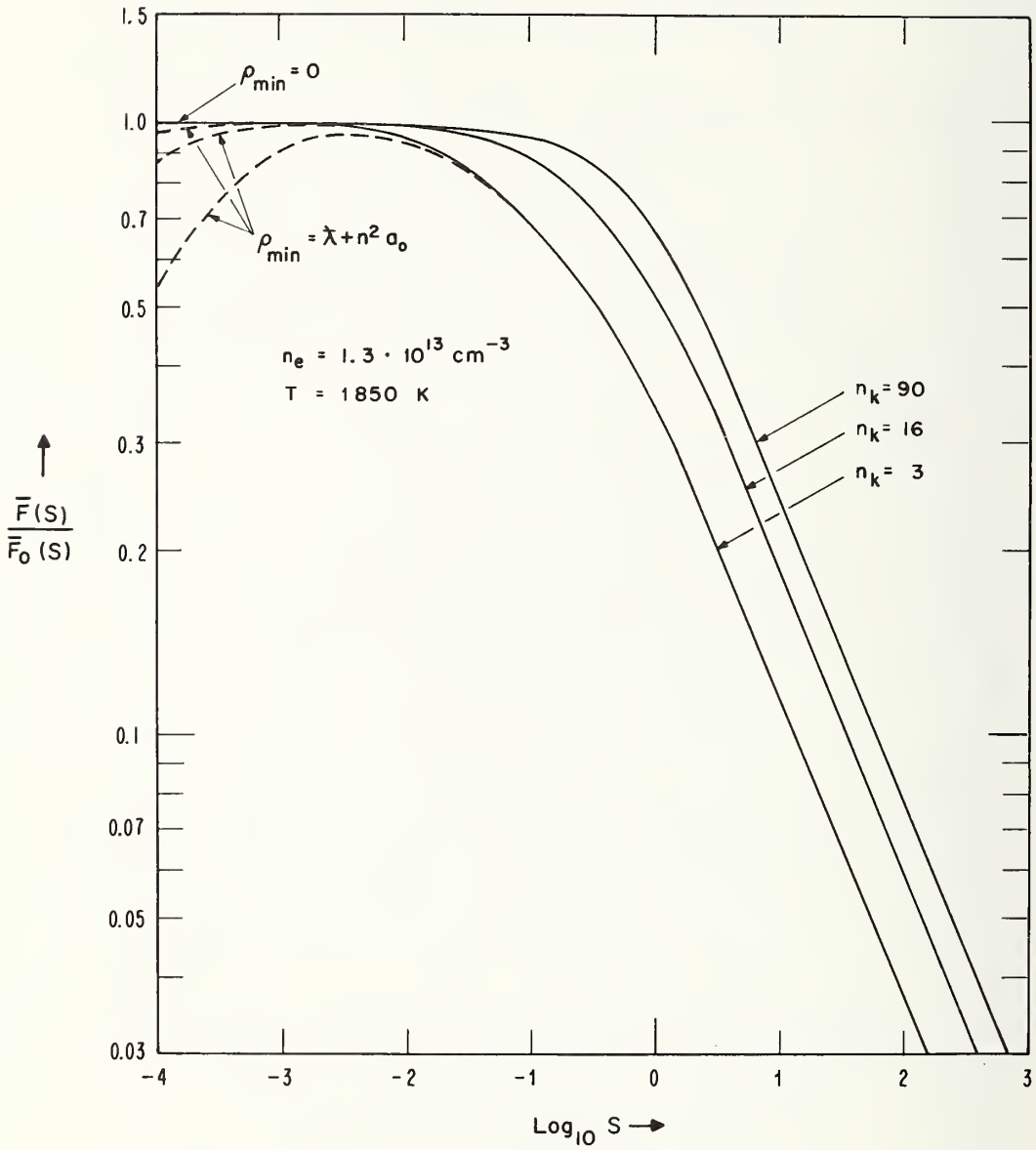

Figure 3. The thermal average $\bar{F}$ of the time development operator normalized with respect to the static, small interaction time asymptote $\bar{F}_o$ as a function of the normalized time $s = \tilde{\omega}_p t$. The two sets of curves are obtained with two different lower cutoff parameters in the ρ-integral, $\rho_{min} = 0$ and $\rho_{min} = \bar{\lambda} + n^2 a_o$. The three different curves in every set correspond to different Stark components characterized by the quantum number $n_k = nq - n'q'$.

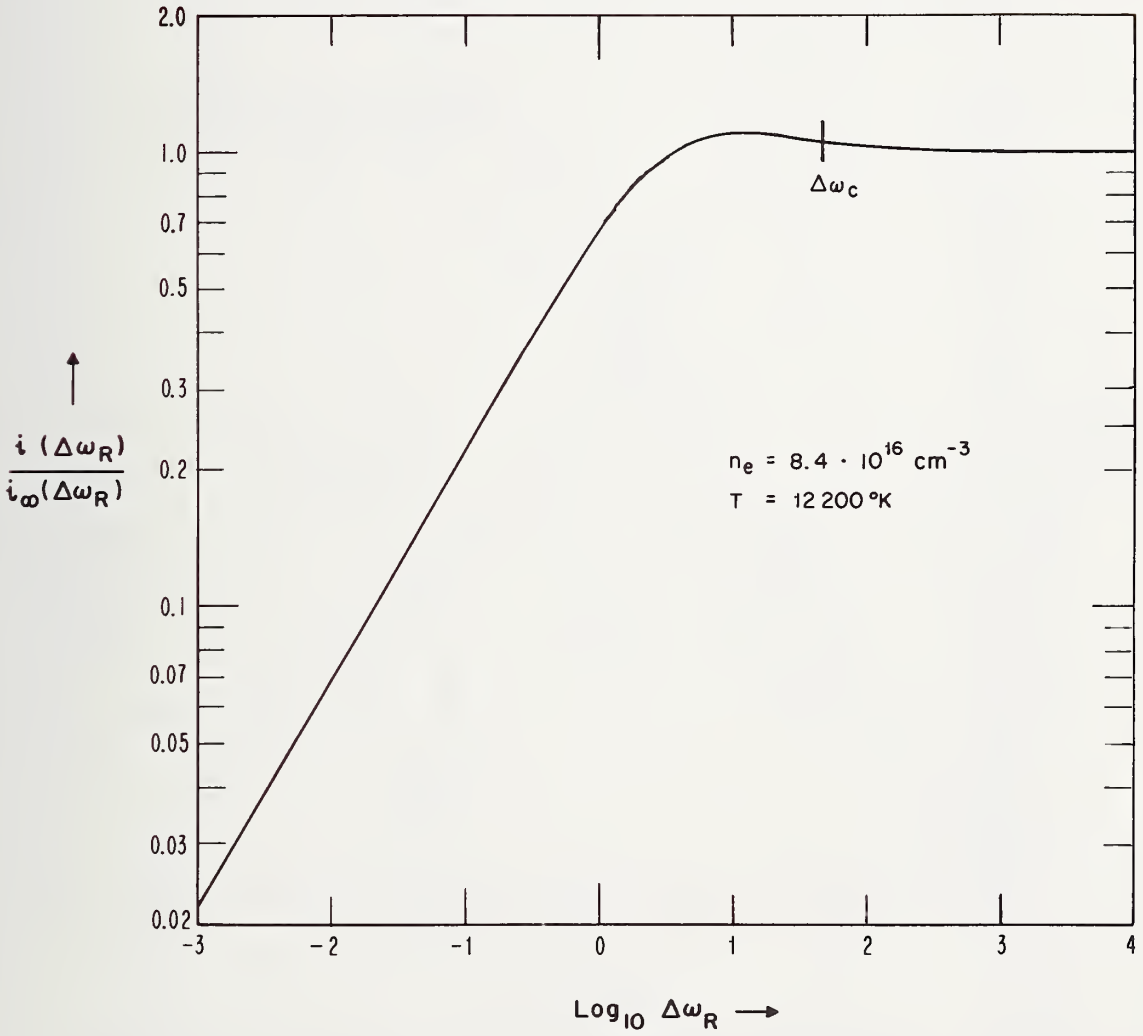

Figure 4. The Fourier transform of the thermal average i, normalized with respect to the static, large frequency limit i_∞ as a function of the normalized frequency $\Delta\omega_R = (\Delta\omega - \Delta\omega_i \cdot \beta)/\tilde{\omega}_p$.

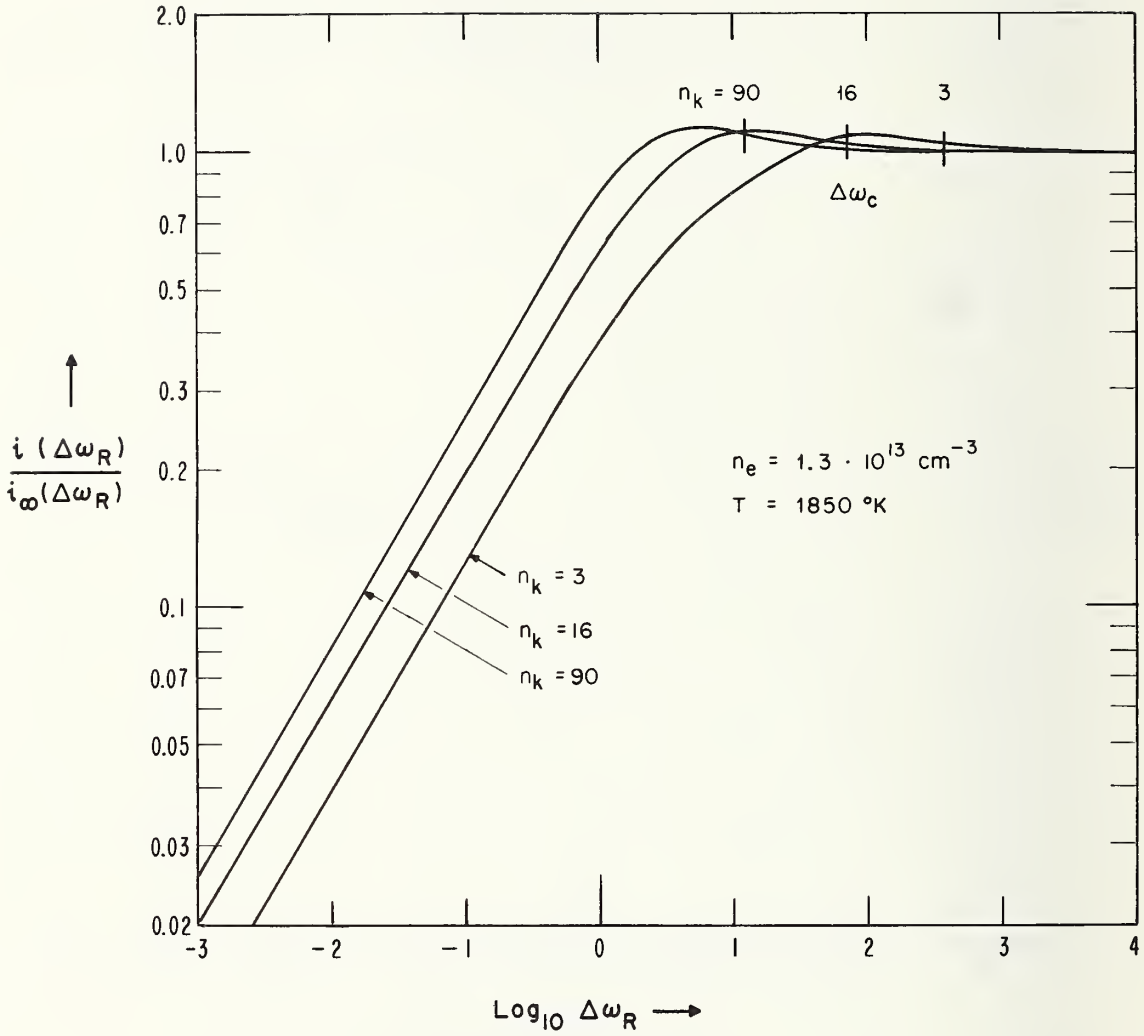

Figure 5. The Fourier transform of the thermal average i, normalized with respect to the static, large frequency limit i_∞ as a function of the normalized frequency $\Delta\omega_R = (\Delta\omega - \Delta\omega_i \cdot \beta)/\tilde{\omega}_p$. The three different curves correspond to different Stark components characterized by the quantum number $n_k = nq - n'q'$.

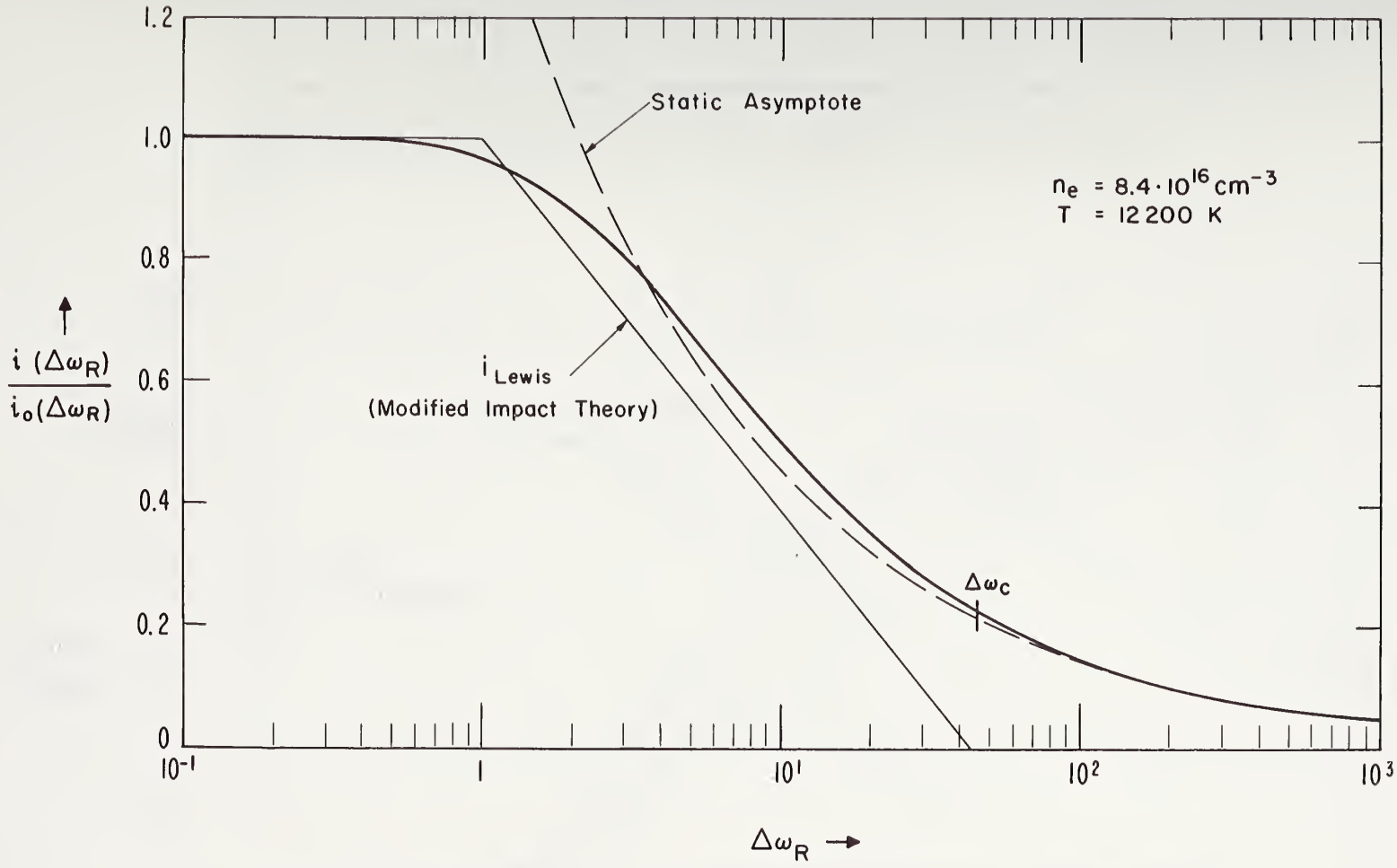

Figure 6. The Fourier transform of the thermal average i, normalized with respect to the small frequency, impact limit i_o as a function of the normalized frequency $\Delta\omega_R = (\Delta\omega - \Delta\omega_i\beta)/\omega_p$.

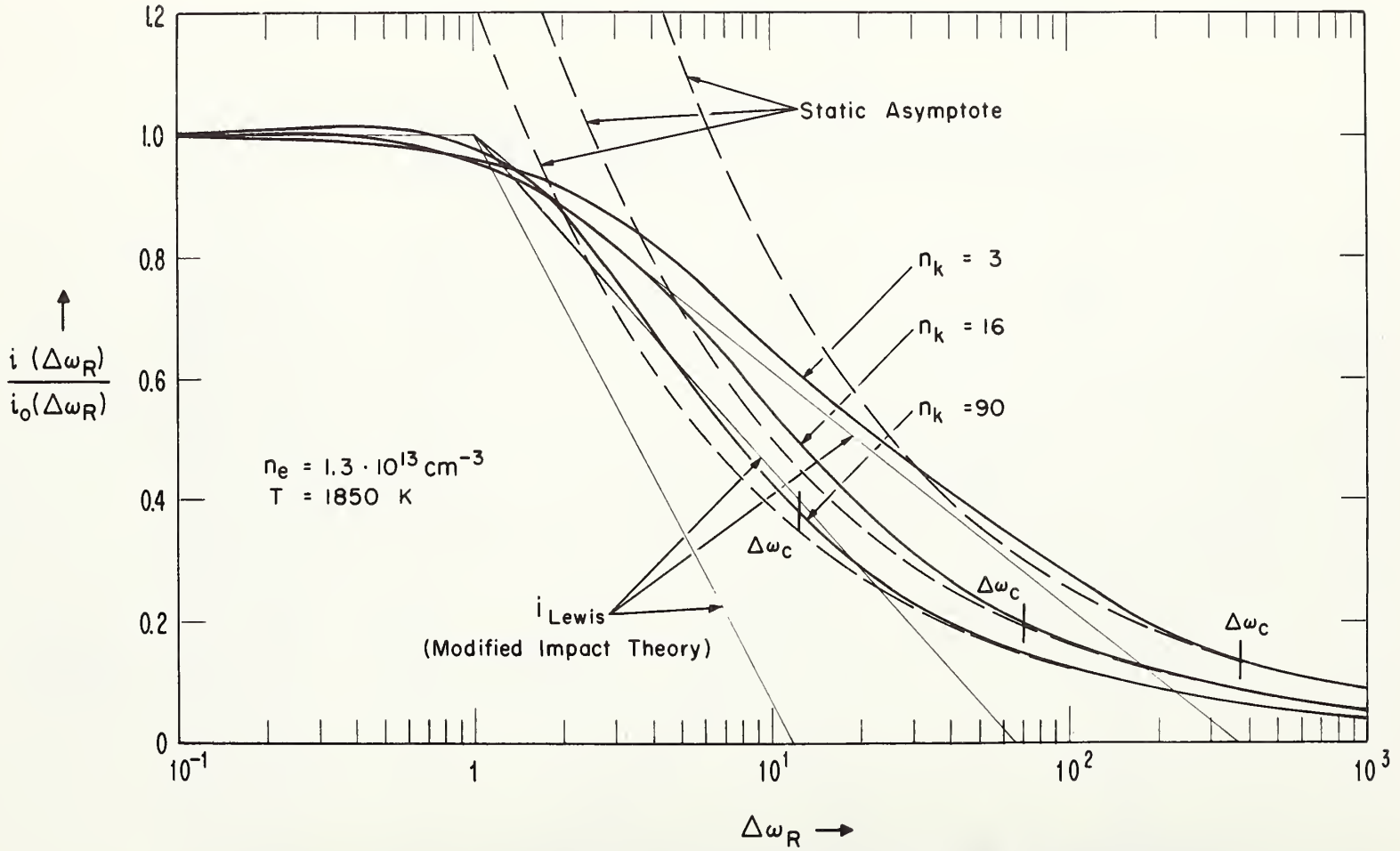

Figure 7. The Fourier transform of the thermal average i, normalized with respect to the small frequency, impact limit i_o as a function of the normalized frequency $\Delta\omega_R = (\Delta\omega - \Delta\omega_i\beta)/\tilde{\omega}_p$. The three sets of curves correspond to different Stark components characterized by the quantum number $n_k = nq - n'q'$.

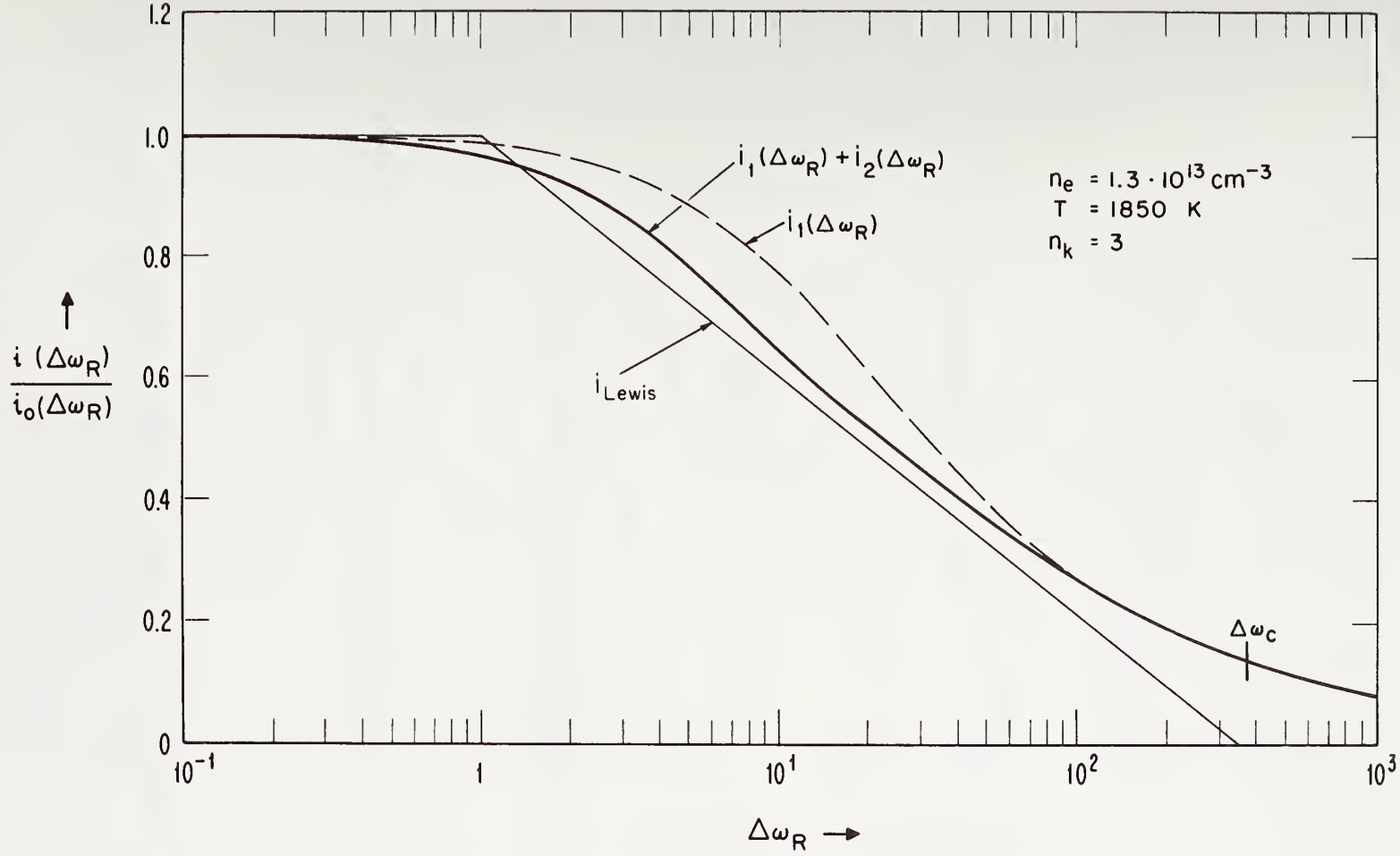

Figure 8. The Fourier transform of the thermal average i, normalized with respect to the small frequency, impact limit i_o is shown as a function of the normalized frequency $\Delta\omega_R = (\Delta\omega - \Delta\omega_i\beta)/\bar{\omega}_p^o$ for a situation where $i_2(\Delta\omega_R)$ defined in Eq. (X.22)) represents an important correction.

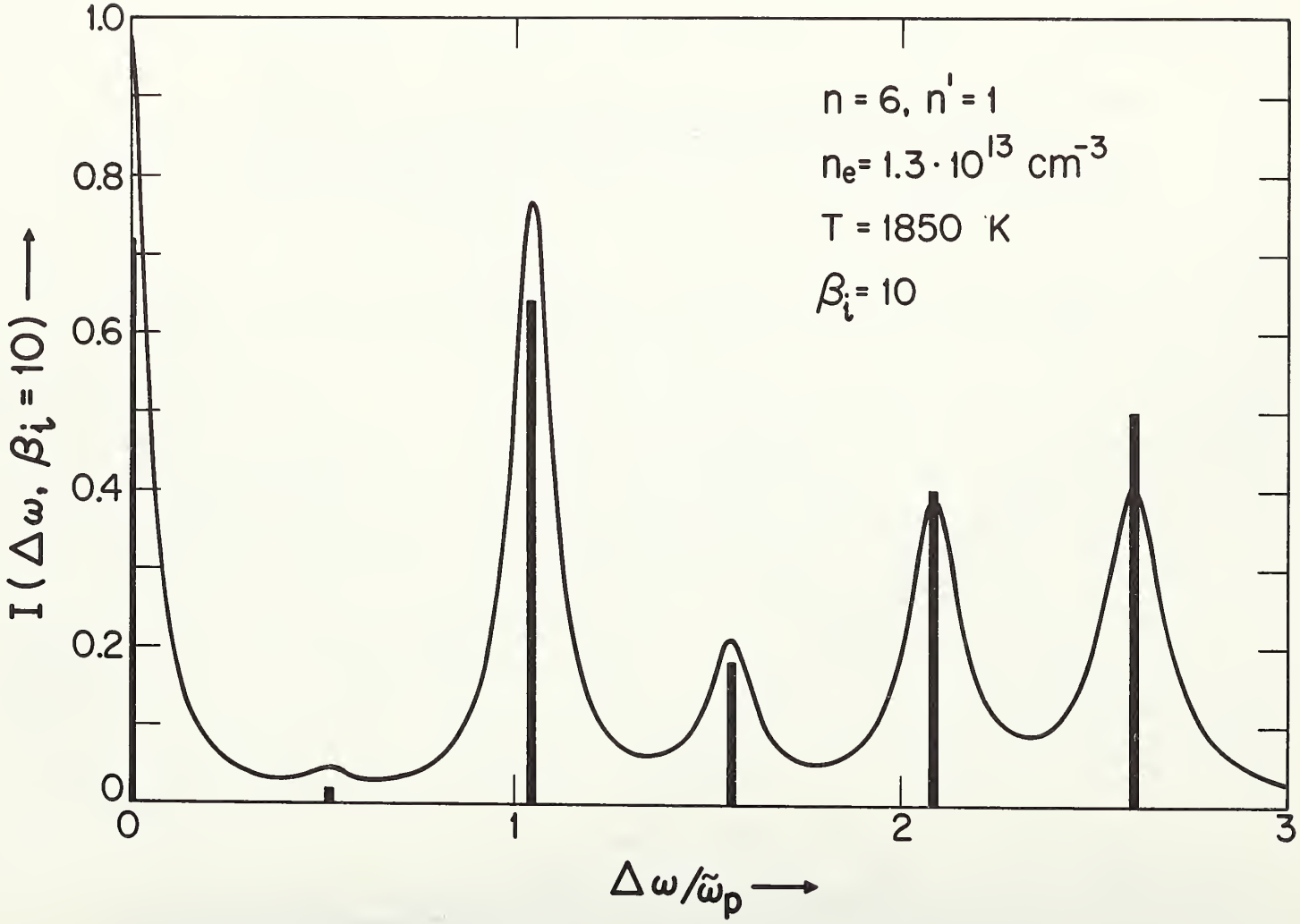

Figure 9. The intensity profile of the Ly_6-line is shown before the final ion field average for a normalized ion field $\beta_i = 10$ demonstrating the electron broadening.

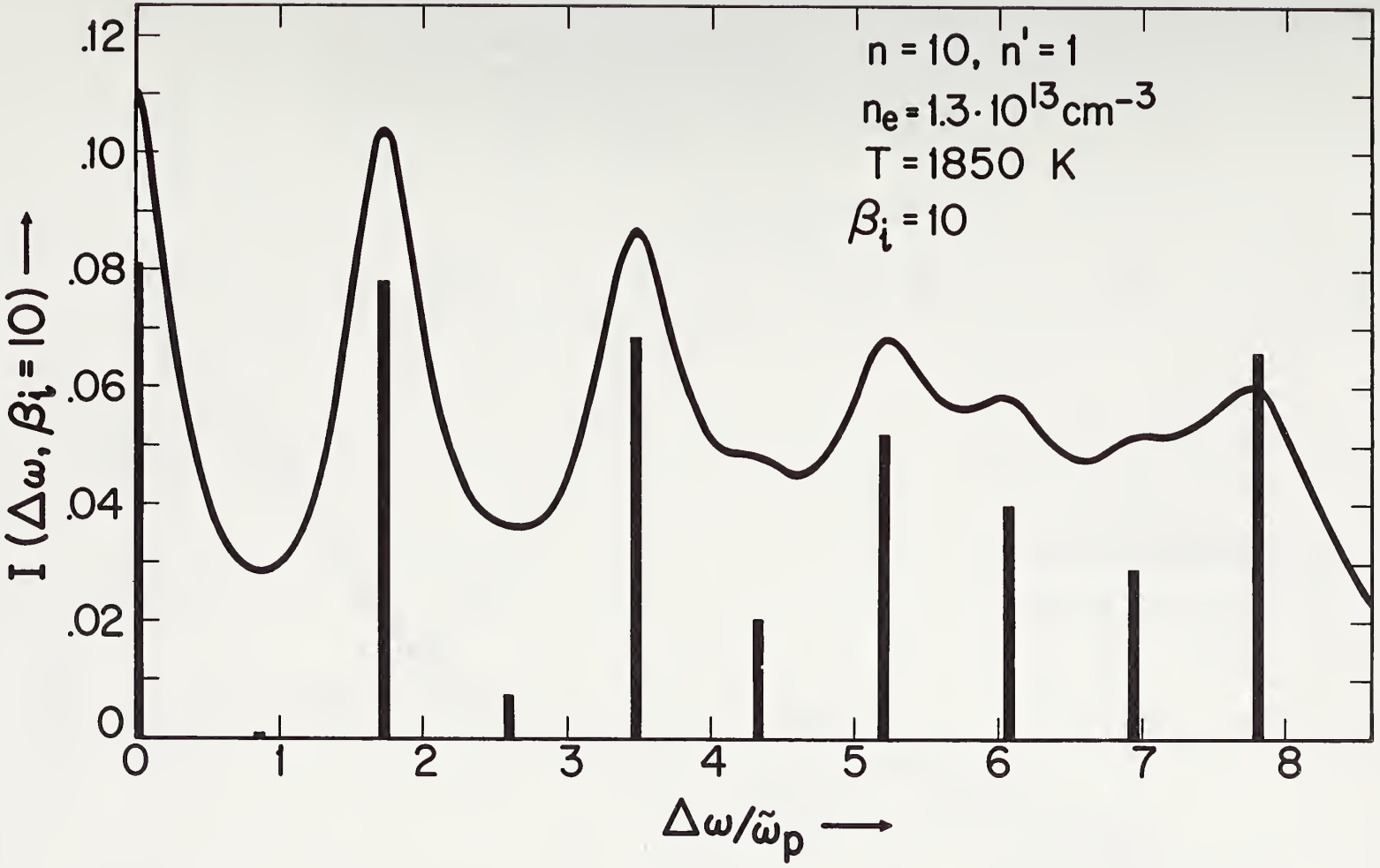

Figure 10. The intensity profile of the Ly_{10}-line is shown before the final ion field average for a normalized ion field $\beta_i = 10$ demonstrating the electron broadening.

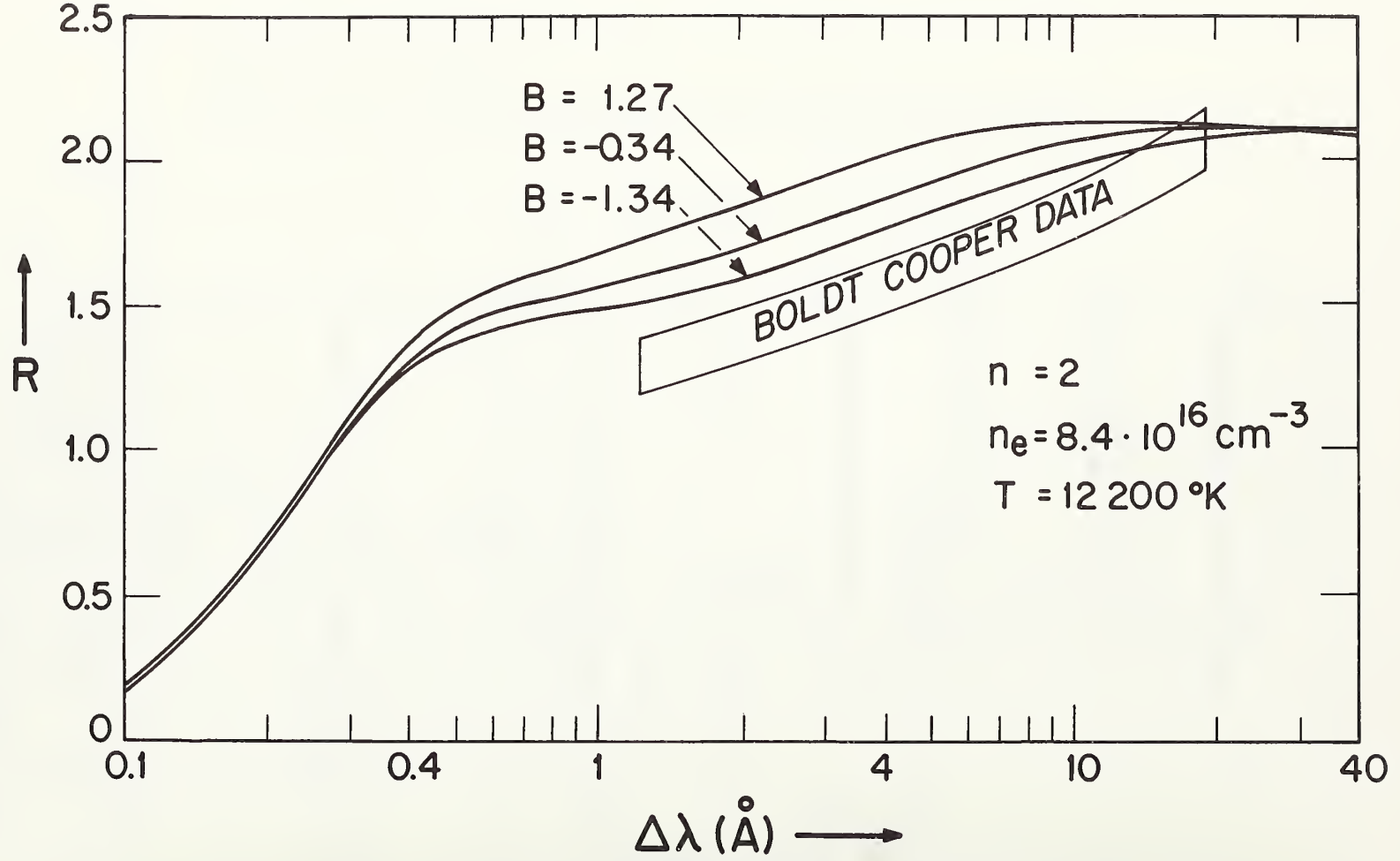

Figure 11. The final Lyman-α profile normalized with respect to the asymptotic Holtsmark $\Delta\lambda^{-5/2}$ - wing (ions only) for three different values of the constant B, whose value depends on the cutoff procedure applied (see explanation in the text).

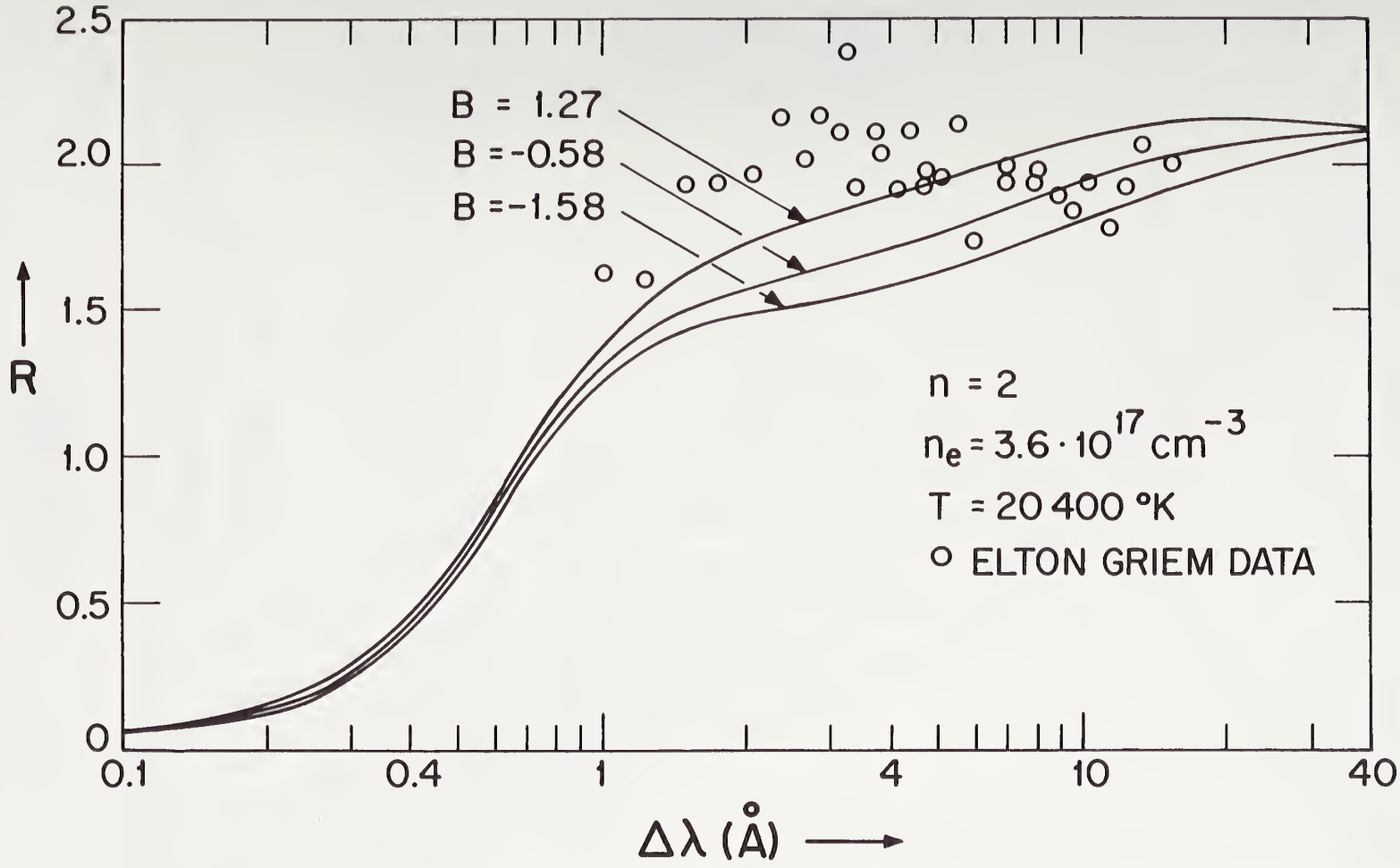

Figure 12. The final Lyman-α-profile normalized with respect to the asymptotic Holtsmark $\Delta\lambda^{-5/2}$-wing (ions only) for three different values of the constant B, whose value depends on the cutoff procedure applied.

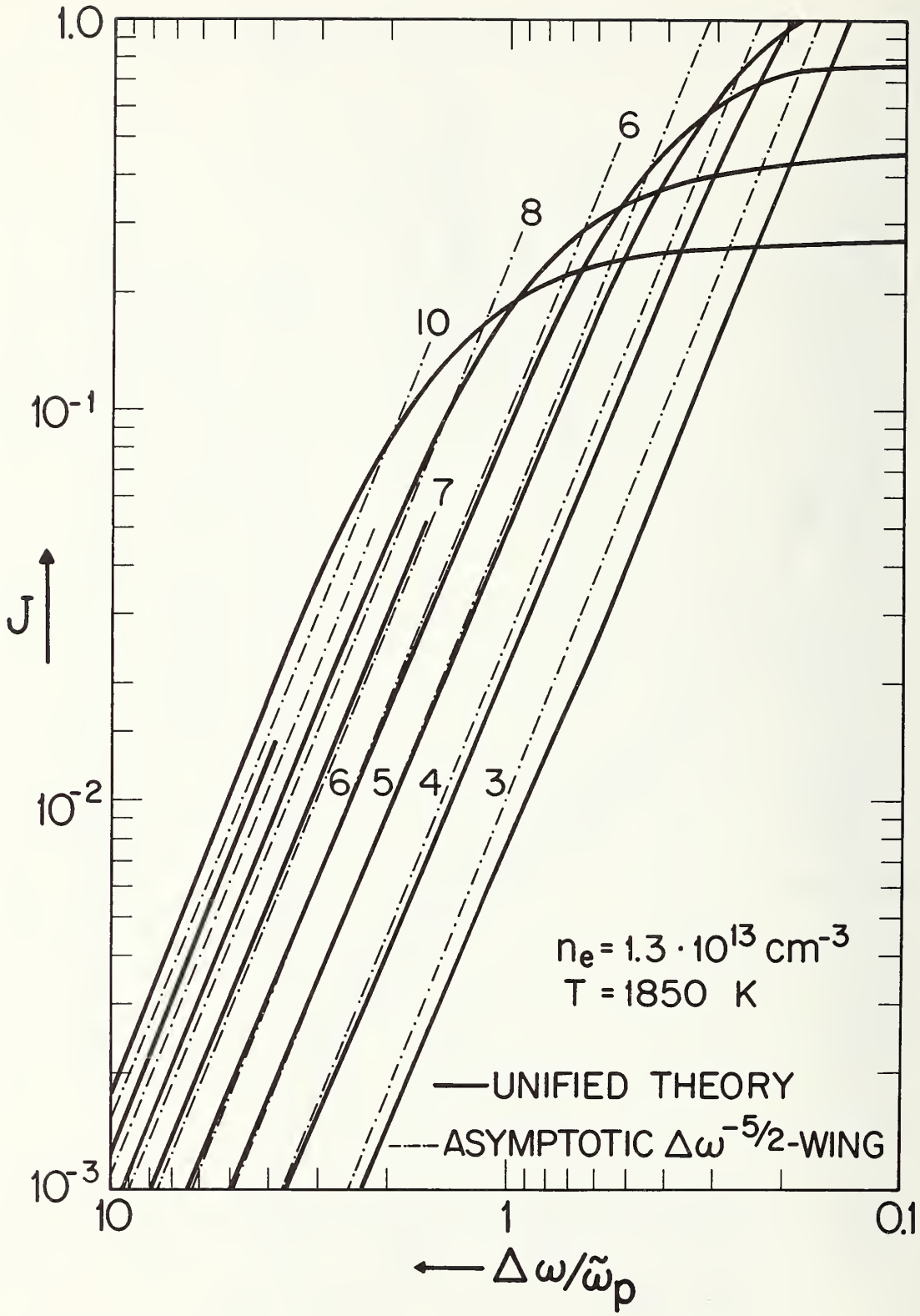

Figure 13. The final line profiles for the density and temperature parameters of Vidal, 1965.

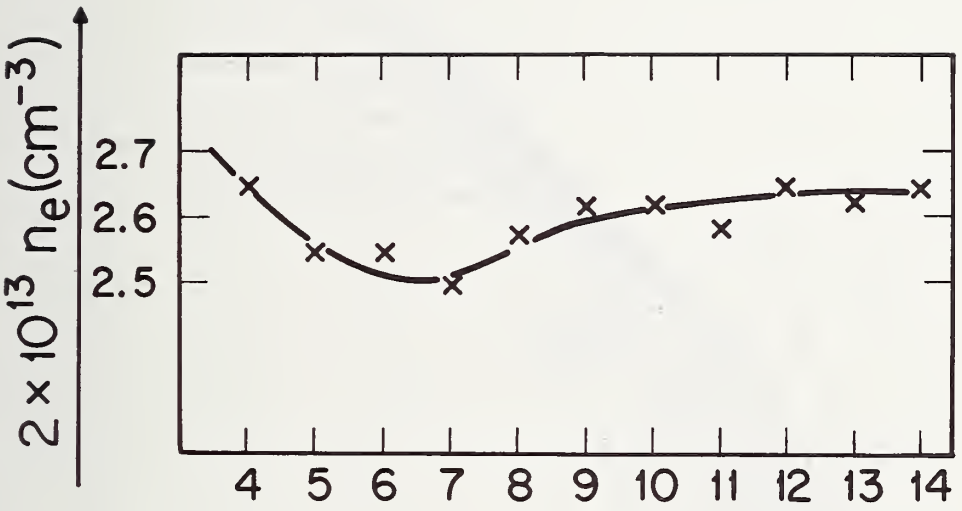

Figure 14. Plot of the electron density values as a function of the principal quantum number n, which have been evaluated by Vidal, 1965, under the assumption that the $\Delta\lambda^{-5/2}$ -wing revealed by the experiment is identical with the asymptotic Holtsmark $\Delta\lambda^{-5/2}$- wing for electrons and ions.

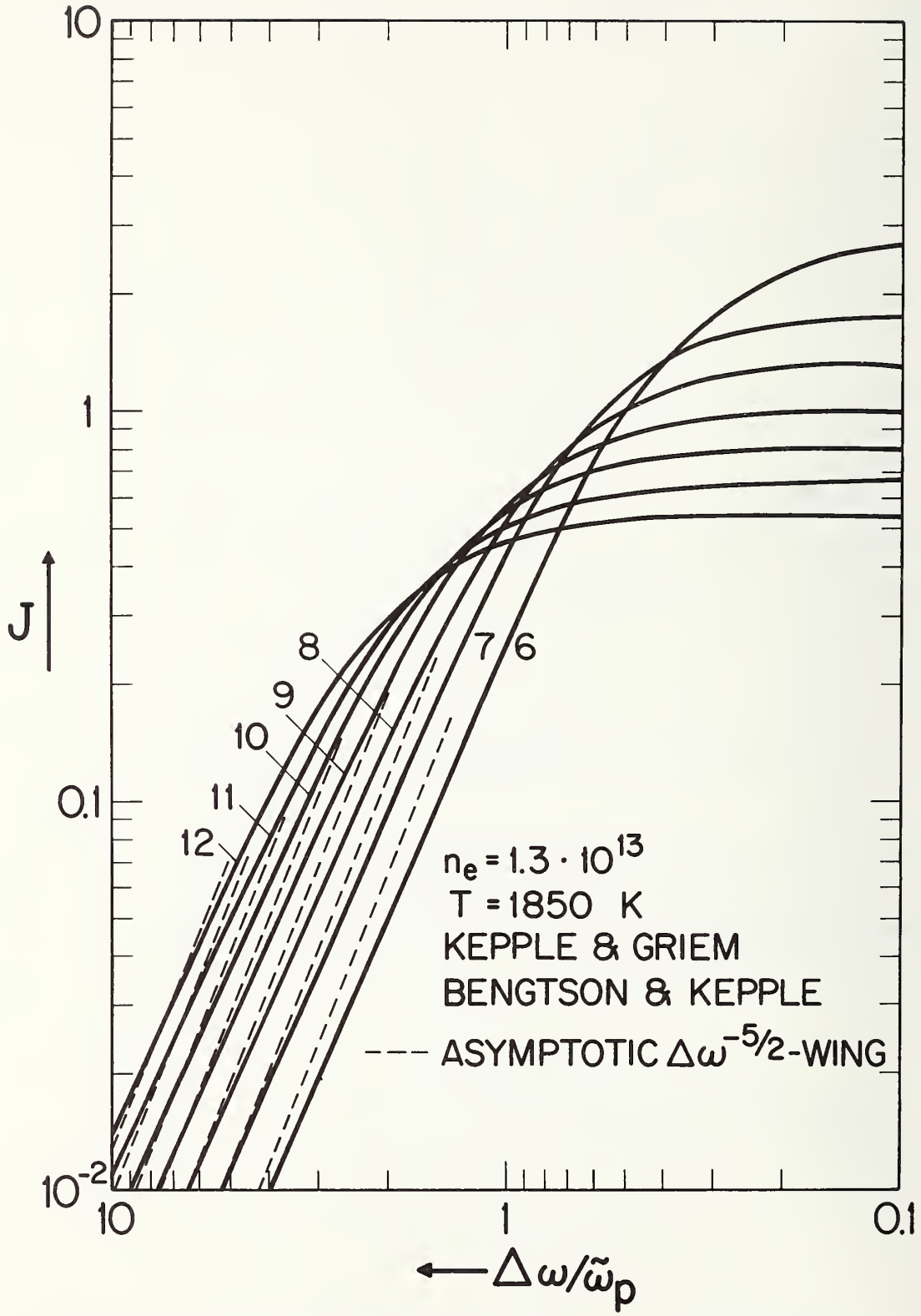

Figure 15. The Balmer line profiles for the density and temperature parameters of Vidal, 1965, as calculated by the indicated authors.

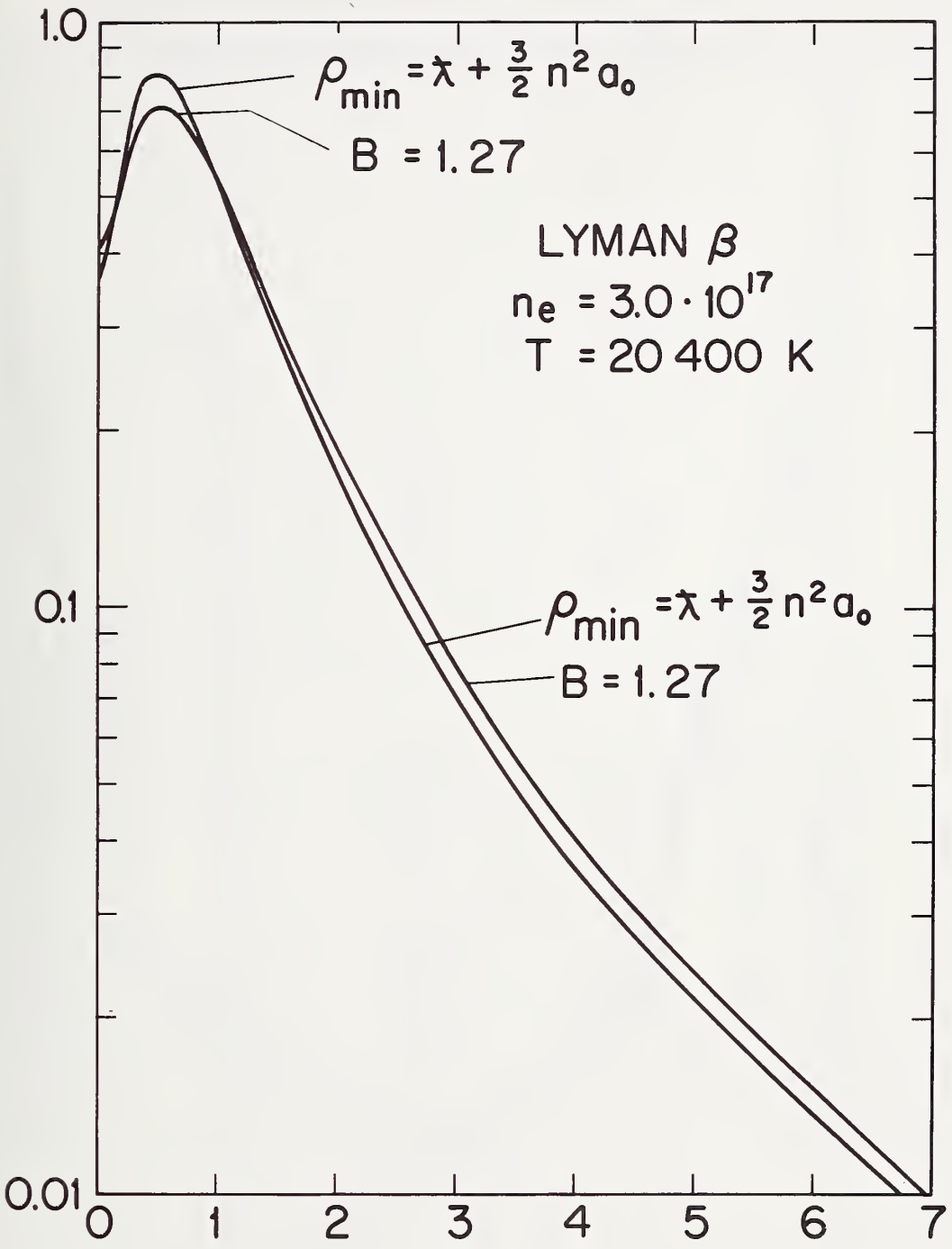

Figure 16. The Lyman-β profile for two different strong collisions cutoffs ρ_{min}.

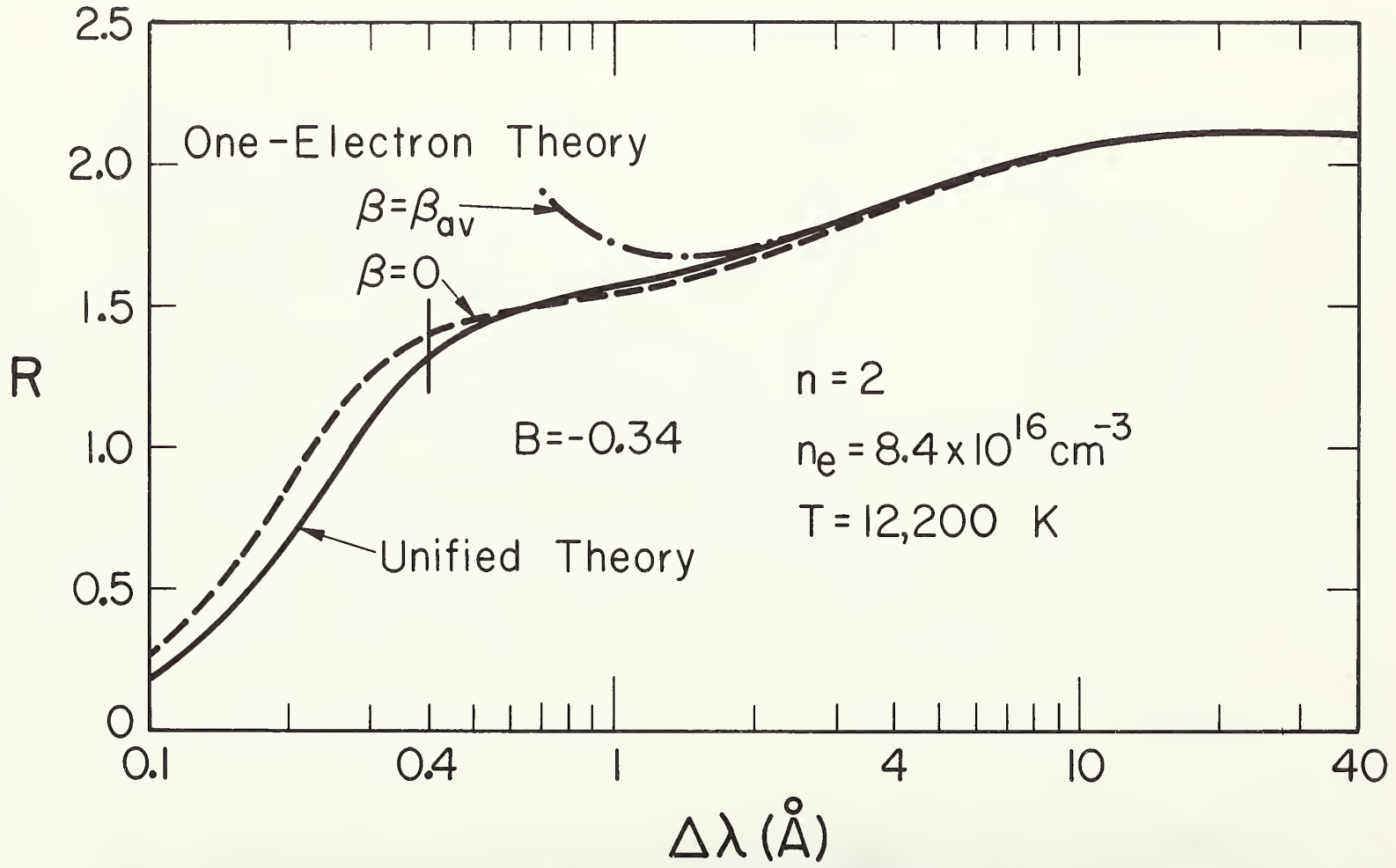

Figure 17. Comparison of the unified theory calculations with the one-electron theory calculations for Lyman-α. The vertical line marks the position of the shifted Stark component for an ion field $\beta=\beta_{av}$.

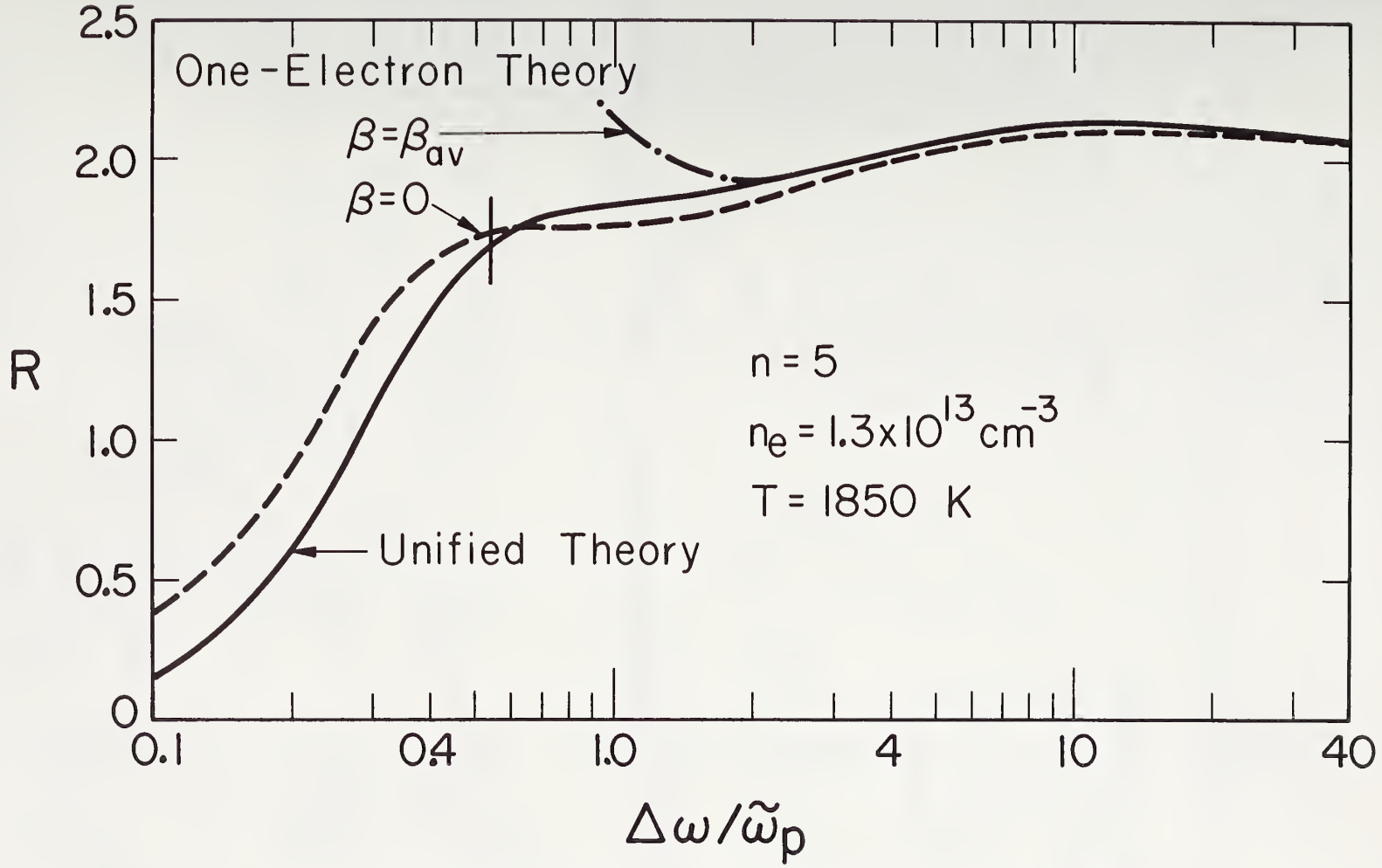

Figure 18. Comparison of the unified theory calculations with the one-electron theory calculations for n=5. The vertical line marks the position of the outermost, shifted Stark component for an ion field $\beta=\beta_{av}$.

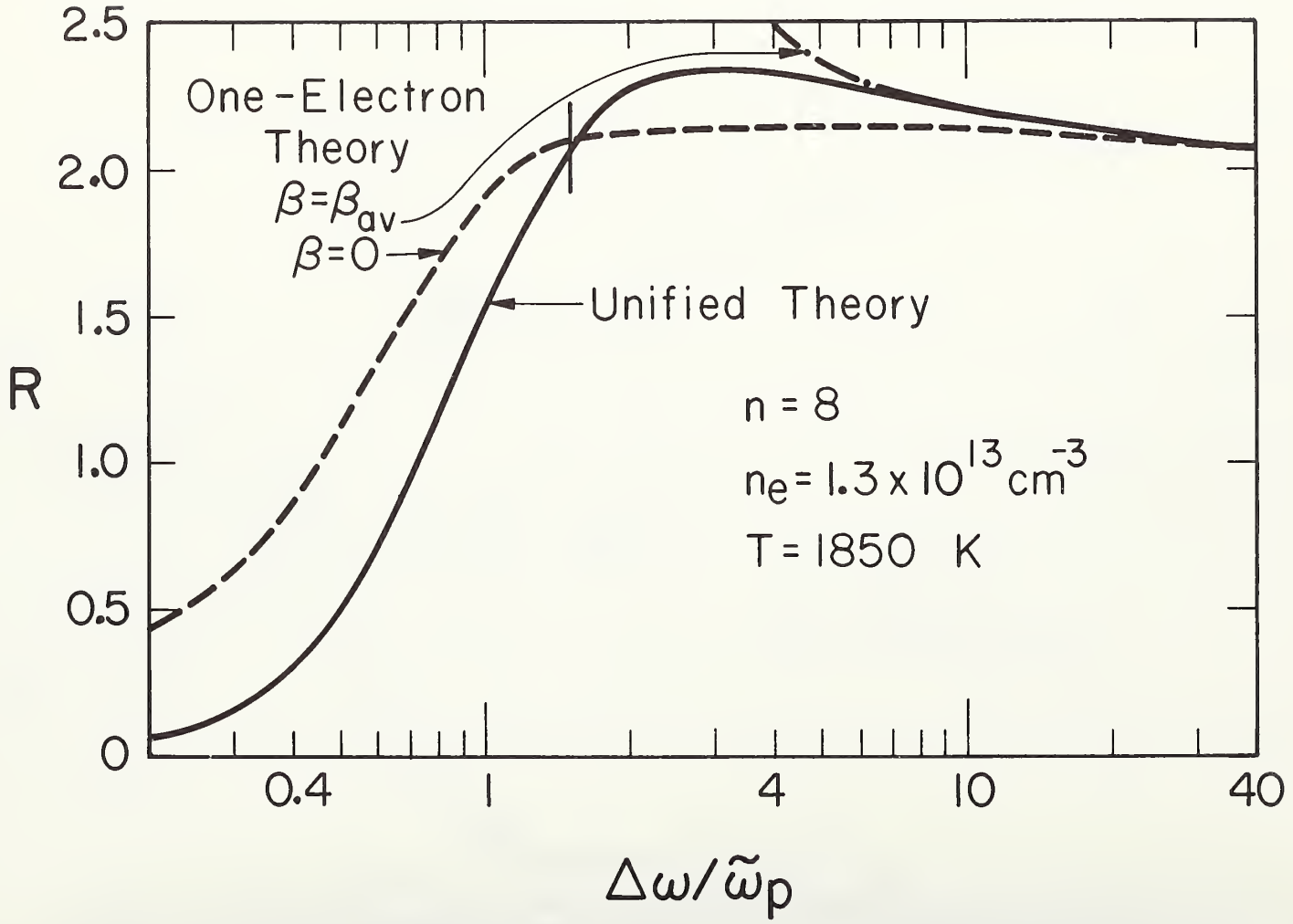

Figure 19. Comparison of the unified theory calculations with the one-electron theory calculations for n = 8. The vertical line marks the position of the outermost, shifted Stark component for an ion field $\beta = \beta_{av}$.

THE NATIONAL ECONOMIC GOAL

Sustained maximum growth in a free market economy, without inflation, under conditions of full employment and equal opportunity

THE DEPARTMENT OF COMMERCE

The historic mission of the Department is "to foster, promote and develop the foreign and domestic commerce" of the United States. This has evolved, as a result of legislative and administrative additions, to encompass broadly the responsibility to foster, serve and promote the nation's economic development and technological advancement. The Department seeks to fulfill this mission through these activities:

MISSION AND FUNCTIONS OF THE DEPARTMENT OF COMMERCE

"to foster, serve and promote the nation's economic development and technological advancement"

Participating with other government agencies in the creation of national policy, through the President's Cabinet and its subdivisions.

- **Cabinet Committee on Economic Policy**
- **Urban Affairs Council**
- **Environmental Quality Council**

Promoting progressive business policies and growth.

- **Business and Defense Services Administration**
- **Office of Field Services**

Assisting states, communities and individuals toward economic progress.

- **Economic Development Administration**
- **Regional Planning Commissions**
- **Office of Minority Business Enterprise**

Strengthening the international economic position of the United States.

- **Bureau of International Commerce**
- **Office of Foreign Commercial Services**
- **Office of Foreign Direct Investments**
- **United States Travel Service**
- **Maritime Administration**

Assuring effective use and growth of the nation's scientific and technical resources.

- **Environmental Science Services Administration**
- **Patent Office**
- **National Bureau of Standards**
- **Office of Telecommunications**
- **Office of State Technical Services**

Acquiring, analyzing and disseminating information concerning the nation and the economy to help achieve increased social and economic benefit.

- **Bureau of the Census**
- **Office of Business Economics**

NOTE: This schematic is neither an organization chart nor a program outline for budget purposes. It is a general statement of the Department's mission in relation to the national goal of economic development.

JULY 1969

☆ U. S. GOVERNMENT PRINTING OFFICE : 1970 O - 381-921

NBS TECHNICAL PUBLICATIONS

PERIODICALS

JOURNAL OF RESEARCH reports National Bureau of Standards research and development in physics, mathematics, chemistry, and engineering. Comprehensive scientific papers give complete details of the work, including laboratory data, experimental procedures, and theoretical and mathematical analyses. Illustrated with photographs, drawings, and charts.

Published in three sections, available separately:

• Physics and Chemistry

Papers of interest primarily to scientists working in these fields. This section covers a broad range of physical and chemical research, with major emphasis on standards of physical measurement, fundamental constants, and properties of matter. Issued six times a year. Annual subscription: Domestic, $9.50; foreign, $11.75*.

• Mathematical Sciences

Studies and compilations designed mainly for the mathematician and theoretical physicist. Topics in mathematical statistics, theory of experiment design, numerical analysis, theoretical physics and chemistry, logical design and programming of computers and computer systems. Short numerical tables. Issued quarterly. Annual subscription: Domestic, $5.00; foreign, $6.25*.

• Engineering and Instrumentation

Reporting results of interest chiefly to the engineer and the applied scientist. This section includes many of the new developments in instrumentation resulting from the Bureau's work in physical measurement, data processing, and development of test methods. It will also cover some of the work in acoustics, applied mechanics, building research, and cryogenic engineering. Issued quarterly. Annual subscription: Domestic, $5.00; foreign, $6.25*.

TECHNICAL NEWS BULLETIN

The best single source of information concerning the Bureau's research, developmental, cooperative and publication activities, this monthly publication is designed for the industry-oriented individual whose daily work involves intimate contact with science and technology—*for engineers, chemists, physicists, research managers, product-development managers, and company executives.* Annual subscription: Domestic, $3.00; foreign, $4.00*.

* Difference in price is due to extra cost of foreign mailing.

NONPERIODICALS

Applied Mathematics Series. Mathematical tables, manuals, and studies.

Building Science Series. Research results, test methods, and performance criteria of building materials, components, systems, and structures.

Handbooks. Recommended codes of engineering and industrial practice (including safety codes) developed in cooperation with interested industries, professional organizations, and regulatory bodies.

Special Publications. Proceedings of NBS conferences, bibliographies, annual reports, wall charts, pamphlets, etc.

Monographs. Major contributions to the technical literature on various subjects related to the Bureau's scientific and technical activities.

National Standard Reference Data Series. NSRDS provides quantitive data on the physical and chemical properties of materials, compiled from the world's literature and critically evaluated.

Product Standards. Provide requirements for sizes, types, quality and methods for testing various industrial products. These standards are developed cooperatively with interested Government and industry groups and provide the basis for common understanding of product characteristics for both buyers and sellers. Their use is voluntary.

Technical Notes. This series consists of communications and reports (covering both other agency and NBS-sponsored work) of limited or transitory interest.

Federal Information Processing Standards Publications. This series is the official publication within the Federal Government for information on standards adopted and promulgated under the Public Law 89–306, and Bureau of the Budget Circular A–86 entitled, Standardization of Data Elements and Codes in Data Systems.

CLEARINGHOUSE

The Clearinghouse for Federal Scientific and Technical Information, operated by NBS, supplies unclassified information related to Government-generated science and technology in defense, space, atomic energy, and other national programs. For further information on Clearinghouse services, write:

Clearinghouse
U.S. Department of Commerce
Springfield, Virginia 22151

Order NBS publications from:

Superintendent of Documents
Government Printing Office
Washington, D.C. 20402

U.S. DEPARTMENT OF COMMERCE
WASHINGTON, D.C. 20230

OFFICIAL BUSINESS

POSTAGE AND FEES PAID
U.S. DEPARTMENT OF COMMERCE